Title
Causes and Consequences of Tree Growth, Injury, and Decay in Sierra Nevada Forest Ecosystems

Author
Cousins, Stella Janet Melugin

Publication Date
2016

Peer reviewed|Thesis/dissertation

Causes and Consequences of Tree Growth, Injury, and Decay in Sierra Nevada Forest Ecosystems

By

Stella Janet Melugin Cousins

A dissertation submitted in partial satisfaction of the

requirements for the degree of

Doctor of Philosophy

in

Environmental Science, Policy, and Management

in the

Graduate Division

of the

University of California, Berkeley

Committee in charge:

Professor John J. Battles, Chair
Professor David D. Ackerly
Professor Scott L. Stephens

Summer 2016

Causes and Consequences of Tree Growth, Injury, and Decay
in Sierra Nevada Forest Ecosystems

by

Stella Janet Melugin Cousins

Abstract

Causes and Consequences of Tree Growth, Injury, and Decay
in Sierra Nevada Forest Ecosystems

by

Stella Janet Melugin Cousins

Doctor of Philosophy in Environmental Science, Policy, and Management

University of California, Berkeley

Professor John J. Battles, Chair

In the course of its long life, a tree confronts environmental conditions that range from natural variation in local weather or regional climate to large scale alteration of the earth's atmosphere. Forest ecosystems are modified and potentially degraded by an array of anthropogenic enterprises, not the least of which is air pollution. Environmental change can alter ecosystem patterns and processes, particularly when effects accumulate over the long term or multiple factors interact. My dissertation research examines two key aspects of forest ecosystem dynamics in response to altered environmental conditions over the long term. First, I examine mortality, and in particular standing dead trees, one of the predominant physical consequences of forest ecosystem stress. This work quantifies the decay patterns of six common species of California's mixed conifer forests, revealing the role of standing dead trees in forest carbon budgets. Next, my research examines influences on the growth and vitality of live trees in the southern Sierra Nevada, a forested region impacted by chronic ozone pollution. This work encompasses the regional patterns of ecosystem exposure to ozone pollution, long term monitoring of ozone-induced injury to ponderosa and Jeffrey pine trees (*Pinus ponderosa* and *Pinus Jeffreyi*), and a description of tree growth responses to pollution in light of their simultaneous responses to climate.

Forest mortality is always an important part of ecosystem processes, but in recent years, elevated mortality rates have increased the relative abundance of dead trees in forests across the Western United States. Though the importance of woody debris to ecosystem processes is clear, the structural and biogeochemical contributions of standing dead trees remain largely unknown. The first chapter of my dissertation characterizes the decay patterns and carbon density of standing dead trees in Sierra Nevada mixed conifer forests, examining traits in six dominant species. I used a dimensional analysis to describe the patterns of wood density, carbon concentration, and net carbon density. As decay class advanced, trees showed a progressively lower density and a small increase in carbon concentration. Net carbon density of the most decayed standing dead trees was only 60% that of live trees. The key characteristics that determined these patterns were species, surface to volume ratio, and relative position within each tree. Decay while standing and estimation of deadwood biomass in large scale inventories also have repercussions in greenhouse

gas accounting. When the measured changes in carbon density were applied to standing dead carbon stock estimates for California mixed conifer forests, the decay-adjusted estimates were 18% (3.66-3.74 teragrams) lower than estimates that did not incorporate change due to decay.

In the second and third chapters, I focus on anthropogenic ozone pollution, a major stressor in southern Sierra Nevada forests. Ozone poses a risk to ecosystems worldwide because of its damaging effects on plant tissues and the carbon fixation they carry out. Ozone is a secondary pollutant formed by the reaction of nitrogen oxides and oxygen in the presence of sunlight and heat. Elevated tropospheric ozone has impacted parts of southern California, the San Joaquin Valley, and the southern Sierra Nevada for more than 40 years. This field-based research relies on data collected in Sequoia and Kings Canyon National Parks and on the Sierra National Forest.

Chapter two investigates the connections between ozone exposure and injury to trees. The tools of this study were a long term air quality monitoring network across a regional gradient of ozone concentration and repeat measures of pollution injury in ponderosa and Jeffrey pines. I used these measures to quantify trends in ozone concentration, assess patterns in ozone-caused foliar injury, and understand tree demographic responses to ozone exposure. Since region-wide observations began in 1991, air quality has improved, but across much of the mixed conifer forest, ozone exposure is still high enough to cause permanent damage to ecosystems. Chlorotic mottle, the key symptom of pollution injury in ponderosa and Jeffrey pines, continues to provide evidence of physiological impacts to trees but has also incrementally declined in recent years. Because growth is a leading indicator of tree vitality and forest ecosystem condition, in this study I also remeasured tree diameters to determine the long term relative growth rates of individuals exposed to ozone pollution. Relative to asymptomatic trees, typical ozone-injured trees from the most polluted sites had growth reduced by up to 24%. Over the 20-year study survival of damaged trees was lowest at high pollution levels, but within the range of rates in similar forests. The pollution-injured pines that make up southern Sierra Nevada forests today clearly have the capacity for recovery, but will continue to bear a legacy of anthropogenic impacts.

In the third chapter, I examine how Sierra Nevada forest ecosystems respond to climatic conditions and chronic ozone pollution, both individually and interactively. The gradient of pollution exposure on the western slope of the southern Sierra Nevada enabled a comparison of annual tree growth under very low to severe summer ozone levels, across sites with shared climatic conditions. I used the Jeffrey pine tree ring record to characterize growth as shaped by these conditions. First, I found that the temperature and precipitation of the preceding winter and summer have an important influence on annual growth. Building on this understanding of climatic dependency, analysis showed that trees exposed to elevated ozone had slower annual growth rates than their counterparts in relatively unpolluted locations. Annual growth rates in severely polluted sites were 8.4-23% lower than predicted growth under conditions that meet current air quality standards. Although the isolated effects of both ozone and water limitation are negative, an antagonistic interaction between these environmental factors was also apparent. As predicted in earlier research, high summer temperatures limited the negative growth impacts of ozone pollution. The likely mechanism for this interaction amongst stressors is stomatal closure, which prevents uptake of ozone into the leaf. These growth losses, attributable to a chronic anthropogenic stressor and modified by prevailing environmental conditions, may facilitate further change in forest processes.

for my family

and other animals

Table of Contents

Acknowledgements

This undertaking would not have been possible without the encouragement and support of my family. I thank my parents for their tireless care and high expectations, and also for feeding myself and my field crews during our research trips. Two siblings with dissertations behind them helped me imagine that I could pull it off and prodded me along the way. My sister also provided many delicious dinners, and the company of her family was especially appreciated when I needed a night off from worrying about quals or an excuse to leave Hilgard at a reasonable hour.

John Battles has served as a generous mentor, critic, and sounding board throughout the last six years. I am grateful for his guidance on analytical approaches, counsel in times of frustration, and uncompromising dedication to scientific rigor. In long drives with John and in even longer meetings, this dissertation took shape as we discussed the merits of ideas and my mind whirled. I thank John for being a truly trustworthy advisor in every sense of the word and for passing his contagious fascination for ecosystem ecology on to me. I also thank my dissertation committee, Scott Stephens and David Ackerly, for their guidance and input on this research. David has contributed more than he may know, having offered me my first opportunity to contribute to research, first paid position in ecology, and first truly dangerous look at plants under a microscope. Thanks also to Joe McBride, who challenged me to dive deep into the long history of ozone pollution in California.

A crowd of collaborators both in the Sierra Nevada and in Berkeley has helped see this project to fruition. Annie Esperanza provided essential data and background information as my ideas developed into research endeavor. Of equal importance, she has also given me an example of a committed scientific career to which I aspire. Ricardo Cisneros and Don Schwiezer also shared both data and expertise, as well as the time of their summer staff. I am grateful to them for their help as I learned the concepts and calculations needed to understand air pollution. My thanks also to Dan Duriscoe, who surveyed many of the plots I revisited in my work and provided field training on essential protocols. At Sequoia and Kings Canyon National Parks, Koren Nydick facilitated permitting twice over and helped make space for field crews, while Tom Warner provided the singular pole pruner without which an entire chapter could not have been carried out. Nate Stephenson and Adrian Das of the USGS provided constructive feedback on methods for studying mortality and decay, as well as sharing their enthusiasm for all things southern Sierra Nevada. At Blodgett Forest Research Station, Rob York and Ken Somers searched out possible snags both actual and metaphorical. Rob has also earned the dubious title of instructor in the art of scientific chainsaw use. I was glad of his patient tutorials, at least when the saw was working. Projects at Blodgett also benefited from the efforts of Amy Mason and careful skill of Pete Zellner. Within ESPM, Roxanne Heglar and Alyssa Fong have helped with events and logistics on innumerable occasions.

Many talented and patient people contributed to the lab and field research that forms the foundation of my dissertation. John Sanders endured the many absurdities of dead wood and measured thousands of tree rings, all while ever fostering stimulating conversation. Debra Swenson was the first person to sign on for field work and the last to proof read. No part would

have been possible without her energy and keen questions, and many long days benefited from her sense of humor and sense of wonder. Eric Olliff, David Soderberg, Alex Javier and Natalie Holt braved yellow jackets, wielded axes, and turned over many a log for the cause; I thank them heartily for their efforts. Erika Blomdahl, Jeneya Fertel, and Clayton Sodergren also played a critical role, both through assistance in the field and through meticulous lab work.

Wonderful labmates past and present have made day to day work in the Battles Lab a pleasure. Maya Hayden, Natalie van Doorn, Carrie Levine, Carmen Tubbesing, Joan Dudney, and Anne Eschtruth have been the people I turned to with a thousand questions and were always the first to join in a minor victory. Marlyse Duguid serves as long distance labmate, and I always value her advice and camaraderie in Ph.D. life and real life. Thanks also to Rebecca Wenk, who will always share her inspiring love of the natural world with us. I look forward to sharing the highs and lows of science with all these colleagues for years to come.

Many friends have leant an understanding ear during this rather long project. Chief among the sufferers are Kari Finstad, Kate Wilkin, and Sara Knox, who have listened to more than their share of my complaints. Lauren Hallett, Luke Macaulay, and Maddie Girard may have wandered in and out of other time zones, but have persistently helped through their encouraging and interesting conversations. Eric Waller deserves special recognition for quality hike planning and long talks about plants. And finally, my thanks to the friends and creatures who have kept checking on me all throughout this adventure, those before, and more to come: the perfectly cromulent Jennifer Bland, Katie Port, Nicholas Chan, Mel Abreu, and my vegetarian roommate, Marmot. I owe them great quantities of wine, many bridge crossings, and a some portion of my remaining sanity.

Financial support for this research was provided in part by the California Energy Commission through contract 500-10-046 and California Air Resources Board agreement 10-778. Graduate student support came from the University of California (UC) Cooperative Extension Graduate Training in Cooperative Extension Pilot Program, the UC Office of the President Carbon Neutrality Initiative Fellowship, UC Division of Agriculture and Natural Resources Renewable Resources Extension Act Grant, a Koshland-UC Berkeley Dissertation Writing Grant, and the Baker-Bidwell, William Carroll Smith and Frank Myers Forestry fellowships.

CHAPTER 1 | Decay patterns and carbon density of standing dead trees in California mixed conifer forests

1. INTRODUCTION

Tree death is a critical process in forest ecosystems. When trees die, the subsequent decay releases carbon to the atmosphere as well as an abundance of resources (e.g., nutrients and energy) into the forest ecosystem (Franklin et al., 1987; Harmon et al., 1986). Decomposition often begins while the tree is still standing (Boddy, 2001; Harmon et al.; 1986; Whittaker et al., 1979). Standing dead (SD) trees store a significant amount of carbon and provide essential habitat for wildlife but also present potential safety and fire hazards (Hilger et al., 2012; Keen, 1955; Knapp, 2015; Raphael and White, 1984). Thus, SD trees play an important role in the ecology and management of forests.

As a direct result of well-documented increases in forest morbidity and mortality, SD trees are becoming more important for forest carbon dynamics. Increasing climatic stress, chronic and widespread air pollution, and pest outbreaks have fueled forest die-offs worldwide, with broad implications for ecosystem structure and function (Allen et al., 2010; Anderegg et al., 2012; Bytnerowicz et al., 2007; Hicke et al., 2013). In the North American West, increases in mortality are widely attributable to warming and increased water deficits (van Mantgem et al., 2009), often in combination with irruptions of bark beetles (Bentz et al., 2010, Ganey and Vojta, 2011). Across the western US from 1997-2010, bark beetles killed trees containing 2-24 teragrams (Tg) of carbon year-1 on over 5 million ha (Hicke et al., 2013; Meddens et al., 2012). Similarly, mountain pine beetle (Dendroctonus ponderosae) related mortality in British Columbia has caused forests there to become a net source of carbon, potentially for many decades (Kurz et al., 2008). Following a severe disturbance such as this, the majority of aboveground carbon stocks may be stored in SD trees (Hagemann et al., 2010). Fire suppression also contributes to increased abundance and decreased average size of dead trees (Stephens, 2004; Stephens and Moghaddas, 2005). Climate change projections and emissions trends indicate a future of exacerbated environmental stress both for California's forests (Battles et al., 2009; Moser et al., 2009, Panek et al., 2013) and forests throughout the western United States (Allen et al., 2010; IPCC, 2007). Additionally, high exposure to ozone pollution that contributes to tree stress and death -- already the norm in parts of California -- is expected in nearly 50% of global forests within this century (Fowler, 1999; Panek et al., 2013). Elevated tree mortality will contribute to a growing deadwood carbon pool and could result in regional increases in GHG emissions (e.g., Kurz et al., 2008).

During the time a dead tree remains standing, a typical sequence of changes occurs leading to an overall reduction in tree size (Domke et al., 2011; Raphael and Morrison, 1987). Tree volume declines through loss of leaves, twigs, and branches, which fall to the forest floor and join the down woody material (DWM) pool (Aakala et al., 2008; Raphael and Morrison, 1987). Concurrent with these dimensional reductions are changes to the tree's physical and chemical properties caused by weathering, decomposition, and insect activity (Harmon et al., 1986; Domke et al., 2011). In many temperate species, wood and bark density decline with advancing

decay, while the carbon content of tissues rises slightly. The net outcome is a decrease in total carbon density (Harmon et al., 2013; Harmon et al., 2011). Size, tree species, and present decay condition are key determinants of wood decay rates (Harmon et al., 1986; Russell et al., 2014; Yatskov et al., 2003)). Parts of the stem can also decay at different rates. For example, contact with soil can increase moisture content and facilitate access for decay organisms, accelerating decomposition near ground level compared to upper portions of the stem (Boddy, 2001; Graham, 1925; Harmon et al., 1986; Maser and Trappe, 1984). Gradients in the density of wood from the originating live tree also shape patterns of decay. For example, conifers typically have higher wood density and carbon concentrations at the base of the stem relative to the upper reaches (Bowyer et al., 2007). SD trees retain substantial necromass for decades (Keen, 1929; Hilger et al., 2012) and sometimes even over a century (Mast et al., 1999). Since SD trees can represent a significant carbon reservoir in many forests, explicitly accounting for SD tree carbon dynamics will refine estimates of forest carbon storage and flux, and improve models of decomposition (Kurz et al., 2009; Litton et al., 2007; Woodall et al., 2008).

In continental US and Canada forests, SD trees form 5 - 35% of aboveground forest biomass (Aakala et al., 2008, Vanderwel, 2008, Woodall, 2008). Conifer forests in the Western US are typically at the upper end of this range, with field-based estimates ranging from 2.4 to 7.2 Mg carbon ha-1 (Woodall et al., 2012, Woodall et al., 2013). Standing dead carbon in California mixed conifer forests specifically is greater still, with an average of 9.5 Mg carbon ha-1 and a total of 20.5 Tg carbon in SD trees (Battles et al., 2014; Gonzalez et al., 2010). SD trees form one of five forest sector carbon pools included in the U.S. National Greenhouse Gas Inventory (NGHGI) (Aalde et al., 2006; EPA, 2015). The NGHGI is in turn used for reporting to international bodies including the Intergovernmental Panel on Climate Change and United Nations (IPCC, 2006; United Nations, 1992). There is also growing demand for accurate accounting of GHG emissions at state and regional levels. California's Global Warming Solutions Act, which requires inventory of storage and emissions of GHG by forests, is one example (State of California, 2006).

Though SD trees are essential to forest processes, incorporation of their physical and chemical transformations into forest inventory and carbon accounting is a relatively recent development (Domke et al., 2013; Fahey et al., 2005; Heath et al., 2011; O'Connell et al., 2012; Woodall, 2012). As previously implemented, the NGHGI and dependent statewide inventories handled SD trees by applying live wood and bark properties to gradually decreasing tree volumes (Battles et al. 2014; Woudenberg et al., 2010; Woodall et al., 2011). The most recent NGHGI reports, based on results from the US Forest Service Forest Inventory and Analysis program (FIA), now also include adjustments for wood decay in SD trees in addition to estimates of whole tree volume loss (O'Connell et al., 2014; EPA, 2015). Biomass and GHG estimates employ a suite of ratios that are used to adjust the density of SD trees according their species and decay class (1:intact - 5:advanced decay) (O'Connell et al., 2014; USFS, 2010). These density reduction ratios rely on the demonstrated correspondence between decay rates of DWM and SD trees. The SD adjustments in use for major mixed conifer species originate from the SD to down dead ratios for softwoods (classes 1-3) and the SD to down dead ratios for all inventoried species (classes 4-5) (Harmon et al., 2011; Harmon et al., 2008). Comparison of DWM and SD density suggests that patterns of density and carbon loss in SD trees differ from those of DWM; for mixed conifer species, sampled SD densities are not yet available (Harmon et al., 2011; Harmon et al., 2013).

Finally, a typical large-scale inventory sets carbon concentration of SD trees at 50% of total biomass (Birdsey, 1992; Fahey et al., 2005; Woodall et al., 2011). However, this assumption underestimates SD tree carbon concentration by 5-10%, as carbon density increases with advancing decay in both hardwood and softwood species groups, including California mixed conifer species (Harmon et al., 2013). Continued improvement in forest carbon estimates requires further quantification of the changes characteristic of SD trees: not only diminishing size, but also distinctly altered physical and chemical properties (Heath et al., 2011, Smith et al., 2003; Woodall et al., 2012).

The goal of this study was to understand the patterns and processes of in situ decay of SD trees in the mixed conifer forests of California. To achieve this goal, we first measured the decline in carbon density (g cm-3) of SD trees along a decay class gradient. We specifically accounted for the contributions of changes in wood density and carbon concentration that occur during decay. We then asked whether patterns in carbon density with advancing decay varied by species, tree size, or vertical position along the tree bole. To scale up the results from our site-based research and to gauge their relevance to carbon management, we used the same tree inventory and decay classification used by the FIA program. Based on previous studies of decay patterns in SD trees (Harmon et al., 2011), our hypothesis was that bole density would decline with decay class. On the basis of carbon measurements from DWM and some SD trees (Harmon et al., 2013), we expected carbon concentration to rise slightly with decay class, but net carbon density to decline. We also anticipated that density losses in SD trees would vary by tree size and species. Given the more rapid decay of woody material in contact with the soil (Maser and Trappe 1984), the base of SD trees was expected to decay faster than the upper bole. Finally, in an application of these measurements, we developed decay-adjusted estimates of SD carbon stock for California mixed conifer forests and compared the outcomes of the live:dead decay ratios from this study with those used by the FIA program. Taking the patterns above into account, we predicted that implementing decay adjustments in biomass inventory would lead to lower estimates of carbon stock in SD trees than alternative unadjusted approaches.

2. METHODS

2.1 Study Areas

Dimensional analysis of SD trees was carried out in mixed conifer forests at Blodgett Forest Research Station (BFRS) and Sequoia National Park. BFRS is situated on the western slope of the Sierra Nevada near Georgetown, California (38°52’ N; 120°40’W; Fig. 1). Six native tree species are commonly found in mixtures of varying proportions: white fir (*Abies concolor*), incense cedar (*Calocedrus decurrens*), coast Douglas-fir (*Pseudotsuga menziesii var. menziesii*), sugar pine (*Pinus lambertiana*), ponderosa pine (*Pinus ponderosa*), and California black oak (*Quercus kelloggii*). The elevation of study sites ranges from 1220 to 1350 meters. Annual precipitation at BFRS averages 1660 mm, with a Mediterranean climate pattern of warm summers (14-17° C) and mild winters (0-9° C). Soils are derived from granodiorite parent material and are considered productive for the region. The study areas at BFRS were heavily cut in the early twentieth century and later regenerated naturally, a land use pattern common throughout the Sierran mixed conifer forest. Prior to European settlement, the north-central Sierra maintained a median fire return interval of 4-5 years and interval range of 2-22 years. The

most recent fire in the sampled stands occurred in 1900 (Stephens and Collins, 2004). After more than a century of fire suppression mixed conifer forests throughout the region now have large accumulations of SD trees and DWM (Stephens and Collins, 2004; Stephens and Moghaddas, 2005). SD tree measurement and collections at BFRS were carried out in both reserve stands and those actively managed with periodic timber harvests.

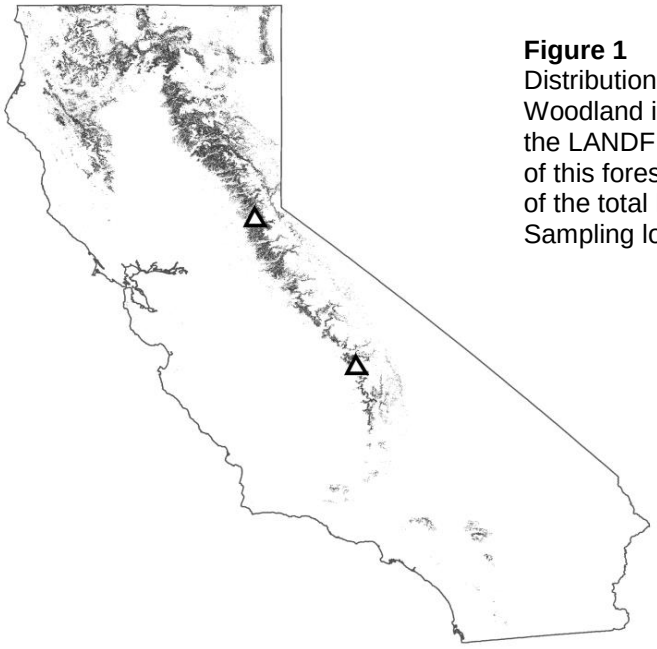

Figure 1
Distribution of Mesic Mixed Conifer Forest and Woodland in California, an existing vegetation type of the LANDFIRE landscape mapping program. Total area of this forest type in California is 2.15 million ha, 5.3% of the total land area in the state (USGS, 2008). Sampling locations are indicated by open triangles

The southern Sierra Nevada study sites are co-located with the US Geological Survey Western Ecological Research Station (USGS-WERC) Forest Demography Study. The long term study conducts an annual inventory of permanent plots, providing crucial estimates of key drivers of forest change. Structural and habitat characteristics of standing dead trees, including FIA decay class, are described during this survey. The five plots with carbon density sampling are dominated by red fir (Abies magnifica) and white fir, with giant sequoia (Sequoiadendron giganteum), incense cedar, and sugar pine also present. All are located in the Giant Forest and Panther Gap areas of Sequoia National Park (36°34'N 118°44'W, Fig. 1). At elevations of 2000-2600 meters, precipitation for these sites averages 1200 mm yr-1 with 35-65% in the form of snow. Soils are coarse loams from granitic parent material. For the Giant Forest grove area, pre-European mean and median fire return intervals are 35 and 30 years (Swetnam et al., 2009). The sampling locations have been without a stand replacing disturbance for several centuries and without any surface fire for at least ten years (Caprio and Swetnam, 1993; Das et al., 2007). Sampled trees from the USGS-WERC sites are SD red fir that were surveyed standing in plots and fell naturally in 2012-2013.

2.2 SD tree measurement and sample collection

Standing dead trees were identified at BFRS and in the USGS-WERC study areas based on previous inventories, observations of site managers, and field surveys. We then used stratified random sampling to select candidate SD trees with the strata defined by species, tree size, and FIA decay class (USFS, 2010). This decay classification is based upon the condition of the tree's

top, branches and twigs, bark, sapwood, and heartwood. It is used for SD trees throughout the FIA's nationwide forest inventory plots (USFS, 2010, after Thomas, 1979). We excluded fire-killed trees and those with severe mechanical wounds from logging operations. Our goal was to have a uniformly distributed sample of trees across the three strata. After selection, SD tree dimensions were measured while standing using a sonic hypsometer (Haglöf Vertex) and a laser dendrometer (Laser Technology Criterion 400; Fig. A1.A). Because broken boles contribute to volume loss and decay, the nature of the break was described: intact (i.e. no break), flat break, tapered break, or stepped break. The dimensions of the broken bole portion were also measured. An experienced sawyer then safely felled the sample trees at his discretion; one tree was excluded and later replaced.

We used dimensional analysis techniques to measure of intact wood, decayed wood, and bark to the whole tree (Whittaker and Woodwell, 1968). We also evaluated differences in decay conditions along the length of the bole to account for the vertical gradients in decay. Our protocol for sampling was adapted from Harmon et al., 2011, with the addition of measurements to characterize and compare specific positions and tissues. Felled trees were marked into 1-3 sections dependent on height (Fig. A1.B): for logs 0-2 m, 1 section; 2-10 m, 2 sections (base and top); and over 10 m, 3 sections (base, middle, and top). To determine full SD tree volume and section properties, the dimensions and attributes of each section were measured: length, diameter, bark thickness, bark extent, and wood hardness (Fig. A1.C). Cross sections 5-15 cm wide were removed with a chainsaw or hand tools from the midpoint of each tree section. When decayed material (soft, delaminated along one or more axes, or unable to hold form under pressure) was present, additional sampling and measurement was carried out. For decomposing or friable samples, the sample dimensions were measured in the field to the nearest millimeter using calipers. For the furthest decayed wood, a pre-measured area was outlined and excavated directly into a sample bag from a larger piece. If present, a bark sample was collected from each section. The cross-sectional cuts were also used to examine interior decay (Fig. A1.D). At each section midpoint, the decay condition (intact, decayed, or absent) of the wood was described by means of three pith-to-bark radial transects, the first random and others at 120° and -120° from the first (Fig. A1.E). By describing the cross sectional surface area, transects were used to calculate the proportion of each section in each decay condition.

2.3 Measurement and analysis of tissue properties

After collection, field (green) volume (cm3) of all wood and bark samples was measured. Bark volume was determined using a displacement gauge after saturation of the sample. The displaced water was collected and weighed to the nearest 0.1 gram. Large cross sections were cut into radial blocks in proportion to the decay conditions present in the sample using a miter saw. Wood and bark samples were dried a minimum of 48 hours at 100-105° C (Bergman, 2010). Tissue density was calculated as the ratio of oven dry mass (g) to field volume at room temperature. This value can also be interpreted as the basic specific gravity (Williamson and Wiemann, 2010).

A minimum of six trees of each species were selected for carbon analysis: three random individuals from decay classes 1-3 and three from classes 4-5 (excepting red fir, for which the sole tree in class 4 was analyzed). Once the minimum was met, we selected additional trees to represent all size classes and tissue types in the analysis. Samples were ground using a number 4

Wiley mill fitted with a 0.5 mm screen. The resultant powder was mixed and >3 g retained for analysis. The University of California Davis Analytical Laboratory performed analysis of total carbon presence by weight by sample combustion in a muffle furnace. This method converts organic and inorganic substances into gases, which are then detected and measured by thermal conductivity/IR detection using a CN Analyzer (Leco Corporation TruSpec; Association of Analytical Communities, 2006). Carbon concentrations were calculated specific to the sample, section, and the entire SD tree.

Tree and section specific properties were calculated by weighting the density and carbon concentration of the component samples by the proportion (by volume) of the four tissue types measured at sampling: intact wood, decayed wood, excavated wood (i.e. galleries) and bark. Total bark-off tree volumes were calculated from measured diameter and height, using taper equations for mixed conifer species in the Sierra Nevada (Biging, 1984; Wensel and Olson 1995). If the bole was broken and live tree height unknown, height was regressed from DBH using coefficients specific to BFRS (Holmen, unpublished data, 1990). Bark volume was added to the tapered tree forms according to each section's volume, field measured bark thickness (nearest 0.1mm), and observed bark presence (nearest 5%). The volume of SD trees that did not conform to a tapered shape was calculated by direct measurement. Finally, total SD volume was allocated to each section and to each tissue type based on the section measurements and radial transects described above. The properties of samples from each tissue type were then assigned to the total volume according to the proportion represented. The final result is a whole tree estimate of carbon concentration (%) and biomass density (g cm-3). Net carbon density (g cm-3 of carbon) was calculated as the product of carbon concentration and biomass density. We also report the ratio of dead tree to live tree density (aka density reduction factor, Harmon et al., 2008). In our calculation, we used our measured dead tree densities (wood and bark) and the live wood and bark densities reported in Miles and Smith (2009). Calculated whole tree properties include both wood and bark. Measures and ratios of density, carbon concentration, and net carbon density were completed on all species. They were summarized across all species and by taxonomic group on the basis of phylogenetic relationship and similar allometry (Jenkins et al., 2003). All reported ratios are calculated for a live bole of the same form and volume; i.e. bole breakage and bark loss do not contribute to lower density ratios.

2.4 Analysis of patterns in SD trees

To examine the effect of species and size on density ratio, we used linear mixed effects analyses (Crawley, 2002; R Core Team, 2014). A mixed effects approach enabled us to describe how the properties of the sampled population differed by species and size, while controlling for the effects of each tree's assigned decay class. The response variables examined were dead:live density ratio and dead:live carbon concentration ratio. Since we expected that trees in different decay classes would inherently vary in their ratios (Harmon et al., 1986; Yatskov, 2003), we controlled for this variation by including decay class in the models as a random effects parameter. Fixed effects parameters were species and surface area to volume ratio (SA:V) (Whittaker and Woodwell, 1967) and species identity was treated as a categorical "dummy variable" for purposes of comparison. Surface area was determined by treating SD trees as smooth-barked conic frustums, with the large diameter measurement at 0-30 cm above ground and the upper diameter at the highest intact point (Whittaker and Woodwell, 1968). Parameter estimates for the linear mixed effects model were calculated using restricted maximum log-

likelihood (REML; Pinheiro et al., 2014). The basis for comparison was white fir, the most common tree species in the mesic mixed conifer forest (FIA Database, 2009).

To examine the importance of stem position on biomass density and carbon concentration, we performed two separate linear mixed effects analyses, with dead:live density ratio and dead:live carbon concentration ratio as response variables. For both models, the sole fixed effects parameter was section (base, middle, or top). The base was compared to middle and top sections because it is in contact with soil fungi and moisture, known factors in promoting decay (Maser and Trappe, 1984). Because each individual SD tree was expected to vary in its properties, tree ID was included in the models as a random intercept. Only trees with two and three sections were included in the analysis (n=103 trees, 251 sections).

For measures of SD tree properties (density, carbon concentration, and net carbon density), we calculated standard errors from whole SD tree values. Measurement uncertainties related to simple and precise measures of length, diameter, and volume are expected to be less than 2% and are not reported. For density and carbon concentration, standard errors of mean whole-tree properties are reported. The uncertainty of SD net carbon density was generated by resampling from 10,000 replications of the analyzed trees (n=76) in a Monte Carlo simulation approach (Liu, 2001). All statistical analyses were conducted in R version 3.1.2 (R Core Team, 2014).

2.5 Carbon stock estimates for California mixed conifer forests

We applied our SD reduction factors to a population of SD trees in the mixed conifer forests in California. FIA plots were geographically selected within the Mediterranean California Mesic Mixed Conifer Forest and Woodland type of the 2008 LANDFIRE existing vegetation type map (USGS, 2008). Year of FIA survey ranged from 2001-2009. Stocks were calculated using three methods: with no decay adjustments applied, with the decay ratios employed by the FIA Program (O'Connell et al., 2014) applied, and with the species and decay class specific ratios developed in this study for density and carbon applied. We then compared the three estimates. For tree species and decay classes not represented in our sample, we used the current FIA SD density and carbon ratios (O'Connell et al., 2014; Harmon et al., 2011).

3. RESULTS

3.1 Standing dead trees sampled

Our sample of 107 standing dead trees ranged from 13.3 to 126.7 cm DBH, with 103 (95%) of trees between, 20 cm and 100 cm DBH (Table 1). Sampling slightly favored trees in advanced decay (classes 3, 4, and 5) with 22 individuals in class 3, 31 in class 4 and 17 in class 5. The average tree was represented by 5 measured samples of wood and bark. Not all combinations of species and size were obtainable in our study locations. Class 2 Douglas-fir and class 1 incense cedar were absent. Due to limitations on destructive sampling in long term forest demography plots, availability of red fir was limited to classes 1, 2, and 4 (Table 1).

Table 1. Standing dead (SD) tree characteristics by species, decay class, and diameter class

Species	Decay class (n)					Diameter class (cm DBH)			Total SD trees
	1	2	3	4	5	12.5-30	30-50	>50	
White fir	5	6	4	10	4	10	10	9	29
Red fir	6	3	0	1	0	4	3	3	10
Incense cedar	0	4	6	3	3	10	5	1	16
Sugar pine	6	1	4	2	2	3	6	6	15
Ponderosa pine	3	1	6	8	5	5	14	4	23
Douglas-fir	4	0	2	7	3	4	6	6	16
All species	24	15	22	31	17	36	44	29	109

3.2 Change in SD tree properties by decay class

3.2.1 Carbon concentration

Mean carbon concentration among trees in all decay classes and species was 52.3%, and ranged from 50.1% to 57.2%. Three hundred seventy-six samples from 76 trees were analyzed. Carbon concentration increased from a mean of 51.4% in all decay class 1 individuals (n=11) to 53.7% in all class 5 individuals (n=14). Similarly, dead:live carbon concentration ratios increased slightly from 1.03 to 1.07, using 50% carbon as the basis for comparison in all live trees (Fig. 2, Table A1). All species showed consistent gains in carbon concentration of 2-6% when comparing class 1 to class 5 trees, but except for true firs, gains were not smoothly distributed by decay class.

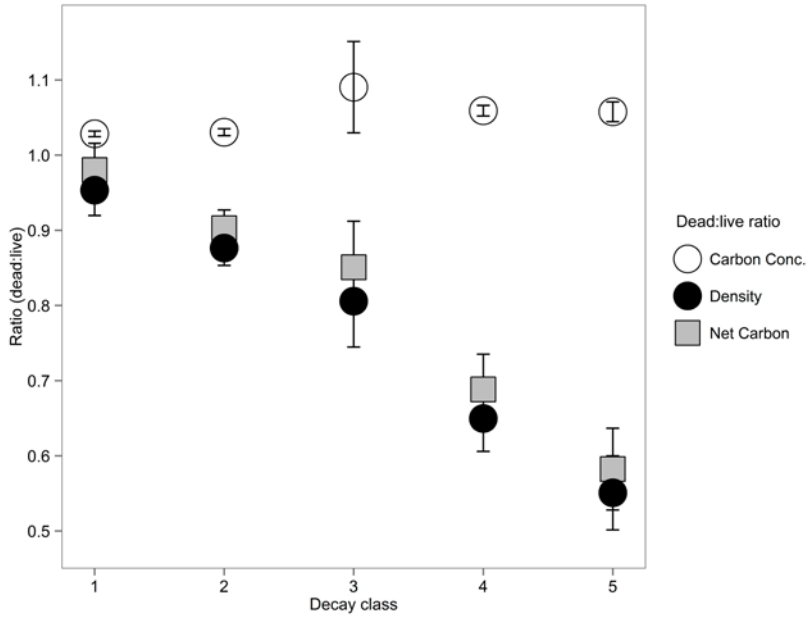

Figure 2
Standing dead tree properties (carbon concentration, density, and net carbon density) relative to live properties for each decay class. Ratios are mean standing dead value: mean live value (Miles and Smith 2009). Density values are from measured SD trees (n=107); carbon concentration and net carbon density values from SD trees (n=76) resampled from Monte Carlo replications. Error bars represent the standard error for all measurements.

3.2.2 Whole-stem density

Whole-stem SD tree density (wood and bark combined in field-measured proportions) declined precipitously as decay class advanced (Fig. 2, Table A1). On average, trees in class 1 had 5% lower density than live trees and a dead:live density ratio of 0.95. Decay classes 2 through 4 then demonstrated progressively lower densities, with a mean difference between decay classes of 10.1%. Trees in class 5 had lost 45% of mean live density (Table A1). Among all individuals, mean SD tree density was 0.29 g cm-3, and ranged (min-max) from 0.04 g cm-3 to 0.44 g cm-3. In a pool of live trees of the same species, size, and bark proportion, mean density would be expected to be 0.38 g cm-3. Density loss patterns varied among tree taxonomic groups. For firs and pines, density declined with decay class (Fig. 3). For example, in class 5, the most advanced decay condition, white fir had only 43% of live density and ponderosa pine had 52%. Incense cedar was the exception to this trend. Though density of all SD cedar was consistently lower than the known live cedar density of 0.35 g cm^{-3}, mean SD cedar density was essentially unchanged as decay class advanced, from 0.28 ± 0.02 g cm^{-3} (mean ± standard error) in class 2 trees to 0.30 ± 0.03 g cm^{-3} in classes 4 and 5 (Fig. 3b; species detail in Tables A1 and A2).

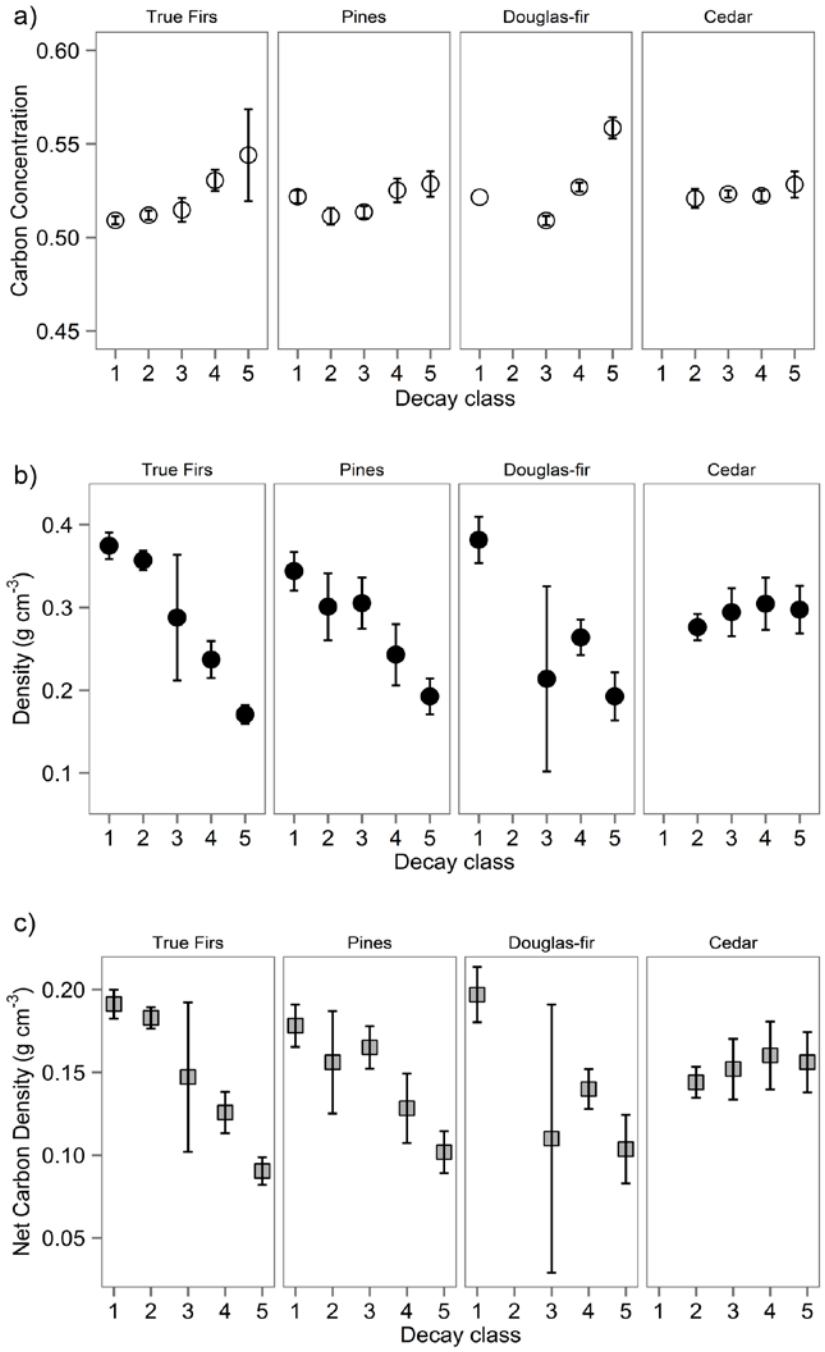

Figure 3
Standing dead tree properties for taxonomic groups by decay class: a) carbon concentration, n = 76, b) density (g cm^{-3}), n=107, and c) net carbon density (g cm^{-3}). In a) and b), values are means of all trees in the group and error bars are standard errors. In c), means and standard error are generated by resampling from 10000 Monte Carlo replicates of the analyzed trees. True firs include white and red fir, pines include sugar and ponderosa pine.

3.2.3 Net carbon density

The net carbon density generally tracked whole-stem SD tree density. However, increased carbon concentration did attenuate density losses to some extent (Fig. 3c). The mean net carbon density ratio among all classes of analyzed SD tree was 0.76 ± 0.29, 3.2% higher than density alone at 0.73 ± 0.03. For class 5 SD trees, mean net carbon density ratio was 0.60 ± 0.06, or 60% of live tree carbon density. Within each tree species, the net carbon density also tracked density losses very closely. Species-level net carbon ratios values were typically 0-6% above the dead:live density ratios (Table A1).

3.2.4 Differences in wood and bark decay patterns

The physical and chemical properties of wood and bark differed, with bark showing overall smaller declines in density with decay class, implying greater resistance to decay than wood (Table 2). As decay class advanced, carbon concentration increased 2-4% in both wood and bark. As in live trees, bark maintained higher carbon concentrations (2.58%) for all species and decay classes. Mean wood density showed larger differences among decay classes, moving from a dead:live density ratio of 0.90 ± 0.04 in all class 1 trees to 0.53 ± 0.05 in class 5 trees. Again the exception to the trend was incense cedar. Its spongy, layered bark was lower in density than wood and its density did not progressively decrease with decay class.

Table 2

Wood and bark properties compared. Mean standing dead:live density ratio and mean carbon concentration for each decay class 1W-5W, wood, and 1B-5B, bark. Standard errors are for tree-level means of all individuals analyzed. Species values are listed separately in the Appendix.

Decay class	Dead:live* density ratio	n	Carbon concentration	n
1 W	0.90 (0.04)	24	0.51 (0.00)	11
2 W	0.84 (0.03)	15	0.51 (0.00)	10
3 W	0.81 (0.06)	22	0.51 (0.00)	14
4 W	0.62 (0.05)	30	0.52 (0.00)	27
5 W	0.53 (0.05)	16	0.53 (0.01)	14
Decay class	Dead:live* density ratio	n	Carbon concentration	n
1 B	1.17 (0.06)	24	0.53 (0.00)	11
2 B	1.01 (0.04)	15	0.53 (0.00)	10
3 B	0.96 (0.06)	21	0.53 (0.00)	13
4 B	0.92 (0.04)	27	0.55 (0.00)	25
5 B	0.87 (0.08)	10	0.57 (0.01)	9

*Live density, Miles and Smith 2009. All other data this study.

Parenthetical values are standard errors

3.3 Factors in changing SD tree density and carbon concentration

To examine the characteristics of SD trees that predict density and carbon loss, we used linear mixed effects models with species and size (measured as the surface area: volume ratio, SA:V) as fixed effect parameters and decay class included as a random effect parameter. Neither species nor SA:V proved to be a significant predictor of dead:live carbon concentration ratio across species (Table 3a). Species identity did have a significant effect on dead:live density ratio (Table 3b). However, compared to white fir, which had a dead:live density ratio of 0.61 ± 0.08, only incense cedar and red fir were statistically distinguishable; both were higher in density. Pine species and Douglas-fir had density ratios similar to that of white fir. Individual tree size was also a positive and significant predictor of dead:live density ratio (Table 3b). Inspection of residual plots showed that the model was consistent with assumptions of homoscedasticity and normality.

Table 3

a) Summary of the linear mixed-effect model explaining variation in dead:live carbon concentration ratio

Explanatory Variable	Estimate	SE	t value	p value
Intercept (white fir)	1.057	0.012	86.845	0.0000***
Red fir	-0.020	0.012	-1.653	0.1031
Incense cedar	-0.002	0.011	-0.197	0.8441
Sugar pine	-0.016	0.011	-1.469	0.1467
Ponderosa pine	-0.005	0.010	-0.492	0.6247
Douglas-fir	0.007	0.010	0.711	0.4797
Surface:Volume	-0.022	0.022	-0.975	0.3332

Parameter estimates are given as contrasts with white fir as the intercept. Model controls for decay class by including it as a random intercept.

Significance codes: < 0.001 *** / < 0.01 ** / < 0.05 *

b) Summary of the linear mixed-effect model explaining variation in dead:live density ratio

Explanatory Variable	Estimate	SE	t value	p value
Intercept (white fir)	0.610	0.078	7.772	0.0000***
Red fir	0.214	0.077	2.785	0.0064**
Incense cedar	0.198	0.065	3.061	0.0029**
Sugar pine	0.090	0.065	1.384	0.1697
Ponderosa pine	0.062	0.057	1.083	0.2816
Douglas-fir	-0.067	0.065	-1.039	0.3012
Surface:Volume	0.250	0.126	1.986	0.0498*

Parameter estimates are given as contrasts with white fir as the intercept. Model controls for decay class by including it as a random intercept.

Significance codes: < 0.001 *** / < 0.01 ** / < 0.05 *

3.4 Importance of position within individual trees

Within individual SD trees, both the carbon concentration and density of tissues differed with position along the bole, as demonstrated in a linear mixed effects analysis (Table 4). For SD trees with two or more sections (103 trees and 251 sections), the dead:live carbon concentration ratios of both top and middle sections were significantly different from the base section (top: $p<0.01$, middle: $p<0.01$). Mean carbon concentrations were highest in the base (dead:live carbon concentration ratio = 1.055 ± 0.004) and top (1.042 ± 0.005) sections, and lowest in the middle (1.033 ± 0.007). Density also varied with position. Top sections had the lowest density ratios overall (0.748 ± 0.030, $p<0.001$) followed by middle sections (0.839 ± 0.031, $p<0.01$), with the highest density ratios found from 0-2 m (base dead:live density ratio = 0.883 ± 0.034, $p<0.001$).

Table 4

a) Summary of the linear mixed-effect model explaining variation in section dead:live carbon concentration ratio

Explanatory Variable	Estimate	SE	t value	p value
Base (intercept)	1.055	0.004	239.059	0.0000***
Middle	-0.022	0.007	-3.196	0.0019**
Top	-0.013	0.005	-2.714	0.0079**

Parameter estimates are given as contrasts with the base (0-2m) section as the intercept. Tree ID was included as a random intercept.

Significance codes: < 0.001 *** / < 0.01 ** / < 0.05 *

b) Summary of the linear mixed-effect model explaining variation in section dead:live density ratio

Explanatory Variable	Estimate	SE	t value	p value
Base (intercept)	0.883	0.031	28.876	0.0000***
Middle	-0.135	0.042	-3.237	0.0015**
Top	-0.140	0.032	-4.395	0.0000***

Parameter estimates are given as contrasts with the base (0-2m) section as the intercept. Tree ID was included as a random intercept.

Significance codes: < 0.001 *** / < 0.01 ** / < 0.05 *

For all sections of the bole, mean dead:live density ratio declined with decay class. The distribution of density ratios had a strongly peaked distribution in early stages of decay (Fig. 4). For classes 1-3 standard error of the mean was 0.022 and kurtosis = 3.41, and distributions were centered only slightly lower than live trees (dead:live ratio = 1.0; Joanes and Gill 1998). In classes 4 and 5, all section density ratios were comparatively lower (skewed left relative to the overall mean) and more platykurtic, or evenly distributed (SE = 0.029, kurtosis = -0.09). This shift in density distribution during advanced decay was especially apparent in top sections (mean = 0.539, SE=0.05, kurtosis = -0.98).

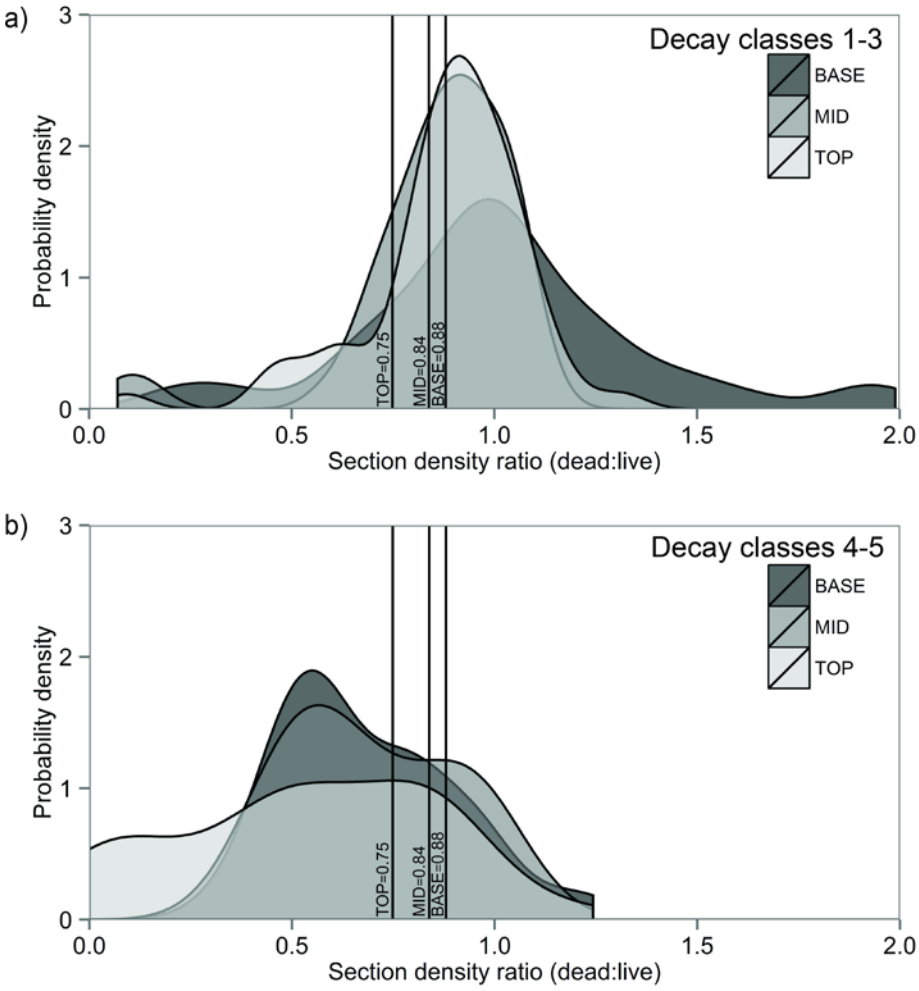

Figure 4
Combined wood and bark density of each section (base, mid, and top) for a) decay classes 1-3 and b) decay classes 4 and 5. Probability density distributions are displayed using a smoothing kernel. The classes 1-3 and classes 4-5 distributions are shown relative to mean section density ratios for decay classes 1-5 (vertical lines): base=0.88, mid=0.84, and top=0.75.

3.5 Regional implications of change in SD tree properties

For the final component of the study, we examined the regional implications of SD tree decay for estimates of aboveground carbon stocks. We compared three stock estimation approaches. The first approach generated an estimate adjusted for the changes in net carbon density as reported above. The second adjusted for changes in net carbon density using the FIA's current density and carbon ratios for mesic mixed conifer forests (Table A4; O'Connell et al, 2014), and the third approach generated an estimate with unchanged wood and bark properties, as previously implemented in continental-scale inventories (Table 5, EPA 2011; Woudenberg et al., 2010). SD tree information (volume, species, and decay class) came from 661 plots in California mesic mixed conifer forests (FIA Database, 2009; USGS, 2008). In these forests, SD tree volume was dominated by white fir, which totaled 2801 m3 and 37.5% of overall SD tree volume. Following in importance were Douglas-fir and sugar pine. The six focal species accounted for 90.8% of total SD volume (6778 of 7465 m3). Mesic mixed conifer forests, California's single most extensive forest type, had a total live aboveground carbon of 117 Mg ha-1 and occupied a land area of 2.15 million ha, or 5.3% of the state's total land area (Fig.1; FIA Database, 2009; USGS, 2008). The decay-adjusted carbon stock of SD trees in mesic mixed conifer forests using both density and carbon ratios was 9.46 Mg C ha-1; the statewide total is 20.33 Tg. Accounting for

decay using current FIA density ratios and 50% carbon results in slightly lower estimates: 9.42 Mg C ha-1 and 20.25 Tg statewide. Compared to this study's standing dead:live ratios, the FIA density ratios applied higher SD tissue densities at lower carbon concentration (Table A4). In both cases, the decay-reduced SD tree stock was about 8% of aboveground live carbon. Using an unadjusted approach yielded a higher stock estimate: SD trees then accounted for 11.16 Mg C ha-1 and a statewide total of 23.98 Tg. The difference in total carbon stock between the estimate using decay adjustments based on our measurements and the estimate with no decay adjustment was 3.66 Tg. Similarly, FIA decay ratios yielded a total carbon stock that was 3.74 Tg lower than the estimate without decay adjustment. Thus, when compared to available methods that incorporate change due to decay, omitting changes in net carbon density yielded an 18.0-18.45% overestimate of the SD tree carbon stock (Table 5).

Table 5

Carbon in standing dead (SD) trees of California mesic mixed conifer forests. Stock estimates use three alternative methods to quantify decay: no adjustment, density and carbon ratios per FIA (O'Connell et al., 2014), and density and carbon ratios per this study. Differences are by comparison to the "no adjustment" method.

	Carbon ha^{-1}	Total SD carbon	C stock difference vs. no adjustment	% C stock difference vs. no adjustment
No adjustment in wood/bark properties	11.16 Mg	23.98 Tg	NA	NA
Density and carbon ratios per FIA	9.42 Mg	20.25 Tg	-3.74 Tg	+18.45%
Density and carbon ratios per this study	9.46 Mg	20.33 Tg	-3.66 Tg	+18.0%

4. DISCUSSION

4.1 Loss of carbon density: theme and variations among taxa

Our findings emphasize that as SD trees advance through the five structural classes widely used to classify decay, they progressively lose carbon. We have described this pathway of decay by the first in situ sampling of multiple species at all stages of decay and by characterizing the changing properties common to standing mixed conifer species specifically.

Across the major mixed conifer species, gradual loss of carbon density is the dominant pattern. SD trees in the most advanced stage of decay (class 5) have about half of the density of live trees. The pattern and extent of declining density in SD trees seen here is consistent with the losses previously observed in SD conifer species. The resulting dead:live ratios also closely match the ratios now implemented by the FIA program (Harmon et al., 2011; O'Connell et al., 2014). As in earlier studies, the SD trees we observed also have higher density than DWM in the same decay class and taxonomic group (Harmon et al, 2011). We attribute the density change in

SD trees primarily to fungal decomposers and breakdown by invertebrates, as has been well established in previous work (Graham, 1925; Harmon et al., 1986; Swift, 1977). The carbon concentration gains we observed over the full course of decay also match the increases seen across northern hemisphere gymnosperm DWM, and the increases in decay classes 3-5 continue the nascent pattern seen in early-stage SD trees (Harmon et al., 2013). The gradual increase of carbon with decay class is likely caused by the activity of brown-rot fungi, which digest hemicellulose and cellulose, leaving behind tissues enriched in comparatively more carbon dense lignin (Gilbertson, 1980). When effects of the two opposing trends are combined, the decline in net carbon density of SD trees is very similar to the decline in whole tree density; the effect of climbing carbon concentration is small by comparison.

The differences in density and carbon concentration we observed in of all SD trees were comparable to the differences reported among live trees (Lamlom and Savidge, 2003; Miles and Smith, 2009). Incense cedar was exceptional among these six species in that its carbon density did not exhibit a directional change with decay class. One explanation for this anomaly may be that incense cedar is abundant in phenolic extractives that inhibit fungi, making it is extremely decay resistant (McDonald, 1973; Scheffer and Cowling, 1966). Even on the forest floor, it maintains high density well into advanced decay stages (Harmon et al., 1987). Furthermore, the predominant cause of death for incense cedar at BFRS is snow or storm breakage (Schurr, 2005). The resultant broken boles are assigned to decay class 3 or 4 on the basis of their form (USFS, 2010), but have no concomitant loss in density. These characteristics suggest that incense cedar's wood traits, allometry, and mortality all have roles in shaping its distinct decay pathway.

4.2 Attributes of SD trees affecting carbon loss

4.2.1 Size and species

Species identity and SA:V, an expression of tree size, were both significant determinants of dead:live density ratio in SD trees. Past studies of decay in DWM have found that although size and decay rate are often negatively correlated (Mackensen et al., 2003; Zell et al., 2009) the relationship of diameter and decay is not always apparent (Radtke et al., 2009). In studies that consider SA, however, both standing and down boles with greater SA have been shown to decay more quickly (Graham and Cromack, 1982). We also observed this pattern. SA:V quantifies the tree's interface that is prone to fungal attack and available for exchange of water and nutrients; it is also tied to other functional relationships (Whittaker and Woodwell, 1967). For example, in surface fuels, SA:V is directly proportional to the quantity converted to gas during flaming combustion (Rothermel, 1983). Our model suggests that for decaying SD trees, SA:V is a more ecologically relevant expression of size than DBH. Size is also a key attribute of SD trees because individuals that stay standing into advanced decay classes are often remnants of very large trees that have a high proportion of heartwood. These remnants have shed some or all of their readily decomposable parts (bark, branches, sapwood) and therefore do not decline in carbon density as steeply as they would if measured in their entirety (Harmon et al., 1987, Yatskov et al., 2003).This is a unique feature of SD trees as compared to DWM and fuels-focused measurements. Because they are handled as individual trees in inventory, it is important to address SD trees' whole-tree properties on the same basis.

4.2.2 Within-tree position

Wood and bark properties vary substantially within an individual, both in live and dead trees (Bowyer et al., 2007; Forest Products Laboratory, 2010). To determine whether the vertical position of wood and bark along the standing bole is important to its decay condition, in our dimensional analysis we sampled the lowest 2 m of the bole and one to two upper sections, dependent on total size. Decomposition agents including root pathogens can readily spread into a tree's base even while the tree is alive (Scharpf, 1993). We therefore expected that contact with the moisture and mycelia of the forest floor would lead to increased decay rates (Harmon et al., 1986) and consequently to larger change in wood and bark properties at the base of SD trees. However, decay rates are also expected to decrease from the base to the top, because the proportion of decay-resistant heartwood decreases with height (Harmon et al., 1986; Hillis, 1977) and because weathering and breakage makes treetops susceptible to rot (Cline et al., 1980). In the trees we sampled with more than two sections, top sections showed the greatest difference from mean live tree density and carbon concentration. This was contrary to our hypothesis, but consistent with underlying tree anatomy. Conifers typically have higher wood density and carbon concentrations at the base (Bowyer et al., 2007), so it appears that the vertical gradients in live trees also hold true in SD trees, despite basal contact with soil and their lack of active defenses. This habit may vary in different forest communities and climates, dependent on the specific agents of decay. In particular, the properties of SD trees in regions where root pathogens are a more common cause of mortality warrant further study.

Both vertical and radial gradients of wood properties have important implications for use of deadwood in forest carbon inventory. Our observations show that it is essential to account for vertical position in determining overall tree tissue condition. Full discs or bark to pith samples are already known to be important for capturing radial variation (Williamson and Wiemann, 2010). But especially for SD trees, the height of the tissue is also relevant to its condition. Continuing work on the radial and longitudinal patterns of density in live trees (i.e. Chave et al., 2009; Wiemann and Williamson, 2014) is a key part of understanding decay patterns, and can offer further gains in the precision and predictability of deadwood inventory.

4.3 Utility of SD tree characteristics for describing ecological patterns

A simple five class system cannot hope to describe the immense range of forms and decay conditions that SD trees exhibit. The widely implemented FIA decay classification system, which categorizes the structural changes in SD trees, was developed on the basis of a single species, Douglas-fir (Thomas et al., 1979; USDA Forest Service, 2010). Despite its limitations, this system was a very effective means of summarizing SD tree properties for California mixed conifer species. Though the classes were not free from overlap, the progress of carbon loss paralleled the visible structural changes quite well. The decay patterns of SD trees also showcase the potential of FIA decay class as a synthetic ecological indicator. Since a wide variety of SD tree and DWM attribute data is now available at continental scale, FIA's decay classification system, already in wide use, may prove a useful proxy for developing models of forest carbon fluxes and resultant GHG emissions (Domke et al., 2013; Woodall et al., 2013). Because decay class is consistently applied in periodic inventories (Woudenberg et al., 2010), static decay class attributes such as reported here can help improve accuracy of both field-based biomass accounting and estimates of biomass change that use a stock change approach (Domke et al., 2013; EPA, 2015; Woodall et al., 2012).

Understanding SD tree decomposition dynamics also helps connect local decay patterns to synoptic ones, strengthening the linkages between real and modeled ecosystems. The SD trees in California's mesic mixed conifer forests generally follow a globally recognized relationship: the plants that share wood and bark traits also share the same decay trajectories (Cornwell et al., 2009). Note, however, that the underlying cause of similar density loss patterns is probably not a simple matter of their similar live wood densities. Instead, shared allometry, functional traits, and life history are more likely drivers of decay trajectories at a grander scale (Chambers et al., 2000, Weedon et al., 2009). Factors in mortality can also predispose certain species to particularly distinctive decay patterns. Examples are the top breakage seen in incense cedar (Shurr, 2005); species resistant to windthrow such as yellow birch (Betula alleghensis), sugar maple (Acer saccharum), and giant sequoia (Canham et al., 2001; York and DeVries, 2013), and the inside-out decomposition of species susceptible to heart rots (i.e. Acacia mangium; Barry et al., 2004). To best reflect the variability of forest ecosystems, species with such distinct decay trends may warrant species-specific decay ratios. Even considering these special cases, widely shared allometric and life history patterns have the potential to serve as the basis for new models of decay processes and carbon transfer, and can help reduce uncertainty in forest process models (Domke et al., 2011; Hilger et al., 2012).

There are some pertinent ecosystem characteristics that our study of decay patterns in SD trees cannot address. Decay class is not necessarily tied to SD tree age or expected longevity, so it is not an informative measure of time since death (Angers et al., 2011; Angers et al., 2012; Waskiewicz, 2007). Therefore differences in properties described here apply to trees with characteristic structures that are the result of decay, but should not be conflated with decay rates. Demographic studies of SD trees, i.e., measures of longevity, fall rates, and associated decay classification, are needed to parameterize the decay rates, carbon residence times, and the expected GHG flux of SD trees (Hilger et al., 2012; Keen, 1955; Raphael and Morrison, 1987). SD tree vital rates vary with species, region, and site, and are also important in influencing the trajectory of forest emissions (Hilger et al., 2012, Morrison and Raphael 1993, Ritchie et al., 2013).

4.4 Implications for measurement and management of changing forests

Accurately accounting for SD carbon is increasingly important, as the abundance of SD trees in mixed conifer and other forest ecosystems is rapidly increasing (Allen et al., 2010; van Mantgem et al., 2009). Rising rates of mortality will supply an increasing quantity of SD trees for future decomposition. The progressive loss of biomass from SD trees will shape carbon transfer rates, potentially influencing biogeochemical and global change processes across time and scale (Friend et al., 2014; Hilger et al., 2012). As standing decay is incorporated into forest carbon inventories and mortality rates climb, greenhouse gas regulated sectors can expect to face lower caps on allowable emissions. Decay patterns and processes are of particular concern in mixed conifer forests, where past forest management and changing climate have also substantially reshaped forest structure (Collins et al., 2011; McIntyre et al., 2015). SD trees are not only becoming more abundant, but are also smaller on average and more dispersed than in historical accounts (Knapp, 2015; Stephens and Moghaddas, 2005). In mixed conifer forests under long term fire suppression, SD trees have higher spatial density and lower average size (Stephens, 2004; Stephens and Moghaddas, 2005). This arrangement of SD trees also increases the risk of

fire spread (Brown et al., 2003). According to our results, these patterns will translate to rising carbon losses from SD trees and also growing importance of SD trees to land managers.

Adjusting carbon density to account for decay provides a lower and a more realistic estimate of standing carbon in California mixed conifer forests. Our measurements of standing trees serve as a comprehensive test of the SD density ratios used by the FIA program, and we find them largely in agreement for these six species. The difference between decay-adjusted and unadjusted stock estimates verifies that the use of carbon density ratios has considerably improved the accuracy of carbon accounting for these forests. Therefore, estimates of dead biomass should specifically include SD trees and adjust the physical and chemical properties of their biomass according to decay condition. Closely related species can be likely be grouped on the basis of their shared decay trajectories, but some species are expected to follow disparate patterns and should be treated accordingly. In detailed analysis, the size and position of SD biomass can also be incorporated. Although SD trees decay in a distinct environment and gradually develop properties unlike either live or down dead trees, many species still lack field-based measurements from standing individuals (Harmon et al., 2011, Harmon et al., 2013). Next steps in describing the decay dynamics of SD trees might extend measurement of standing trees, establish baseline demographic rates, and expand to unmeasured species and forest communities. Adding time, climatic, and taxonomic elements to SD decay patterns will further trace the path of living forests toward their fate in the soil and air.

Roles

SC and JB designed the study; SC, JS, RY, and JB selected sites and supervised data collection; SC, JS, and JB analyzed and interpreted data; SC composed the article; RY and JB edited the article. Support for this research was provided by California Energy Commission contract 500-10-046 and California Air Resources Board agreement 10-778. The funding agencies had no involvement in study design or publication.

ACKNOWLEDGEMENTS

The authors gratefully acknowledge those who assisted with sample collection and preparation: D. Swenson, D. Soderberg, E. Olliff, A. Javier, N. Holt, C. Sodergren, E. Blomdahl, and J. Battles. We particularly thank P. Zellner for safely felling trees and K. Somers for assistance with tree selection. Additionally, we are grateful to cooperators A. Das and N. Stephenson of the USGS - Western Ecological Research Station and K. Nydick of the National Park Service for their assistance with research in Sequoia National Park. Comments from S. Stephens and two anonymous reviewers improved the manuscript.

APPENDIX A

Supplementary data associated with this article can be found in Appendix A.

REFERENCES

Aakala, T., Kuuluvainen, T., Gauthier, S., De Grandpre, L., 2008. Standing dead trees and their decay-class dynamics in the northeastern boreal old-growth forests of Quebec. Forest Ecology and Management 255, 410-420.

Aalde, H., Gonzalez, P., Gytarsky, M., Krug, T., Kurz, W.A., Ogle, S., Raison, J., Schoene, D., Ravindranath, N.H, Elhassan, N.G., Heath, L.S., Higuchi, N., Kainja, S., Matsumoto, M., Sánchez, M.J.S., Somogyi, Z., 2006. Forest Land. In Intergovernmental Panel on Climate Change. National Greenhouse Gas Inventory Guidelines. Institute for Global Environmental Strategies, Hayama, Japan.

Allen, C.D., Macalady, A.K., Chenchouni, H., Bachelet, D., McDowell, N., Vennetier, M., Kitzberger, T., Rigling, A., Breshears, D.D., Hogg, E.H., Gonzalez, P., Fensham, R., Zhang, Z., Castro, J., Demidova, N., Lim, J.H., Allard, G., Running, S.W., Semerci, A., Cobb, N., 2010. A global overview of drought and heat-induced tree mortality reveals emerging climate change risks for forests. Forest Ecology and Management 259, 660-684.

Anderegg, W., Kane, J., Anderegg, L., 2012. Consequences of widespread tree mortality triggered by drought and temperature stress. Nature Climate Change 3. DOI: 10.1038/NCLIMATE1635

Angers, V.A., Bergeron, Y., Drapeau, P., 2012. Morphological attributes and snag classification of four North American boreal tree species: Relationships with time since death and wood density. Forest Ecology and Management 263, 138-147

Angers, V.A., Gauthier, S., Drapeau, P., Jayen, K., Bergeron, Y., 2011. Tree mortality and snag dynamics in North American boreal tree species after a wildfire: a long-term study. International Journal of Wildland Fire 20:751-763.

Association of Analytical Communities. 2006. Official Method 972.43. Microchemical Determination of Carbon, Hydrogen, and Nitrogen, Automated Method, in Official Methods of Analysis of AOAC International, 18th edition, Revision 1, 2006. Chapter 12, pp. 5-6, AOAC International, Gaithersburg, MD.

Barry, K.M., Irianto, R.S.B., Santoso, E., Turjaman, M., Widyati, E., Sitepu, I., Mohammed, C.L., 2004. Incidence of heart rot in harvest-age Acacia mangium in Indonesia, using a rapid survey method. Forest Ecology and Management 190, 273-280

Battles, J.J., Gonzalez, P., Robards, T., Collins, B.M., Saah, D.S., 2014. Final Report: California Forest and Rangeland Greenhouse Gas Inventory Development. California Air Resources Board Agreement 10-778. http://www.arb.ca.gov/research/apr/past/10-778.pdf

Battles, J.J., Robards, T., Das, A., Stewart, W., 2009. Projecting climate change impacts on forest growth and yield for California's Sierran mixed conifer forests. California Climate

Change Center, March 2009. CEC-500-2009-047-D; prepared for the California Energy Commission.

Bentz, B.J., Régnière, J., Fettig, C.J., Hansen, E.M., Hayes, J.L., Hicke, J.A., Kelsey, R.G., Negrón, J.F., Seybold, S.J., 2010. Climate Change and Bark Beetles of the Western United States and Canada: Direct and Indirect Effects. BioScience 60, 602-613.

Bergman, R., 2010. Drying and Control of Moisture Content and Dimensional Changes. Chapter 13 in Forest Products Laboratory (Ross, R. J.) 2010. Wood handbook : wood as an engineering material. Centennial ed. General Technical Report FPL ; GTR-190. Madison, WI : U.S. Dept. of Agriculture, Forest Service, 2010: 1 v

Biging, G.S., 1984. Taper Equations for Second-Growth Mixed Conifers of Northern California. Forest Science 30:1103-1117.

Birdsey, R.A., 1992. Carbon storage and accumulation in United States forest ecosystems. Gen. Tech. Rep. WO-59. Washington, DC: U.S. Department of Agriculture, Forest Service. 51 p.

Boddy, L., 2001. Fungal community ecology and wood decomposition processes in angiosperms: from standing tree to complete decay of coarse woody debris. Ecological Bulletins 49: 43-56.

Bowyer, J.L., Shmulsky, R., Haygreen, J.G., 2007. Forest Products and Wood Science, an introduction. 5th ed. Blackwell Publishing, Ames, IA.

Brown, J.K., Reinhardt, E.D., Kramer, K.A., 2003. Coarse woody debris: managing benefits and fire hazard in the recovering forest. USDA For. Serv. Gen. Tech. Rep. RMRS-GTR-105.

Bytnerowicz, A., Omasa, K., Paoletti, E., 2007. Integrated effects of air pollution and climate change on forests: a northern hemisphere perspective. Environmental Pollution 147.3, 438-445.

Chambers J.Q., Higuchi, N., Schimel J.P., Ferreira, L.V., Melack J.M., 2000. Decomposition and carbon cycling of dead trees in tropical forests of the central Amazon. Oecologia, 122, 380–388.

Canham, C.D., Papaik, M.J., Latty, E.F., 2001. Interspecific variation in susceptibility to windthrow as a function of tree size and storm severity for northern temperate tree species. Canadian Journal of Forest Research 31, 1–10. DOI: 10.1139/cjfr-31-1-1

Caprio, A.C., Swetnam, T.W., 1993. Historic fire regimes along an elevational gradient on the west slope of the Sierra Nevada, California. USDA Forest Service Gen. Tech. Rep. INT-GTR-320.

Chave, J., Coomes, D., Jansen, S., Lewis, S.L., Swenson, N.G., Zanne, A.E., 2009. Towards a worldwide wood economics spectrum. Ecology Letters 12, 351-366.

Cline, S.P., Berg, A.B., Wight, H.M., 1980. Snag Characteristics and Dynamics in Douglas-Fir Forests, Western Oregon. Journal of Wildlife Management 44, 773-786.

Collins B.M., Everett, R.G., Stephens, S.L., 2011. Impacts of fire exclusion and recent managed fire on forest structure in old growth Sierra mixed-conifer forests. Ecosphere 2:art51. doi: 10.1890/ES11-00026.1

Cornwell, W.K., Cornelissen, J. H.C., Allison, S.D., Bauhus, J., Eggleton, P., Preston, C.M., Scarff, F., Weedon, J.T., Wirth, C., Zanne, A.E., 2009. Plant traits and wood fates across the globe: rotted, burned, or consumed? Global Change Biology 15, 2431-2449.

Crawley, M.J., 2002. Statistical Computing: An Introduction to Data Analysis using S-Plus. Wiley, Hoboken, NJ. 772 pp.

Das, A., Battles, J., Stephenson, N., van Mantgem, P., 2007. The relationship between tree growth patterns and likelihood of mortality: a study of two tree species in the Sierra Nevada. Canadian Journal of Forest Research 37, 580-597.

Domke, G.M., Woodall, C.W., Smith, J.E., 2011. Accounting for density reduction and structural loss in standing dead trees: implications for forest biomass and carbon stock estimates in the United States. Carbon Balance and Management 6:14.

Domke, G.M., Woodall, C.W., Walters, B.F., Smith, J.E., 2013. From Models to Measurements: Comparing Downed Dead Wood Carbon Stock Estimates in the U.S. Forest Inventory. PLoS ONE 8, e59949.

Fahey, T.J., Siccama, T.G., Driscoll, C.T., Likens, G.E., Campbell, J., Johnson, C.E., Battles, J.J., Aber, J.D., Cole, J.J., Fisk, M.C., Groffman, P.M., Hamburg, S.P., Holmes, R.T., Schwarz, P.A., Yanai, R.D., 2005. The Biogeochemistry of Carbon at Hubbard Brook. Biogeochemistry 75, 109-176.

Forest Products Laboratory, 2010. Wood handbook—Wood as an engineering material. General Technical Report FPL-GTR-190. Madison, WI: U.S. Department of Agriculture, Forest Service, Forest Products Laboratory. Robert Ross, Editor. 508 p.

Forest Inventory and Analysis Database, 2009. FIADB 5.1. Available: http://apps.fs.fed.us/fiadb-downloads/datamart.html.

Fowler, D., Cape, J., Coyle, M., Flechard, C., Kuylenstierna, J., Hicks, K., Derwent, D., Johnson, C., Stevenson, D., 1999. The global exposure of forests to air pollutants. Water Air and Soil Pollution 116, 5-32.

Franklin, J.F., Shugart, H.H., Harmon, M.E., 1987. Tree death as an ecological process. BioScience 37, 550-556.

Friend, A.D., Lucht, W., Rademacher, T.T., Keribin, R., Betts, R., Cadule, P., Ciais, P., Clark, D.B., Dankers, R., Falloon, P.D., Ito, A., Kahana, R., Kleidon, A., Lomas, M.R., Nishina, K., Ostberg, S., Pavlick, R., Peylin, P., Schaphoff, S., Vuichard, N., Warszawski, L., Wiltshire, A., Woodward, F.I., 2014. Carbon residence time dominates uncertainty in

terrestrial vegetation responses to future climate and atmospheric CO2. Proceedings of the National Academy of Sciences 111, 3280-3285.

Ganey, J.A., Vojta, S.C., 2011. Tree mortality in drought-stressed mixed-conifer and ponderosa pine forests, Arizona, USA. Forest Ecology and Management 261, 162–168.

Gilbertson, R.L., 1980. Wood-rotting fungi of North America. Mycologia 72, 1–49.

Gonzalez, P., Asner, G.P., Battles, J.J., Lefsky, M.A., Waring, K.M., Palace, M., 2010. Forest carbon densities and uncertainties from Lidar, QuickBird, and field measurements in California. Remote Sensing of Environment 114, 1561-1575.

Graham, S.A., 1925. The Felled Tree Trunk as an Ecological Unit. Ecology 6, 397-411.

Graham, R.L., and Cromack, K., Jr., 1982. Mass, nutrient content and decay rate of dead boles in rain forests of Olympic National Park. Canadian Journal of Forest Research 12, 511-521.

Hagemann, U., Moroni, M.T., Shaw, C.H., Kurz, W.A., Makeschin, F., 2010. Comparing measured and modelled forest carbon stocks in high-boreal forests of harvest and natural-disturbance origin in Labrador, Canada. Ecological Modelling 221, 825-839.

Harmon, M.E., Cromack Jr, K., Smith, B.G., 1987. Coarse woody debris in mixed-conifer forests, Sequoia National Park, California. Canadian Journal of Forest Research 17, 1265-1272.

Harmon, M.E., Fasth, B., Woodall, C.W., Sexton, J., 2013. Carbon concentration of standing and downed woody detritus: Effects of tree taxa, decay class, position, and tissue type. Forest Ecology and Management 291, 259-267. doi:10.1016/j.foreco.2012.11.046

Harmon, M.E., Franklin, J.F., Swanson, F.J., Sollins, P., Gregory, S.V., Lattin, D., Anderson, N.H., Cline, S.P., Asumne, N.G., Sedell, J.R., Lienkaemper, W., Cromack, K., Jr., and Cummings, K.W. 1986. Ecology of coarse woody debris in temperate ecosystems. Adv. Ecol. Res. 15, 133–302. doi:10.1016/S00652504(08)60121-X.

Harmon, M.E., Woodall, C.W., Fasth, B., Sexton, J., 2008. Woody detritus density and density reduction factors for tree species in the United States: a synthesis. Gen. Tech. Rep. NRS-29. Newtown Square, PA: U.S. Department of Agriculture, Forest Service, Northern Research Station. 84 p.

Harmon, M.E., Woodall, C.W., Fasth, B., Sexton, J., Yatkov, M., 2011. Differences between standing and downed dead tree wood density reduction factors: A comparison across decay classes and tree species. Res. Pap. NRS-15. Newtown Square, PA: U.S. Department of Agriculture, Forest Service, Northern Research Station. 40 p.

Heath, L.S., Smith, J.E., Skog, K.E., Nowak, D.J., Woodall, C.W., 2011. Managed Forest Carbon Estimates for the US Greenhouse Gas Inventory, 1990-2008. Journal of Forestry 109, 167-173.

Hicke, J.A., Meddens, A.J.H., Allen, C.D., Kolden, C.A., 2013. Carbon stocks of trees killed by bark beetles and wildfire in the western United States. Environmental Research Letters 8, 035032. doi: 10.1088/1748-9326/8/3/035032

Hillis, W.E., 1977. Secondary changes in wood. Recent Advances in Phytochemistry 11, 247-309

Hilger, A.B., Shaw, C.H., Metsaranta, J.M., Kurz, W.A., 2012. Estimation of snag carbon transfer rates by ecozone and lead species for forests in Canada. Ecological Applications 22, 2078-2090.

Holmen, S.P. 1990. Height-diameter regression tables from forest inventory at Blodgett Forest Research Station. Unpublished dataset.

Intergovernmental Panel on Climate Change (IPCC), 2006. Agriculture, Forestry, and Other Land Use. In IPCC. National Greenhouse Gas Inventory Guidelines. Institute for Global Environmental Strategies, Hayama, Japan.

Intergovernmental Panel on Climate Change (IPCC), 2007. Climate change 2007: the physical science basis. In Contribution of Working Group I to the Fourth Assessment Report of the Intergovernmental Panel on Climate Change. S. Solomon, D. Qin, M. Manning, Z. Chen, M. Marquis, Avery, B., Tignor, M. and Miller, H.L. (eds). Cambridge University Press, Cambridge, UK, 996 pp.

Isenberg, I.H., 1980. Pulpwoods of the United States and Canada, 3rd edition. Volume I-Conifers. Institute of Paper Chemistry, Appleton, WI. Revised by ML. Harder and L. Louden.

Jenkins, J.C., Chojnacky, D.C., Heath, L.S., Birdsey, R.A., 2003. National-Scale Biomass Estimators for United States Tree Species. Forest Science 49, 12-35.

Joanes, D.N, Gill, C.A., 1998. Comparing measures of sample skewness and kurtosis. The Statistician 47, 183-189.

Keen, F.P., 1955. The rate of natural falling of beetle-killed ponderosa pine snags. Journal of Forestry 53, 720-723.

Keen, F.P. 1929. How soon do yellow pine snags fall? Journal of Forestry 27, 735-737.

Knapp, E.E., 2015. Long-term dead wood changes in a Sierra Nevada mixed conifer forest: Habitat and fire hazard implications. Forest Ecology and Management 339, 87-95.

Kurz, W.A., Dymond, C.C., Stinson, G., Rampley, G.J., Neilson, E.T., Carroll, A.L., Ebata, T., Safranyik, L., 2008. Mountain pine beetle and forest carbon feedback to climate change. Nature 452, 987-990.

Kurz, W.A., Dymond, C.C., White, T.M., Stinson, G., Shaw, C.H., Rampley, G.J., Smyth, C., Simpson, B.N., Neilson, E.T., Trofymow, J.A., Metsaranta, J., Apps, M.J., 2009. CBM-

CFS3: A model of carbon-dynamics in forestry and land-use change implementing IPCC standards. Ecological Modelling 220, 480-504.

Lamlom, S.H., Savidge, R.A., 2003. A reassessment of carbon content in wood: variation within and between 41 North American species. Biomass & Bioenergy 25, 381-388.

Litton C.M., Raich, J.W., Ryan, M.G., 2007. Carbon allocation in forest ecosystems. Global Change Biology 13, 2089–2109.

Liu, J.S., 2001. Monte Carlo strategies in scientific computing. Springer series in statistics. Springer-Verlag, New York, New York, USA

Mackensen J., Bauhus J., Webber, E. 2003. Decomposition rates of coarse woody debris-a review with particular emphasis on Australian species. Aust J Bot 51:27-37.

van Mantgem, P.J., Stephenson, N.L., Byrne, J.C., Daniels, L.D., Franklin, J.F., Fule, P.Z., Harmon, M.E., Larson, A.J., Smith, J.M., Taylor, A.H., Veblen, T.T., 2009. Widespread Increase of Tree Mortality Rates in the Western United States. Science 323, 521-524.

Maser, C., Trappe, J., 1984. The seen and unseen world of the fallen tree. USDA-FS Pacific Northwest Forest and Range Experiment Station General Technical Report PNW-164, 56 pp.

Mast, J.N., Fulé, P.Z., Moore, M.M., Covington, W.W., Waltz, A.E.M., 1999. Restoration of presettlement age structure of an Arizona ponderosa pine forest. Ecological Applications 9, 228 –239.

McIntyre, P.J., Thorne, J.H., Dolanc, C.R., Flint, A.L., Flint, L.E., Kelly, M., Ackerly, D.D., 2015. Twentieth-century shifts in forest structure in California: Denser forests, smaller trees, and increased dominance of oaks. Proceedings of the National Academy of Sciences. Published online before print January 20, 2015, doi: 10.1073/pnas.1410186112

McDonald, P., 1973. Incense-cedar…an American wood. FS-226. United States Department of Agriculture Forest Service, Pacific Southwest Forest and Range Experiment Station, Berkeley, California.

Meddens, A.J.H., Hicke, J.A., Ferguson, C.A., 2012. Spatiotemporal patterns of observed bark beetle-caused tree mortality in British Columbia and the western United States Ecological Applications 22, 1876–91

Miles, P.D. and W. B. Smith. 2009. Specific gravity and other properties of wood and bark for 156 tree species found in North America. Res. Note NRS-38. Newtown Square, PA: U.S. Department of Agriculture, Forest Service, Northern Research Station. 35 p.

Morrison, M. L., and M. G. Raphael. 1993. Modeling the Dynamics of Snags. Ecological Applications 3:322-330.

Moser, S., G. Franco, S. Pittiglio, W. Chou, and D. Cayan. 2009. The Future Is Now: An Update on Climate Change Science Impacts and Response Options for California. California

Energy Commission, PIER Energy-Related Environmental Research Program. CEC-500-2008-071.

O'Connell, B. M., LaPoint, E.B., Turner, J.A., Ridley, Boyer, D., Wilson, A.M., Waddell, K.L., Christenson, G., Conkling, B.L., 2012. The Forest Inventory and Analysis Database: Database description and user guide version 5.1.2 for Phase 2. U.S. Department of Agriculture, Forest Service. 488 p. Available: http://www.fia.fs.fed.us/library/database-documentation/.

O'Connell, B. M., LaPoint, E.B., Turner, J.A., Ridley, T., Pugh, S.A., Wilson, A.M., Waddell, K.L., Conkling, B.L., 2014. The Forest Inventory and Analysis Database: Database description and user guide version 6.0.1 for Phase 2. U.S. Department of Agriculture, Forest Service. 748 p. Available: http://www.fia.fs.fed.us/library/database-documentation/.

Panek, J., Saah, D., Esperanza, A., Bytnerowicz, A., Fraczek, W., Cisneros, R., 2013. Ozone distribution in remote ecologically vulnerable terrain of the southern Sierra Nevada, CA. Environmental Pollution 182, 343-356.

Pinheiro, J., Bates, D., DebRoy, S., Sarkar, D., 2014. Package 'nlme', Linear and Nonlinear Mixed Effects Models. Documentation: http://cran.r-project.org/web/packages/nlme/nlme.pdf

R Core Team, 2014. R: A language and environment for statistical computing. R Foundation for Statistical Computing, Vienna, Austria. URL http://www.R-project.org/.

Radtke, P.J., Amateis, R.L., Prisley, S.P., Copenheaver, C.A. Chojnacky, D.C., Pittman J.R., Burkhart, H.E., 2009. Modeling production and decay of coarse woody debris in loblolly pine plantations. For Ecol Manage 257:790-9.

Raphael, M.G., White, M. 1984. Use of snags by cavity-nesting birds in the Sierra-Nevada. Wildlife Monographs 86:1-66.

Raphael, M.G., Morrison, M.L., 1987. Decay and Dynamics of Snags in the Sierra Nevada, California. Forest Science 33:774-783.

Ritchie, M.W., Knapp, E.E., Skinner, C.N., 2013. Snag longevity and surface fuel accumulation following post-fire logging in a ponderosa pine dominated forest. Forest Ecology and Management 287, 113-122.

Rothermel, R.C., 1983. How to Predict the Spread and Intensity of Forest and Range Fires. US Department of Agriculture, Forest Service, Intermountain Forest and Range Experiment Station, Ogden, UT, p. 161.

Russell, M., Woodall, C., Fraver, S., D'Amato, A., Domke, G., Skog, K., 2014. Residence Times and Decay Rates of Downed Woody Debris Biomass/Carbon in Eastern US Forests. Ecosystems 17, 765-777.

Scharpf, R. F., tech coord., 1993. Diseases of Pacific Coast Conifers. USDA Forest Service Agricultural Handbook 521. 199 p.32, 58.

Scheffer, T.C., Cowling, E.B., 1966. Natural Resistance of Wood to Microbial Deterioration. Annual Review of Phytopathology 4, 147-168.

Schurr, F., 2005. Incense cedar growth studies and observed mortality at Blodgett Forest Research Station. Presentation to the California Forest Pest Council, November 2005. Available at http://caforestpestcouncil.org/2008/07/2005-cfpc-annual-meeting-online-proceedings/ ; accessed November 2014.

Smith, J.E., Heath, L.S., Jenkins, J.C., 2003. Forest Volume-to-Biomass Models and Estimates of Mass for Live and Standing Dead Trees of U.S. Forests. Gen. Tech. Rep. NE-298. Newtown Square, PA: U.S. Department of Agriculture, Forest Service, Northeastern Research Station. 57 p.

State of California, 2006. California Global Warming Solutions Act. California Health and Safety Code Section 38561. 2006. California Legislative Information, November 2014.

Stephens, S.L. 2004. Fuel loads, snag abundance, and snag recruitment in an unmanaged Jeffrey pine-mixed conifer forest in Northwestern Mexico. Forest Ecology and Management 199, 103-113.

Stephens, S.L. and Collins, B.M. 2004. Fire regimes of mixed conifer forests in the north-central Sierra Nevada at multiple spatial scales. Northwest Science 78: 12-23.

Stephens, S.L., Moghaddas, J.J., 2005. Fuel treatment effects on snags and coarse woody debris in a Sierra Nevada mixed conifer forest. Forest Ecology and Management 214, 53–64.

Swetnam, T.W., Baisan, C.H., Caprio, A.C., Brown, P.M., Touchan, R., Anderson, R.S., Hallett, D.J., 2009. Multi-Millennial Fire History of the Giant Forest, Sequoia National Park, California, USA. The Journal of the Association for Fire Ecology 5, 120-127.

Swift, M.J., 1977. The ecology of wood decomposition. Sci. Prog. 64, 175-199.

Thomas, J.W., (technical editor) 1979. Wildlife habitats in managed forests of the Blue Mountains of Oregon and Washington. USDA-Forest Service Agriculture Handbook Number 553. Published in cooperation with the Wildlife Management Institute Washington, D.C. and the U.S. Department of Interior Bureau of Land Management.

Thomas, J.W., Anderson, R.G., Maser, C., Bull, E.L., 1979. Snags. P. 60–77 in: Wildlife habitat in managed forests, Thomas, J.W. (ed.). USDA Forest Service, Washington, D.C.

United Nations, 1992. UN General Assembly, United Nations Framework Convention on Climate Change : resolution / adopted by the General Assembly, 20 January 1994, A/RES/48/189, Available online: http://unfccc.int/essential_background/convention/background/items/1353.php accessed November 2014

United States Department of Agriculture, Forest Service (USFS), 2010. Forest Inventory and Analysis national core field guide Volume 1: field data collection procedures for phase 2 plots, version 5.0. Available online: http://www.fia.fs.fed.us/library/field-guides-methods-proc/

United States Department of the Interior, Geological Survey (USGS), 2008. LANDFIRE: LANDFIRE 1.1.0 Existing Vegetation Type layer. Available online: http://landfire.cr.usgs.gov/viewer/

U.S. Environmental Protection Agency (EPA), 2015. Inventory of U.S. greenhouse gas emissions and sinks: 1990-2013. US-EPA 430-R-15-004.

U.S. Environmental Protection Agency (EPA), 2011. Inventory of U.S greenhouse gas emissions and sinks: 1990-2009. US-EPA 430-R-11-005.

Vanderwel, M.C., Thorpe, H.C., Shuter, J.L., Caspersen, J.P., Thomas, S.C., 2008. Contrasting downed woody debris dynamics in managed and unmanaged northern hardwood stands. Canadian Journal of Forest Research 38, 2850-2861.

Waskiewicz, J.D., Fule, P.Z., Beier, P., 2007. Pine Snags in Northern Arizona. Western Journal of Applied Forestry 22, 233-240.

Weedon, J.T., Cornwell, W.K., Cornelissen, J.H., Zanne, A.E., Wirth, C., Coomes, D.A., 2009. Global meta-analysis of wood decomposition rates: a role for trait variation among tree species? Ecology Letters 12:45-56.

Wensel, L.C., Olson, C.M., 1995. Tree taper model volume equations. Hilgardia 62, December 1995.

Whittaker, R.H., Woodwell, G.M., 1967. Surface Area Relations of Woody Plants and Forest Communities. American Journal of Botany 54:931-939.

Whittaker, R.H., Woodwell, G.M., 1968. Dimension and production relations of trees and shrubs in the Brookhaven Forest, New York. Journal of Ecology. 56(1): 1-25.

Whittaker, R.H., Likens, G.E., Bormann, F.H., Easton, J.S., and Siccama, T.G., 1979. The Hubbard Brook Ecosystem Study: Forest Nutrient Cycling and Element Behavior. Ecology 60:203–220. http://dx.doi.org/10.2307/1936481

Wiemann, M.C., Williamson, G.B., 2014. Wood specific gravity variation with height and its implications for biomass estimation. Research Paper FPL-RP-677. Madison, WI: U.S. Department of Agriculture, Forest Service, Forest Products Laboratory. 9 p.

Williamson, G.B., Wiemann, M.C., 2010. Measuring Wood Specific Gravity ... Correctly. American Journal of Botany 97:519-524.

Woodall, C.W., 2012. Where Did the US Forest Biomass/Carbon Go? Journal of Forestry, March 2012. Vol. 110 Issue 2, p 113-114.

Woodall, C.W., Heath, L.S., Smith, J.E., 2008. National inventories of down and dead woody material forest carbon stocks in the United States: Challenges and opportunities. Forest Ecology and Management 256, 221-228.

Woodall, C.W., Heath, L.S., Domke, G.M., Nichols, M.C., 2011. Methods and equations for estimating aboveground volume, biomass, and carbon for trees in the U.S forest inventory, 2010. Gen Tech Rep NRS-88 USDA Forest Service, Northern Research Station.

Woodall, C.W., Domke, G.M., MacFarlane, D.W., Oswalt, C.M., 2012. Comparing field- and model-based standing dead tree carbon stock estimates across forests of the US. Forestry. 85: 125-133.

Woodall, C.W., Waddell, K.L., Oswalt, C.M., Smith, J.E., 2013. Standing dead tree resources in forests of the United States. In: Potter, Kevin M.; Conkling, Barbara L., eds. 2013. Forest Health Monitoring: national status, trends, and analysis 2010. Gen. Tech. Rep. SRS-GTR-176. Asheville, NC: U.S. Department of Agriculture Forest Service, Southern Research Station. 85-94

Woudenberg, S.W., Conkling, B.L., O'Connell, B.M., LaPoint, E.B., Turner, J.A., Waddell, K.L., 2010. The Forest Inventory and Analysis Database: Database description and user's manual version 4.0 for Phase 2. Gen Tech Rep RMRS-GTR-245 USDA Forest Service, Rocky Mountain Research Station.

Yatskov, M., Harmon, M.E., Krankina, O.N., 2003. A chronosequence of wood decomposition in the boreal forests of Russia. Canadian Journal of Forest Research 33:1211-1226.

York, R.A., DeVries, R., 2013. Snow Damage Patterns in Maturing Mixed-Species Plantations of the Sierra Nevada. Western Journal of Applied Forestry 28, 174-176.

Zell, J., Kandler, G., Hanewinkel, M., 2009. Predicting constant decay rates of coarse woody debris--a meta-analysis approach with a mixed model. Ecological Modelling 220:904-12.

Chapter 1 Appendix A. Supplementary material

Figure A1. Dimension Analysis of Standing Dead Trees

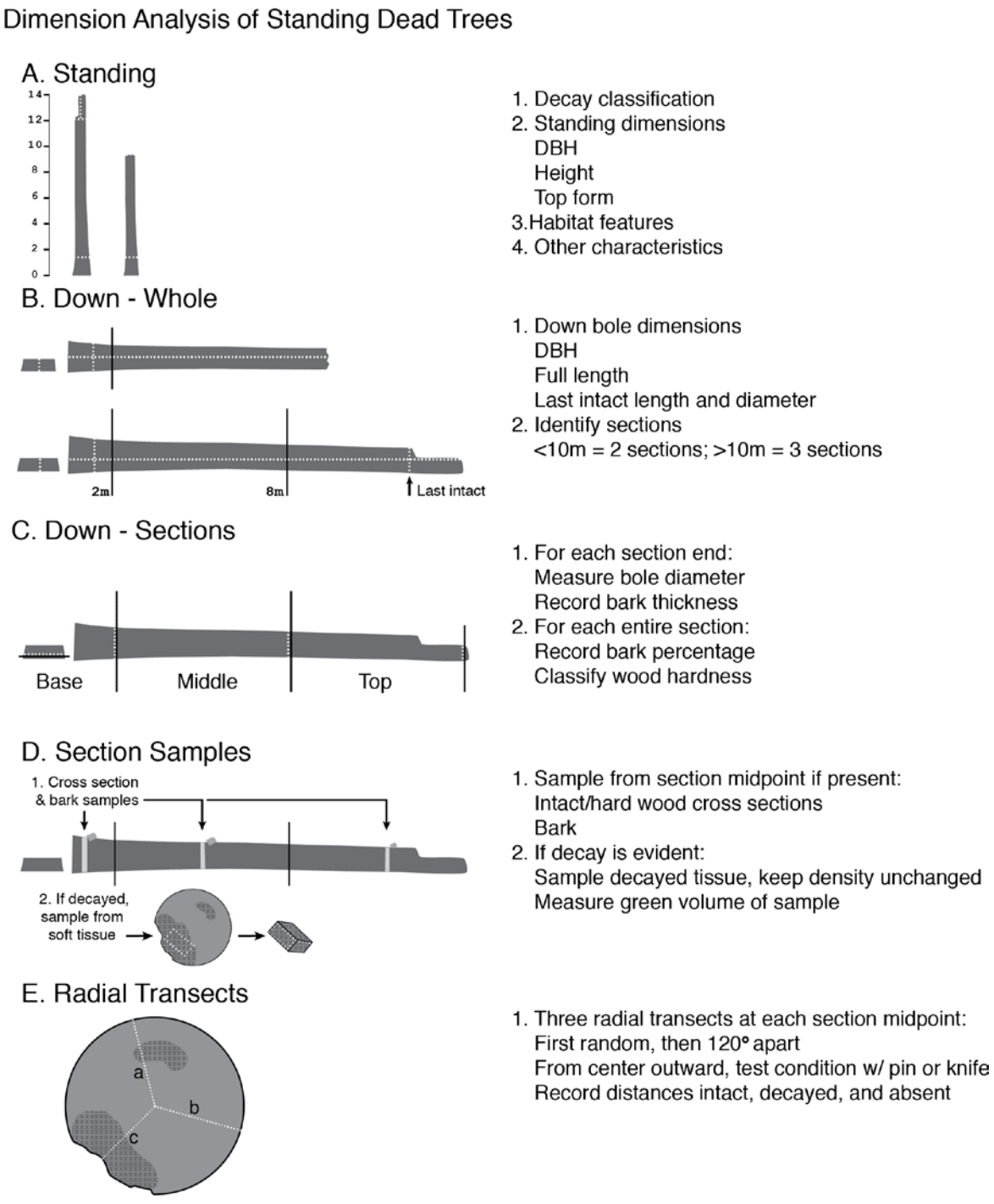

Chapter 1 Appendix A. Supplementary material

Table A1:
Density, carbon concentration, and net carbon density of SD trees for all species. Property measurements, dead:live ratios and standard errors of each for decay classes 1-5. Standard errors refer to all whole analyzed trees.

Decay class	SD density (g/cm^3)	Dead:live* density ratio	n
1	0.36 (0.01)	0.95 (0.03)	24
2	0.33 (0.01)	0.88 (0.02)	15
3	0.29 (0.02)	0.81 (0.06)	22
4	0.25 (0.02)	0.65 (0.04)	30
5	0.21 (0.02)	0.55 (0.05)	16
Decay class	SD carbon concentration (%)	Dead:live** C concentration ratio	n
1	51.37 (0.24)	1.03 (0.00)	11
2	51.45 (0.23)	1.03 (0.00)	10
3	51.51 (0.21)	1.03 (0.00)	14
4	52.72 (0.28)	1.05 (0.01)	27
5	53.71 (0.54)	1.07 (0.01)	14
Decay class	SD net carbon density (g/cm^3)	Dead:live** net C ratio	n
1	0.18 (0.01)	0.94 (0.04)	11
2	0.16 (0.01)	0.89 (0.03)	10
3	0.15 (0.01)	0.85 (0.07)	14
4	0.13 (0.01)	0.68 (0.05)	27
5	0.11 (0.01)	0.60 (0.06)	14

**Live density, Miles and Smith 2009. All other data this study*

***Live carbon concentration 50%*

Parenthetical values are standard errors

Chapter 1 Appendix A. Supplementary material

Table A2

Properties of standing dead trees (wood and bark combined) for all species and decay classes sampled.

Species	Decay class	SD density (g/cm^3)	Dead:live* density ratio	n (trees)	SD carbon concentration	Dead:live** net C ratio	n (trees)
white fir	1	0.37 (0.03)	0.92 (0.08)	5	0.51 (0.01)	0.86 (0.10)	3
white fir	2	0.35 (0.02)	0.86 (0.04)	6	0.51 (0.01)	0.84 (0.13)	2
white fir	3	0.29 (0.08)	0.72 (0.19)	4	0.51 (0.01)	0.90 (0.01)	2
white fir	4	0.22 (0.02)	0.56 (0.04)	10	0.53 (0.01)	0.60 (0.04)	9
white fir	5	0.17 (0.01)	0.43 (0.02)	3	0.54 (0.02)	0.46 (0.05)	2
red fir	1	0.38 (0.02)	1.01 (0.04)	6	0.51 (0.00)	0.97 (0.02)	4
red fir	2	0.37 (0.00)	0.98 (0.02)	3	0.51 (0.00)	1.00 (0.01)	3
red fir	4	0.40 (NA)	1.05 (NA)	1	0.52 (NA)	1.10 (NA)	1
incense cedar	2	0.28 (0.02)	0.85 (0.05)	4	0.52 (0.01)	0.84 (0.03)	3
incense cedar	3	0.29 (0.03)	0.91 (0.09)	6	0.52 (0.00)	1.02 (0.13)	3
incense cedar	4	0.30 (0.03)	0.93 (0.10)	3	0.52 (0.00)	0.97 (0.11)	3
incense cedar	5	0.30 (0.03)	0.86 (0.08)	3	0.53 (0.01)	0.91 (0.10)	3
sugar pine	1	0.34 (0.04)	0.99 (0.10)	6	0.52 (0.00)	1.09 (0.07)	2
sugar pine	2	0.26 (NA)	0.76 (NA)	1	0.52 (NA)	0.79 (NA)	1
sugar pine	3	0.26 (0.05)	0.76 (0.16)	4	0.52 (0.00)	0.79 (0.17)	4
sugar pine	4	0.26 (0.03)	0.75 (0.09)	2	0.52 (0.00)	0.78 (0.08)	2
sugar pine	5	0.19 (0.01)	0.55 (0.04)	2	0.52 (0.00)	0.56 (0.04)	2
ponderosa	1	0.36 (0.01)	0.96 (0.04)	3	0.53 (NA)	0.98 (NA)	1
ponderosa	2	0.34 (NA)	0.91 (NA)	1	0.51 (NA)	0.93 (NA)	1
ponderosa	3	0.34 (0.04)	0.89 (0.09)	6	0.51 (0.01)	0.98 (0.03)	3
ponderosa	4	0.24 (0.05)	0.63 (0.12)	8	0.53 (0.01)	0.61 (0.18)	6
ponderosa	5	0.20 (0.03)	0.52 (0.08)	5	0.53 (0.01)	0.55 (0.12)	4
Douglas-fir	1	0.38 (0.03)	0.85 (0.06)	4	0.52 (NA)	0.74 (NA)	1
Douglas-fir	3	0.21 (0.11)	0.48 (0.25)	2	0.51 (0.00)	0.49 (0.26)	2
Douglas-fir	4	0.26 (0.02)	0.59 (0.05)	6	0.53 (0.00)	0.62 (0.05)	6
Douglas-fir	5	0.19 (0.03)	0.43 (0.07)	3	0.56 (0.01)	0.48 (0.07)	3

**Live density, Miles and Smith 2009. All other data this study*

***Live carbon concentration 50%*

Values in parentheses are standard errors

Table A3

Standing dead wood properties and bark properties for all species and decay classes sampled

Species	Decay class	Mean SD wood density (g/cm^3)	SD wood dead:live* density ratio	n (trees)	SD wood carbon concentration	n (trees)	Mean SD bark density (g/cm^3)	SD bark dead:live* density ratio	n (trees)	SD bark carbon concentration	n (trees)
white fir	1	0.37 (0.03)	0.86 (0.07)	5	0.50 (0.01)	3	0.66 (0.09)	1.17 (0.16)	5	0.53 (0.01)	3
white fir	2	0.35 (0.02)	0.78 (0.05)	6	0.50 (0.00)	2	0.61 (0.05)	1.09 (0.10)	6	0.54 (0.00)	2
white fir	3	0.29 (0.08)	0.68 (0.2)	4	0.51 (0.00)	2	0.48 (0.09)	0.86 (0.17)	4	0.53 (0.01)	2
white fir	4	0.22 (0.02)	0.50 (0.04)	10	0.52 (0.01)	9	0.43 (0.02)	0.77 (0.03)	10	0.56 (0.01)	9
white fir	5	0.17 (0.01)	0.38 (0.06)	3	0.53 (0.03)	2	0.32 (0.10)	0.57 (0.18)	3	0.59 (0.01)	2
red fir	1	0.38 (0.02)	1.01 (0.04)	6	0.51 (0.00)	4	0.47 (0.07)	1.07 (0.15)	6	0.52 (0.00)	4
red fir	2	0.37 (0)	0.98 (0.02)	3	0.51 (0.00)	3	0.43 (0.03)	0.98 (0.07)	3	0.52 (0.01)	3
red fir	4	0.40 (NA)	1.10 (NA)	1	0.52 (NA)	1	0.42 (NA)	0.95 (NA)	1	0.52 (NA)	1
incense cedar	2	0.28 (0.02)	0.82 (0.06)	4	0.52 (0.00)	3	0.24 (0.01)	0.97 (0.05)	4	0.53 (0.01)	3
incense cedar	3	0.29 (0.03)	0.93 (0.11)	6	0.52 (0.00)	3	0.20 (0.03)	0.82 (0.11)	6	0.52 (0.00)	3
incense cedar	4	0.30 (0.03)	0.95 (0.11)	3	0.52 (0.00)	3	0.21 (0.01)	0.85 (0.05)	3	0.52 (0.00)	3
incense cedar	5	0.30 (0.03)	0.86 (0.08)	3	0.53 (0.01)	3	0.22 (NA)	0.90 (NA)	1	0.53 (NA)	1
sugar pine	1	0.34 (0.04)	0.91 (0.12)	6	0.52 (0.00)	2	0.47 (0.04)	1.35 (0.11)	6	0.54 (0.00)	2
sugar pine	2	0.26 (NA)	0.72 (NA)	1	0.51 (NA)	1	0.34 (NA)	0.98 (NA)	1	0.53 (NA)	1
sugar pine	3	0.26 (0.05)	0.85 (0.08)	4	0.51 (0.00)	4	0.38 (0.00)	1.08 (0.01)	3	0.54 (0.00)	3
sugar pine	4	0.26 (0.03)	0.74 (0.08)	2	0.52 (0.01)	2	0.39 (NA)	1.11 (NA)	1	0.54 (NA)	1
sugar pine	5	0.19 (0.01)	0.54 (0.05)	2	0.52 (0.00)	2	0.37 (NA)	1.04 (NA)	1	0.55 (NA)	1
ponderosa pine	1	0.36 (0.01)	0.94 (0.08)	3	0.53 (NA)	1	0.38 (0.06)	1.08 (0.16)	3	0.52 (NA)	1
ponderosa pine	2	0.34 (NA)	0.93 (NA)	1	0.50 (NA)	1	0.30 (NA)	0.87 (NA)	1	0.54 (NA)	1
ponderosa pine	3	0.34 (0.04)	0.87 (0.09)	6	0.50 (0.01)	3	0.37 (0.05)	1.05 (0.15)	6	0.54 (0.01)	3
ponderosa pine	4	0.24 (0.05)	0.63 (0.12)	8	0.53 (0.01)	6	0.37 (0.04)	1.04 (0.12)	6	0.53 (0.00)	5
ponderosa pine	5	0.20 (0.03)	0.53 (0.09)	5	0.53 (0.01)	4	0.35 (0.02)	1.01 (0.06)	2	0.54 (0.00)	2
Douglas-fir	1	0.38 (0.03)	0.76 (0.06)	4	0.52 (NA)	1	0.5 (0.05)	1.14 (0.12)	4	0.53 (NA)	1
Douglas-fir	3	0.21 (0.11)	0.44 (0.25)	2	0.50 (0.00)	2	0.47 (0.05)	1.07 (0.11)	2	0.54 (0.00)	2
Douglas-fir	4	0.26 (0.02)	0.50 (0.06)	6	0.51 (0.01)	6	0.45 (0.01)	1.04 (0.02)	6	0.57 (0.01)	6
Douglas-fir	5	0.19 (0.03)	0.34 (0.05)	3	0.54 (0.02)	3	0.44 (0.00)	1.00 (0.01)	3	0.59 (0.01)	3

**Live density, Miles and Smith 2009. All other data this study*

Values in parentheses are standard errors

Chapter 1 Appendix A. Supplementary material

Table A4
Standing dead density ratios for California mixed conifer species per USFS Forest Inventory and Analysis program (Harmon et al., 2011; O'Connell et al., 2014)

	Decay class	Live density (g/cm^3)	Dead:live density ratio	Uncertainty	Sample info*
white fir	1	0.37	0.996	0.021	a
white fir	2	0.37	0.873	0.018	a
white fir	3	0.37	0.625	0.054	a
white fir	4	0.37	0.541	0.213	b
white fir	5	0.37	0.541	0.213	b
red fir	1	0.36	1.04	0.017	a
red fir	2	0.36	1.08	0.051	a
red fir	3	0.36	0.626	0.054	a
red fir	4	0.36	0.467	0.213	b
red fir	5	0.36	0.467	0.213	b
incense cedar	1	0.37	1.04	0.074	a
incense cedar	2	0.37	0.972	0.035	a
incense cedar	3	0.37	1.011	0.059	a
incense cedar	4	0.37	0.596	0.218	b
incense cedar	5	0.37	0.596	0.218	b
sugar pine	1	0.34	1.04	0.038	a
sugar pine	2	0.34	0.906	0.014	a
sugar pine	3	0.34	0.735	0.054	a
sugar pine	4	0.34	0.517	0.213	b
sugar pine	5	0.34	0.517	0.213	b
ponderosa pine	1	0.38	0.925	0.011	a
ponderosa pine	2	0.38	1.007	0.02	a
ponderosa pine	3	0.38	1.154	0.061	a
ponderosa pine	4	0.38	0.481	0.213	b
ponderosa pine	5	0.38	0.481	0.213	b
Douglas-fir	1	0.45	0.892	0.015	a
Douglas-fir	2	0.45	0.831	0.017	a
Douglas-fir	3	0.45	0.591	0.054	a
Douglas-fir	4	0.45	0.433	0.213	b
Douglas-fir	5	0.45	0.433	0.213	b

*Sample info: a: Genera sampled, b: Species and genus not sampled. (Harmon et al., 2011, Appendix D)

CHAPTER 2 | Impacts of chronic ozone exposure on tree growth and survival

1. INTRODUCTION

Ozone at ground level causes serious damage to plants and directly threatens ecosystem health (Chappelka and Samuelson 1998, Karnosky et al. 2007, Krupa et al. 2001). Today's global mean tropospheric O_3 is double pre-industrial concentrations (Gauss et al. 2006) and projected to continue climbing as precursor emissions increase and the atmosphere warms (Forster 2007, Sitch et al. 2007). The effects of O_3 on plant carbon assimilation, stomatal conductance, and growth result in agricultural losses of $14-26 billion worldwide (Van Dingenen et al. 2009). However, air pollution impacts are by no means limited to cultivated plants. Fully one-half of the planet's forests are also expected to be exposed to toxic levels of O_3 within this century (Fowler et al. 1999, The Royal Society). In the United States, the Environmental Protection Agency recently strengthened the National Ambient Air Quality Standards (NAAQS) to 0.070 parts per million (ppm)(3 year average of the annual fourth-highest maximum daily 8-hour concentration) in recognition of the threat that tropospheric O_3 poses to vegetation, and in turn, public welfare (U.S. Environmental Protection Agency 2015). Yet, forest ecosystems in some regions have already experienced decades of exposure to elevated O_3 (Miller et al. 1972). Today, these chronically polluted sites hold valuable lessons about how trees respond to past and predicted O_3 pollution.

Trees exposed to O_3 suffer molecular-scale breakdown in the mechanisms of photosynthesis, (Heath 1987, Matyssek et al. 2003) decreased CO_2 assimilation in leaves, and consequent declines in net primary productivity (NPP)(Reich and Amundson 1985, Ainsworth et al. 2012). Leaves are often visibly damaged and exhibit premature senescence (Miller et al. 1963, Grulke and Balduman 1999). Reduced root biomass and altered stomatal behavior are also prevalent (Grulke and Balduman 1999, Grulke et al. 2007, Kellomäki and Wang 1997). These individual tree responses integrate into profound impacts on forests, ecosystems, and even climate (Ainsworth et al. 2012, Bytnerowicz et al. 2013b, U.S. Environmental Protection Agency 2007). For example, biomass accumulation is 7% lower in trees grown in present-day ambient O_3 concentrations than those growing in 10 parts per billion (ppb). Based on increases in precursor pollutants, tree biomass accumulation is projected to decline an additional 11% by 2050 (Wittig et al. 2009, Volz and Kley 1988). Decreases in water use efficiency have also been documented in O_3 polluted forests (Sun et al. 2012). Elevated O_3 contributes to weakened defenses against biotic and abiotic stressors, facilitating insect attacks and increasing the risk of fire (Karnosky et al. 2007, Eatough Jones et al. 2004, Grulke 2009). In the context of continued global change, the plant physiological impacts of O_3 pollution reduce the land-carbon sink and ultimately increase atmospheric CO_2 (Sitch et al. 2007).

The western slope of the southern Sierra Nevada has ranked among the world's most O_3 polluted regions for over 40 years (Carroll et al. 2003, National Park Service - Air Resources Division 2013, Panek et al. 2013b). Chronic O_3 pollution endangers the health of the vast conifer forests

protected in the region's National Parks and National Forests. Though air quality has improved in recent years, (San Joaquin Valley Air Pollution Control District 2007, San Joaquin Valley Air Pollution Control District 2010) the region frequently exceeds the primary and secondary NAAQS for O_3(Panek et al. 2013a, Cisneros et al. 2010, U.S. Environmental Protection Agency 2015). Ambient concentrations reach a maximum in mid and late summer,(Grulke et al. 2002) driven primarily by photochemical reactions and regional air circulation (Beaver and Palazoglu 2009). The characteristic chlorotic mottle of pine needles that indicates O_3 damage was first observed here in 1971 (Figure 1A; Miller and Millecan 1971). High O_3 exposure has resulted in injury to ponderosa (*Pinus ponderosa* Laws) and Jeffrey pines (*P. Jeffreyi* Grev. & Balf.), as observed at many sites along the western slope throughout the 1980s and 1990s (Arbaugh et al. 1998, Miller et al. 1982). These species also exhibited O_3 related growth declines in experimental trials (Temple and Miller 1994) and in the San Bernardino mountains, (McBride et al. 1975) but reported effects on tree growth in the southern Sierra Nevada are variable (Peterson et al. 1991, Peterson and Arbaugh 1988, Peterson et al. 1987).

Though the damage to trees inflicted by acute O_3 exposure is well documented, we are just beginning to understand how chronic air pollution affects forests. Repeated and prolonged stress events, especially declines in growth, predispose trees to mortality (Pedersen 1998, Das et al. 2007). Most long term studies of O_3 impacts on forests are experimental, using active manipulation of O_3 and other greenhouse gases, primarily in young, actively managed forests (for example, in open topped containers or in combination with free-air CO_2 enrichment) (Ainsworth et al. 2012, Wittig et al. 2007, Wittig et al. 2009). These investigations have established that a range of flowering and coniferous trees exhibit growth declines after 5-10 years of exposure. Despite the value of these experiments, they are necessarily limited to the time elapsed since installation (King et al. 2005, Matyssek et al. 2010). Longitudinal and retrospective studies are free of this limitation, and have the additional benefit of capturing ecosystem dynamics under field conditions, including annual and multi-year droughts (Braun et al. 2014, Juknys et al. 2014). In the case of the southern Sierra Nevada, variation in water availability exerts a powerful influence over the growth and death of trees (Stephenson 1998, van Mantgem et al. 2009). Thus, in order to understand the long term ecosystem effects of O_3, we need to understand the combined impacts of O_3 exposure and drought stress on trees under field conditions.

The purpose of this study is to quantify the impact of chronic O_3 pollution in southern Sierra Nevada forests and to characterize tree responses to long term O_3 exposure. We ask three key questions: first, what are the recent trends in O_3 exposure and injury throughout the region's forests? Second, to what extent does chronic O_3 exposure cause injury in trees that are also impacted by drought and other stressors? Finally, what are the growth and mortality responses of forests that experience long term exposure to O_3 pollution? We answer these questions using long term air quality monitoring co-located with repeated assessments of tree condition and foliar damage.

2. METHODS AND MATERIALS

2.1 Study design

This region-wide study encompasses eight sites with coupled monitoring of forest vegetation and air quality. Sites are distributed across a gradient of O_3 exposures on the western slope of the southern Sierra Nevada, ranging from severely polluted (summer averages over 55 ppb) to low exposure levels (summer averages under 30 ppb) (Figure 1B; Panek et al. 2013a, Cisneros et al. 2010). Three of these, Giant Forest, Grant Grove, and Shaver Lake, (here after "long term sites") were routinely assessed for O_3 exposure and tree injury starting in 1991. Work was carried out in connection with the Sierra Cooperative Ozone Impact Assessment Study (SCOIAS) and the Forest Ozone Response Study (Project FOREST) through 2001 (Bytnerowicz et al. 2003, Arbaugh and Bytnerowicz 2003). Five more sites were added in 2011 to extend the earlier work. Tree injury and air quality at these short term sites was assessed 2011-2013.

Each site consists of 50-150 mature trees, arranged in tagged permanent study plots within 12.2 km of an O_3 monitoring instrument. At long term sites, the monitors are on average 1 km (maximum of 2.43 km) from study plots. Sites and trees are stratified across the gradient of O_3 exposure. Ozone injury surveys and forest measurements were completed yearly 1991-1994, then again in either 2000 (Giant Forest, Grant Grove) or 2001 (Shaver Lake). Surveys of both long and short term sites were completed in 2011 and 2012.

2.2 Site and sampling descriptions

Forest sites are dominated by ponderosa pine, Jeffrey pine, or both, with white fir (*Abies concolor* Lindley), incense-cedar (*Calocedrus decurrens* Florin), sugar pine (*P. lambertiana* Doug.), and black oak (*Quercus kelloggii* Newb.) also present. Research plot locations were selected based on proximity to existing air quality monitoring infrastructure and dominance of O_3 sensitive species. Mature pines over 16.5 cm (6.5 inches) diameter at breast height (DBH) from all canopy classes were selected for injury surveys. Dominant, codominant, and open grown trees make up the majority of individuals. During each visit, an injury survey, measurements of DBH, and classification of the tree's canopy was completed. Only healthy trees, defined by the absence of pests, pathogens, and physical damage, exclusive of O_3 injury, were followed in the long term study. This was in order to ensure the survival of sufficient individuals to meet statistical requirements for at least 20 years (Miller et al. 1996). We followed this same protocol in selecting new individuals, and trees that acquired signs of disease or physical damage during the course of the study were excluded.

These forests experience a Mediterranean climate with hot, dry summers and mild wet winters. Precipitation is 30-60% snow and ranges from 930-1100mm annually across the eight sites (Stephenson 1988, Western Regional Climate Center 2015). Ninety-five percent of rain and snow falls October-May; accordingly, annual climatic water deficits are reported for the water year, 1 October – 30 September (Flint et al. 2013). Sites are managed primarily as natural and recreational landscapes, with no record of timber harvest within 80 years. A single plot at Shaver Lake is the exception; here 15 trees were excluded from mortality calculations due to harvest. Low-severity fires have occurred within the past 20 years in parts of the Grant Grove, Sugarloaf Basin, and Atwell Mill sites, with no discernable impacts to health of trees in the survey (See also SI 1. Research Site Details)

2.3 Monitoring and indexing O_3 exposure

Ambient O_3 concentrations were measured with ozone analyzers using the UV absorption method. During the study, active measurement of summer hourly O_3 concentrations was continuous at Giant Forest and intermittent at six other sites (Carroll and Dixon 1993, Carroll and Dixon 1995, California Environmental Protection Agency - Air Resources Board 2015, National Park Service - Air Resources Division 2015; see also SI 2. Measuring O_3 exposure; Table SI-1 Site monitoring details). When active, the analyzers sample at least every 30 seconds, then average hourly if >75% of data points for the hour are present. Cumulative O_3 exposure was expressed using the W126 exposure index, a cumulative concentration-weighted index that weights higher concentrations of O_3 using a sigmoidal curve centered at 70 ppbv (Lefohn and Runeckles 1987; see SI 2. Measuring O_3 exposure). Previous studies in this system have found that the W126 exposure index is a strong predictor of vegetation injury (Arbaugh et al. 1998). Cumulative exposure indices also provide a meaningful link to the physiological drivers of oxidative injury, particularly effective flux (Grulke et al. 2002, Musselman et al. 2006). Recent strengthening of the NAAQS for O_3 to 70 ppb provides ecosystem protections equal to a limit of 17 ppm-hours in terms of a 3-year W126 index (U.S. Environmental Protection Agency 2015).

We calculated W126 in two ways to capture both daytime and 24-hour O_3 exposures, because both daytime and nighttime stomatal conductance contribute to vegetation impacts (Grulke et al. 2004, Massman 2004). Although stomatal conductance of O_3 is typically lower at night, plants can be more susceptible during this time, a pattern that should be considered in quantifying exposure (Musselman and Minnick 2000). Since higher elevation sites in the Sierra Nevada can have highest concentrations at night and nocturnal conductance can be significant, a 12-hour W126 underestimates exposure. In this study, $W126_{12}$ is computed from 8:00-20:00 daily and July-September annually. $W126_{24}$ includes all hourly measurements from June-September (Bytnerowicz et al. 2013a, U.S. Forest Service et al., Lefohn and Runeckles 1987; see SI 2. Measuring O_3 exposure). To examine the temporal trends in exposure index, we used linear mixed effects analyses (Crawley 2002). A mixed effects approach allows an assessment of whether region-wide $W126_{24}$ is increasing or decreasing over time while controlling for preexisting differences in exposure between sites by treating them as random effects. Parameter estimates were calculated using restricted maximum log-likelihood (REML)(Pinheiro et al. 2014). This and all other analysis was completed in R version 3.2.2 (R Core Team 2016).

2.4 Ozone injury of trees

Injury of trees was assessed in the field following the Ozone Injury Index (OII) method (Miller et al. 1996). Maximum OII is 100, corresponding to a severely injured tree, with more than 40% of leaf area affected by chlorotic mottle. OII=0 signifies a tree with no symptoms of ozone injury (see SI 3. OII). To examine the temporal trends in tree injury, we again used linear mixed effects analyses (Crawley 2002) with OII as the response variable, year as fixed effect, and site as a random effect.

The relationship between exposure and injury was characterized using linear regression. Previous work suggests that a linear form is appropriate for this relationship (Arbaugh et al. 1998). To match the biological accumulation of O_3 injury on pine needles, regressions were fit to both a four year cumulative $W126_{24}$ and single-year $W126_{24}$. To assess whether chronic exposure has resulted in stronger or weaker injury responses over time, we used a linear mixed effects

approach with OII as the response variable. Fixed effects, $W126_{24}$ and year, were grouped by 4 year periods and tree ID was the random effect.

2.5 Assessing tree survival and growth

In repeated field surveys, the DBH of each tree was re-measured to determine growth. Relative growth rate (RGR) was calculated for measurement periods 1991-2001 and 2001-2011 using these start and end period measurements. RGR is expressed as percent annual change in DBH:

$$(1) \qquad RGR = \frac{\ln dbh_b - \ln dbh_a}{b-a}$$

where a=time at start and b=time at end. We examined the response of RGR to tree and environmental characteristics using linear mixed effects models.(Crawley 2002) OII, climatic water deficit,(Flint et al. 2013) DBH, species, the interaction of OII and deficit, and the interaction of OII and species were included as fixed effects parameters in the initial model. Since trees are expected to vary in susceptibility, tree ID was included as a random effects parameter. An information theoretic approach (Akaike's Information Criterion) was used to compare the relative performance of reduced candidate models to the full initial model (Burnham and Anderson 2002). Before including RGR values in the linear mixed effects analysis, the difference in DBH between measurements was used to identify outlying growth patterns. Periods with change in DBH +/- 2 standard deviations (SD) beyond the mean were re-examined against field records, and any errors found were corrected. The RGRs that remained +/- 3 SD beyond the mean (n=4) were excluded from further analysis (Eitzel et al. 2015).

To evaluate the demographic impact of long term pollution exposure, we first used a Kaplan-Meier approach to describe survival probability at intervals over the 20-year period (Kaplan and Meier 1958). Individuals were interval and right censored. Interval censored trees died between field visit years, with mortality confirmed in person after the fact. Right censored trees were both live trees and those without confirmed mortality (i.e. removed from the study before its conclusion). Survival analyses were conducted using the "survival" and "interval" packages in R (Fay and Shaw 2010, R Core Team 2016, Therneau 2015). Annual mortality rates were computed per Sheil and May (Sheil and May 1996) where

$$(2) \qquad m = 1 - \left[1 - \frac{No - Nt}{No}\right]^{1/t}$$

for N_0 = individuals alive at time zero and t=time elapsed. Analysis of growth and survival was completed using only individuals from long term sites (n=450).

3. RESULTS

3.1 Regional and temporal ozone patterns

Air quality in the southern Sierra is improving, but O_3 exposure is still severe across a large portion of the region (Figure 2A-B). Low-mid elevation locations on the western slope, as well as sites near major drainages, continue to experience the highest O_3 exposure (Panek et al. 2013a). At Giant Forest, where the NPS has maintained the longest continuous record of O_3 observations in the region, the 3 year mean $W126_{12}$ decreased from 49.2 ppm-hours in 1992 to

33.6 ppm-hours in 2012. Elevated but more moderate exposures were present at Shaver Lake (2011 3-year mean $W126_{12}$ = 15.19; Table SI-2). In the region we surveyed, O_3 pollution is least severe where farthest removed from sources of primary pollutants; locations farther east and at higher elevation generally have the cleanest air, particularly areas away from roads (Figure 1B, Figure 2A). For example, Florence and Huntington Lakes have annual $W126_{12}$ ranging from 5.9-16.9 ppm-hours in recent years. Across all sites, average summer exposure to O_3 decreased 1.5% per year from 1991-2013. The decrease was equally apparent in both $W126_{12}$ and $W126_{24}$. For $W126_{12}$, a linear mixed effects model with year as the fixed effect and site as a random effect shows a loss of 0.76 ppm-hours per year (SE = ± 0.04; t = -28.86; $p < 0.001$). In a model of the same form, $W126_{24}$ decreased 1.21 ppm-hours per year (SE = ± 0.02; t = -31.74; $p < 0.001$).

Trees in the region face both annual and episodic drought stress alongside chronic O_3 exposure. During the years of the study, there was no trend in climatic water deficit across all research sites. From 1991-2014, mean annual climatic water deficit at long term study sites (Shaver Lake, Grant Grove, and Giant Forest) was 634.9 mm (SD = ± 1.98). Similarly, mean annual deficit at all eight sites over the same period was 633.6 mm (SD = ± 34.9; range = 562.5 to 680.2).(Flint et al. 2013) Deficit varies much more between years within site (mean interannual range = 305.5 mm, SD = ± 85.2, than between sites (range of site means = 109.0 mm), and annual variation is coherent across sites in the study.

3.2 Injury to pines

Pollution injury to ponderosa and Jeffrey pines persists but the severity has recently started to decline, tracking improvements in air quality. Mean tree injury (OII) declined over time at all sites with long term injury monitoring (Figure 2B). Supporting evidence for the declines in injury comes from a linear mixed effects model in which the fixed effect is year and random effect is site (Coefficient value = -0.6848, SE = ± 0.05, t = -13.53, $p<0.001$). In this model, not only is the slope negative, but year is also a significant predictor of OII within site. The largest decreases in OII were observed at the two most seriously polluted sites in the study: Giant Forest (OII decrease from 44.66 ± 1.33 in 1991 to 28.86 ± 2.14 in 2012) and Grant Grove (from 40.84 ± 1.52 in 1991 to 19.52 ± 1.85 in 2012). Locations with absent and very low injury include Sugarloaf Basin (0.30 ± 0.28) and Florence Lake (OII = 0, no injury observed). Other sites in the region had intermediate levels of O_3 injury: Shaver Lake, a moderately polluted site, also showed declines in OII (Figure 2B, SI Table 3). Among all trees in the long term study, declines were primarily attributable to lower OII (i.e., less injury) of the same individual trees. The proportion of surveyed trees exhibiting any chlorotic mottle (OII > 0) also showed a small net decrease at the two most polluted sites.

3.3 Relationship between injury and environmental factors

Although O_3 exposure and tree injury have both lessened in recent years, extant trees have endured polluted air for decades, while also withstanding annual and multi-year droughts. Under these conditions, to what degree does chronic O_3 exposure determine injury severity? Linear regressions of both a four year cumulative $W126_{24}$ (4 year sum $W126_{24}$), and single-year $W126_{24}$ showed that higher ambient O_3 exposures are significant predictors of increased tree injury (OII) (Figure 3). The regression relationship for $W126_{24}$ is OII= 0.33 ($W126_{24}$) ± 0.08; R2=0.48, t=4.33, $p<0.001$. The relationship between ambient exposure and OII is stronger over time than that of any given year. This is evident in the 4 year sum $W126_{24}$ regression relationship: OII= 0.11($W126_{24}$) + 0.02; R2=0.60, t=4.78, $p<0.001$). However, annual climatic water deficit did not

influence the severity of tree pollution injury. In the same models that show a strong role for annual O_3 exposure, the inclusion of water deficit and a deficit by injury interaction term indicated that neither of these is a significant predictor of OII (for OII = $W126_{24}$ + Deficit + $W126_{24}$:Deficit ($p = 0.49$ and 0.17, respectively).

To assess whether chronic exposure contributed to stronger or weaker injury responses over time, we used a linear mixed effects approach with OII as response. Fixed effects $W126_{24}$ and year were grouped into three periods of four years each. Analysis showed that injury response varied though time, but did not suggest any directional shift ($p < 0.001$ for all factors). It follows that over the long term, individual tree responses to ambient O_3 exposure neither strengthened nor weakened.

3.4 Impacts on tree growth and survival

The most informative model of RGR ultimately included the fixed effects of OII, DBH, tree species, and the interaction of species with OII, with the random effect of individual tree ID number ($\Delta AIC = 10.06$). This relationship shows that growth is reduced in O_3 injured trees (Figure 4). Tree size and species are also significant predictors of growth ($p < 0.001$ for all predictors). In this model, the interaction term can be interpreted as a difference in the growth responses of ponderosa and Jeffrey pines to O_3 injury. Ponderosa pine therefore sustains larger growth losses than Jeffrey pine, as illustrated by its steeper negative slope (Figure 4). According to this growth model, an uninjured tree (i.e., OII = 0) of mean DBH at the three long term study sites grew a modest 1% in DBH each year (ponderosa pine 1.22%, Jeffrey pine 0.93%). Thus, for a Jeffrey pine of mean DBH, the RGR in recent years at Giant Forest (2012 mean OII = 28.8) is 0.78% DBH/year: a loss of 15.2% of typical yearly growth compared to a theoretical year without O_3 injury (Figure 4). An average ponderosa pine at Shaver Lake in2011 (2011 mean OII = 10.7) would be expected to have losses of 5.6% per year. These growth responses represent a considerable improvement over conditions two decades ago, when average injury at Giant Forest would correspond to ponderosa pine growth losses of 23.7% compared to an uninjured tree at the same site.

The forest site with most severe O_3 pollution and highest observed injury, Giant Forest, had the lowest overall Kaplan-Meier survival probability, at 84.7%. Study trees in Grant Grove fared somewhat better, with 89.3% surviving. 97.1% survived at comparatively less polluted Shaver Lake (See Table SI-4) Annual mortality rates follow a similar pattern, at 0.57, 0.50, and 0.07 percent mortality per year, respectively. Sites with greatest O_3 exposures did sustain the highest mortality, though the differences were not significant ($\chi 2 = 4.0648$, $p = 0.131$). The proportion of trees surviving at each of the sites remained within the typical distribution of total mortality rates in similar Sierra mixed conifer stands (van Mantgem and Stephenson 2007).

4. DISCUSSION

Our results demonstrate that chronic O_3 pollution in the southern Sierra Nevada leads to lower rates of tree growth and survival. These findings provide a unique long term view of how forests respond to this damaging secondary pollutant of increasing global importance. In quantifying the relationships between exposure, injury, and resultant growth and survival, our study clarifies the impacts of chronic pollution on trees in natural ecosystems and also confirms their capacity for resistance and recovery.

4.1 Implications of exposure and injury

Declines in both O_3 exposure and injury to trees are promising evidence that years of air pollution can be ameliorated and even reversed. We found that daytime and nighttime O_3 are declining at nearly the same rate, with $W126_{12}$ and $W126_{24}$ declining by the same percentage annually per year; O_3 injury has followed suit. Improvements in air quality were first seen in the San Joaquin Valley, the local source of most precursor pollutants that reach Sierra forests (Beaver et al. 2010, San Joaquin Valley Air Pollution Control District 2010). The most polluted sites, Grant Grove and Giant Forest, register 3 year mean $W126_{12}$ of 40.3 and 33.6 in 2012, still well above the EPA's recommended exposure limit of 17 ppm-hours (EPA Final Rule 2015; see Table SI-2). These levels of exposure continue to pose a risk to both ecosystems and people (Cisneros et al. 2010). As such, O_3 and other pollutants are major stressors for Park and Forest resources, and continued efforts to improve air quality in the region are critical to secure these gains. Through foliar injury surveys, we also confirmed that pollution injury is absent in the forest sites farthest removed from sources of primary pollution. Our results support recent distribution models that predict some parts of the region do not experience damaging O_3 exposures on a regular basis (Panek et al. 2013a).

New, lower EPA standards for human and ecosystem health will help preserve areas with the least compromised air quality and build on recent gains. But there is also a real possibility that these improvements will be eroded by changing climate and growing population of the region. Though per capita emissions are dropping,(Perry and Next10.org 2015) the population of the San Joaquin Valley is projected to continue climbing (California Department of Finance 2014) and warmer summers will strengthen stagnation events (Zhao et al. 2011). The result is expected O_3 declines of just 3-9% through 2050 (Steiner et al. 2006). California exemplifies the intersection of anthropogenic and climatic ecosystem stressors, but extensive temperate and tropical forests are also predicted to follow this trajectory, reaching O_3 levels that cause significant plant productivity losses by 2100 (Fowler et al. 1999, The Royal Society, Ainsworth et al. 2012). In addition to the forest impacts occurring elsewhere in California (Lake Tahoe, (Bytnerowicz et al. 2004) Yosemite/Central Sierra, (Carroll et al. 2003, Duriscoe and Stolte 1990) and the San Bernardino mountains, where this "X-disease" was first identified, Miller et al. 1963, Arbaugh et al. 1998) tropospheric O_3 pollution already causes injury under forest conditions across the globe. Impacted coniferous forests are well documented in the eastern United States, (Chappelka and Samuelson 1998, Karnosky et al. 2007) Mexico City, (de Bauer and Hernández-Tejeda 2007) eastern China, (Feng et al. 2014, Wan et al. 2014) the Alps, (Braun et al. 2014) and much of the Mediterranean Basin, from Spain to Italy (Kefauver et al. 2012, Paoletti 2006).

4.2 Linkages between long term exposure and tree injury

Our second question examines the extent of O_3 exposure's importance for injury under forest conditions. We found that cumulative O_3 exposure is strongly linked to OII, but not to water deficit. By continuing the efforts of Project FOREST and the SCOIAS, we have documented one of the longest records of elevated O_3 and resulting injury under forest conditions (Matyssek et al. 2010, Matyssek et al. 2012, Pretzsch et al. 2010). The linear relationship of exposure to tree response is comparable to that found in previous work across both the western slope of the Sierra Nevada and the San Bernardino mountains (Arbaugh et al. 1998, Salardino and Carroll 1998). Other common indices of ambient exposure, such as SUM0 and SUM06, share this strong linear relationship with injury in pines (Arbaugh et al. 1998). A cumulative index of exposure is well

matched to tree life history and specifically to the physiology of leaf tissue exposure to O_3. Within a single growing season, ponderosa pine exhibits declines in both gross photosynthesis and C assimilation that follow cumulative O_3 exposure (Grulke et al. 2002). Additionally, pine needles, while most active in their youngest years, continue C assimilation throughout their life; typically 4-5 years in ponderosa and 6-8 years in Jeffrey pine at these sites (Munz and Keck 1973, Patterson and Rundel 1989). The close link we found between $W126_{24}$ and injury supports the EPA's finding that cumulative, concentration weighted indices are the most biologically appropriate for assessing vegetation and ecosystem damage (U.S. Environmental Protection Agency 2013, 2015, Panek et al. 2002). Furthermore, $W126_{24}$ is important for capturing elevated O_3 in mountainous ecosystems during late evening and early morning hours. We expect that measures of stomatal conductance would also strongly correspond with injury, potentially even more so than a simple index (e.g. Braun et al. 2014 and Paoletti and Manning 2007). When focusing on the responses of natural vegetation in a mountain landscape, however, less monitoring-intensive indices like W126 are better suited. These indices may also be more practical in worldwide locations where meteorological and eco-physiological data is scarce.

The apparent variation in the exposure/injury relationship can be attributed to local and individual patterns of O_3 uptake. A tree will only sustain internal damage from O_3 if the pollutant is taken up via the stomata,(Reich 1987) and studies suggest that dry summers mediate stomatal O_3 flux. Thus, the effects of drought could prevent the impacts of elevated O_3 for individual trees or even whole forests (Grulke et al. 2002, Panek 2004, Grulke et al. 2003). This effect potentially contributes to lower-than-predicted injury in trees with greater water deficits (i.e. below the line, Figure 3). Despite this facultative role of water availability, our analysis found that in two ten year periods, annual water deficit did not relate to tree injury. This is potentially explained by both the high inter-annual variability of deficit relative to O_3 injury and the intentional design of the OII method to rate only damage caused by O_3. Chronic pollution has not altered the underlying pattern of injury response for trees in this study: over twenty years, trees have neither acclimated nor weakened. Considering that all trees were mature at initial surveys in 1991, this finding for trees under field conditions and prolonged stress is fully consistent with studies noting changes in sensitivity between plant developmental stages, but little change through time within mature individuals (Grulke and Miller 1994, Momen et al. 1997).

4.3 Tree growth declines and their consequences

Ponderosa and Jeffrey pines with evidence of O_3 injury also exhibit slowed growth rates under field conditions. Though estimates of growth reduction in mature trees vary widely, the extent of damage seen here agrees with some of the earliest damage observations in these species (McBride et al. 1975) and also with more recent field observations and physiological models. The relative biomass loss (RBL) that supports the NAAQS for O_3 is based on ponderosa pine seedlings exposed to $W126_{12}$ of 46.37 (20.5% RBL, measured in chambers) and mature trees (3.1% RBL, modeled in var. scopolorum; Constable and Taylor 1997, U.S. Environmental Protection Agency 2014). Previous work on Jeffrey pines in the southern Sierra reports losses of 11% in O_3 damaged individuals, (Peterson et al. 1987) but efforts to attribute growth losses of similar magnitude in injured ponderosa pines were not as conclusive (Peterson et al. 1991, Peterson and Arbaugh 1988). Arbaugh and others reported declines in basal area increment in the San Bernardino Mountains ranging from 7.8–23.2% during 1950-1974, when O_3 exposures reached their most extreme (Arbaugh et al. 1999). The growth effects in these forests were

attributed to the compound effects of O_3, drought, and N deposition. Later estimates of O_3 specific effects in the same region model biomass losses at 20.9% in 1980-85 and 10.3% in 1995-2000, after substantial improvements in air quality (Hogsett et al. 2007). With current field observed relative growth losses in injured trees ranging from 5.6-15.2%, the pines in this study confirm that elevated O_3 contributes to substantial reductions in growth for trees in the southern Sierra. Our analysis of growth further reveals that at equal O_3 injury levels, ponderosa pine growth exhibits slightly larger pollution impacts than Jeffrey pine growth, a distinction also observed in earlier work (Miller et al. 1983).

The key implications of reduced RGRs for injured trees are impacts to individual tree vitality and ultimately to forest productivity. Growth is a leading indicator of tree health, and slowed growth is often the herald of imminent mortality (Franklin et al. 1987, Keane et al. 2001, Das et al. 2007). But even before death, the chronic stress of decades of O_3 pollution transforms forest ecosystems. Outcomes of trees weakened by O_3 include increased susceptibility to successful bark beetle attack (Eatough Jones et al. 2004, Grulke 2009) and increased susceptibility to common pathogenic fungi (James et al. 1980, Fenn et al. 1990). Forests with such impacts are also prone to increased risk of wildfire and elevated mortality (Grulke 2009). We found that the survival rate of selected study trees in O_3 polluted sites did not differ from the survival of canopy trees in the forest at large (van Mantgem and Stephenson 2007). However, the sites with most exposure did exhibit the lowest survival, a pattern also found in a separate survey of the southern Sierra from 1977-2000 (Carroll et al. 2003). Part of the trees' relatively high survival rates can be ascribed to the intentional selection of healthy individuals to initiate monitoring and removal of diseased trees from observation during the course of the study, both choices that increase total survival rates. Since trees must be alive to provide information about their O_3 injury, the measurement of tree injury and measurement of demographic rates are necessarily at cross purposes. This project was designed to achieve the former, while relevant information on the latter emerged over time (Carroll et al. 2003, Miller et al. 1996).

Scaling from leaf and seedling O_3 effects, to mature, whole organism responses has long been a challenge due to the complexity of defense and compensation mechanisms at play (Kolb and Matyssek 2001, Samuelson and Kelly 2001). Similarly, scaling from single tree to ecosystem responses presents many uncertainties, but offers many applications in characterizing ecological dynamics and deciphering land-atmosphere interactions (Ainsworth et al. 2012). To better understand ecosystem effects, the roles of compound stress and the importance of climate should be accounted for. We investigated these links via climatic water deficit, finding that it was not a significant predictor of average growth rates among trees in the long term study. The importance of annual water deficit is potentially muted by our growth measurements, which were averaged over two ten year periods. To describe pollution's ecosystem impacts more completely, annual resolution data on tree growth, such as tree ring analysis, would better address the question of how O_3 response interacts with drought response.

In examining both tree growth and injury together, we found that tree vigor is compromised over the long term but also that the forest can recover from damage, albeit more slowly than the atmosphere can. The severity of foliar injury has lessened since 1991; remaining negative growth impacts may follow suit in the years to come. There is precedent for reversal of the effects of chronic pollution on forests, and if air quality continues to improve the Sierra may present another example (Battles et al. 2014, Likens et al. 1996, Thomas et al. 2013). But because trees

are very long lived and well equipped to endure centuries of adverse conditions, decades may pass before a change is realized (Bormann 1985, Smith et al. 2009). Injured trees now make up a transformed ecosystem that will carry a legacy of pollution impacts for many years to come and amplify the negative effects of fire suppression. Even at new extremes of anthropogenic air pollution, tree defenses are remarkably effective against chronic oxidative damage. Therefore, long term monitoring of both tree condition and forest O_3 exposure is critical for understanding the consequences of air pollution beyond experimental settings.

Though O_3 is a relatively short-lived pollutant in the troposphere, the effects of chronic exposure are evident in the foliar injury and growth of trees over the long term. Decades of severe O_3 pollution have accrued in damage to ponderosa and Jeffrey pines in the southern Sierra Nevada, and exposure continues to cause harm at many sites. Though air quality in the region is now improving, impacts to forests are still emerging and diligent work is needed to perpetuate recent gains. Tree responses to common pollutants form an important component of overall vegetative response to global change. The linkages between exposure and environmental processes are the foundation for critical load thresholds and regulations that protect natural resources (Fenn et al. 2011, U.S. Environmental Protection Agency 2014). With O_3 exposure in global forests expected to tread the same path that these California forests have already traveled, understanding tree responses here will help anticipate atmospheric pollution effects that have yet to be realized.

ACKNOWLEDGEMENTS

John Battles, University of California Berkeley, Annie Esperanza, National Park Service, and Ricardo Cisneros and Don Schweizer, University of California Merced, provided essential support and guidance on the development and completion of this work. They are acknowledged for their substantial contributions to the research.

Research was conducted with the permission of the National Park Service, study SEKI-00380. We thank USFS Region 5 Air Program for sharing air quality data (http://app.airsis.com/USFS/) and Susan Schilling for maintaining and sharing Project FOREST data. Thanks to Koren Nydick and Tom Warner for help with absolutely essential logistics and equipment. The authors also thank Dan Duriscoe for help training the field crew and leading earlier surveys. Debra Swenson, Eric Olliff, David Soderberg, John Sanders, Natalie Holt, Alex Javier, Lupe Amezquita, Maria Cisneros, and Juan Rodriguez were instrumental in forest data collection. We are further grateful to Erik Meyer, Heather Veerkamp, Becky Lindstrom, and Ariane Sarzotti for maintaining O_3 instrumentation and data. David Ackerly and Scott Stephens provided useful comments on the draft manuscript. Partial funding was provided by the California Energy Commission under contract 500-10-046. Stella Cousins was supported by the Baker-Bidwell Fellowship, the William Carroll Smith Plant Pathology Fellowship, and UC President's Carbon Neutrality Initiative Fellowship.

FIGURES AND TABLES

A)

B)

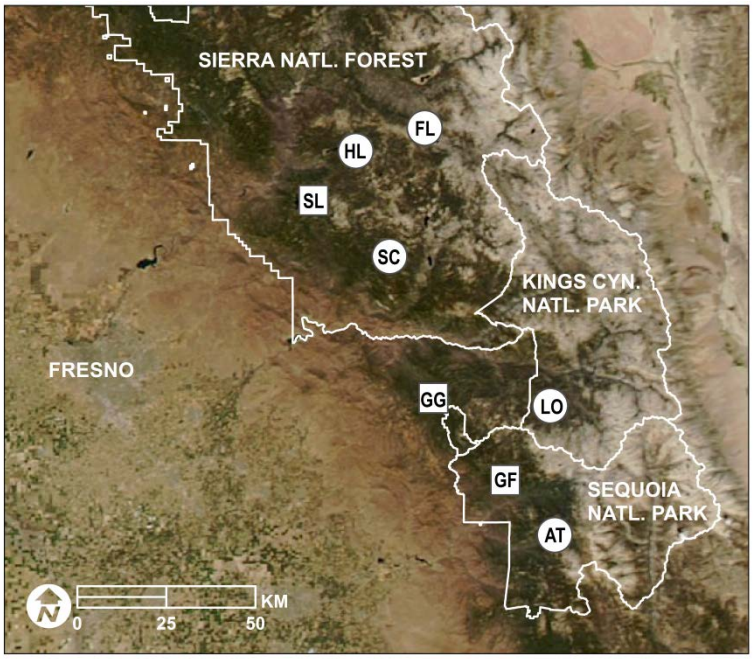

Figure 1
A)

Chlorotic mottle affecting Jeffrey pine needles under forest conditions. Mottle presents as pale yellow areas indicative of injury to internal tissues. Pale brown discoloration, visible at left, is generally caused by weather damage. Photo and map: S. Cousins

B)

Research sites, Sierra National Forest and Sequoia and Kings Canyon National Parks, California. Squares indicate long term study sites, 1991-2012: SL, Shaver Lake; GG, Grant Grove, and GF, Giant Forest. Circles indicate short term sites, added 2011-2012. FL, Florence Lake; HL, Huntington Lake; SC, Snow Corral; LO, Sugarloaf Basin; AT, Atwell Mill. (Photo: AQUA, September 2014)

A)

B)

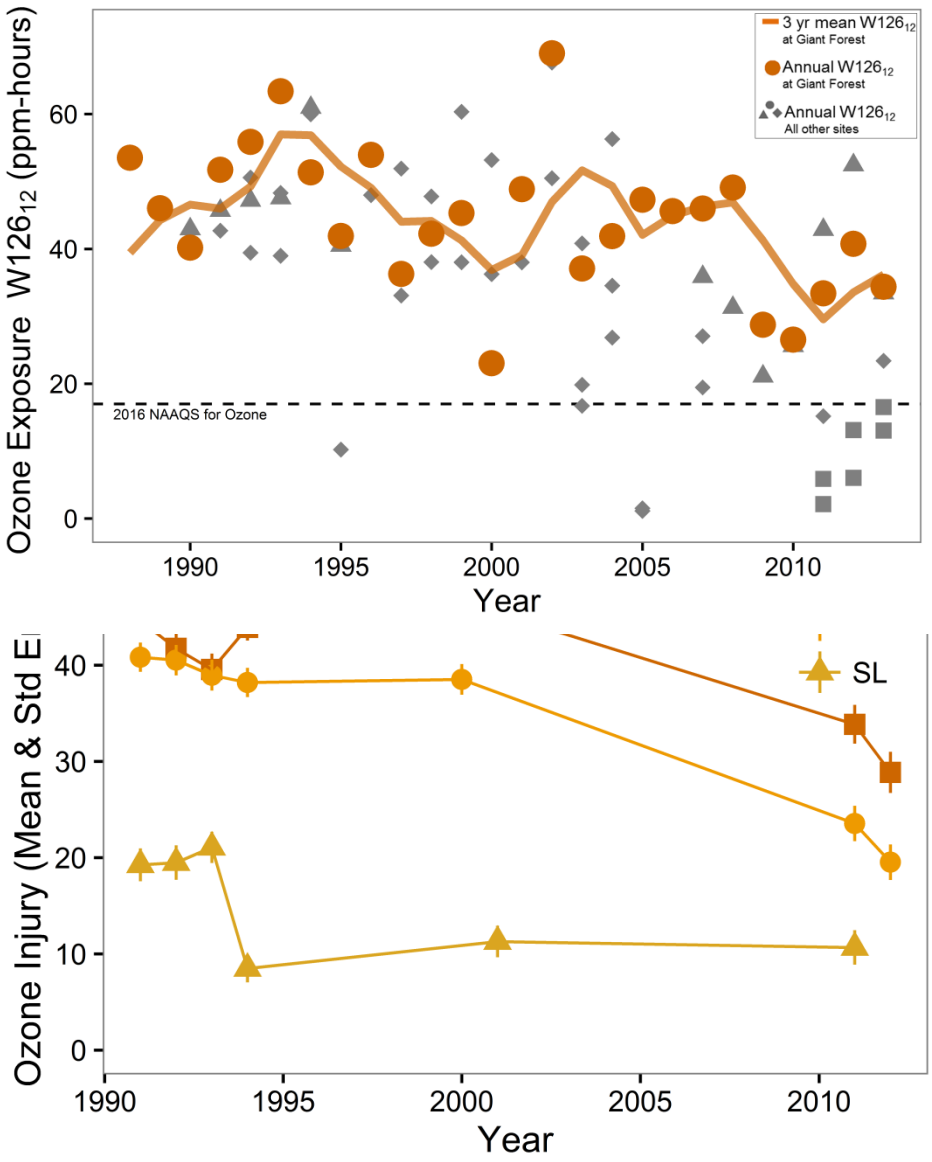

Figure 2

A) Ozone exposure ($W126_{12}$, July-September) at Giant Forest (circles) and other southern Sierra Nevada sites, 1991-2013. Sites with intermittent monitoring include Grant Grove (triangles), Shaver Lake, Atwell Mill, and Snow Corral (diamonds), and most recently, Florence Lake and Huntington Lake (squares). As of October 2015, the National Ambient Air Quality Standard for ozone provides protection equivalent to a limit of 17 ppm-hours in terms of a 3-year W126 index. See Supporting Information Tables 1-2 for additional detail.

B) Mean ozone injury index (OII) declined from 1991-2012 at all long term sites: Giant Forest, Grant Grove, and Shaver Lake. OII is a weighted measure of tree injury; see Figure 2 for appearance of ozone damaged pine needles and Supporting Information 3. Ozone Injury Index for survey methods.

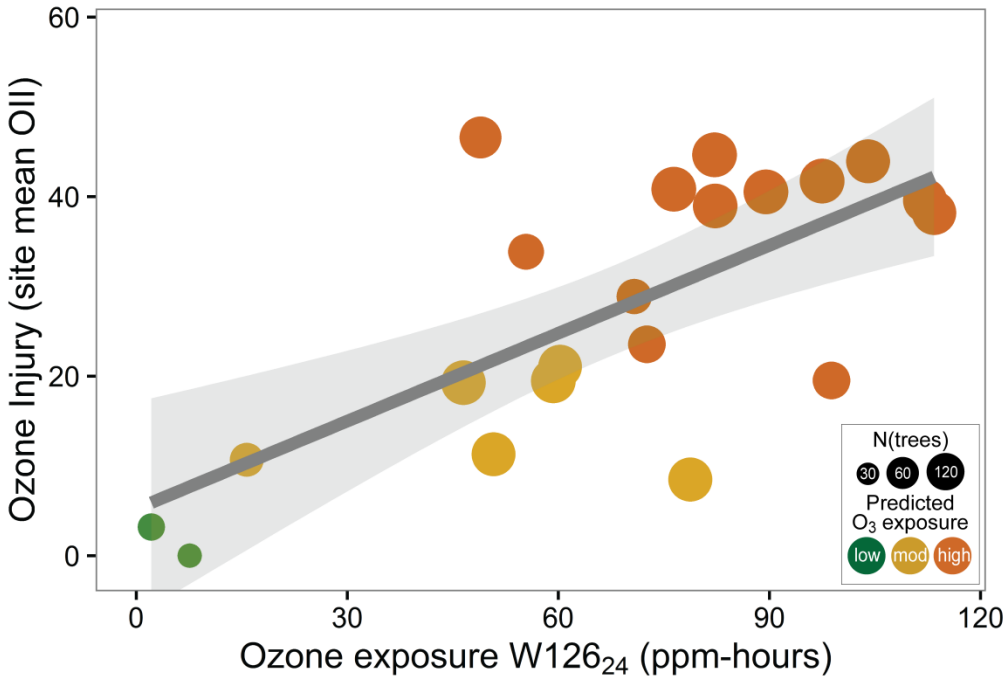

Figure 3
Regression of tree injury (OII) on O_3 exposure ($W126_{24}$) The relationship across all observed trees is OII= 0.33 ($W126_{24}$) ± 0.08; R^2=0.48, t=4.33, p<0.001. Gray shading indicates 95% confidence interval. With 4 year cumulative $W126_{24}$ (not pictured), the relationship strengthens: OII= 0.11($W126_{24}$) + 0.02; R^2=0.60, t=4.78, p<0.001). Predicted summer O_3 exposure per reference 32.

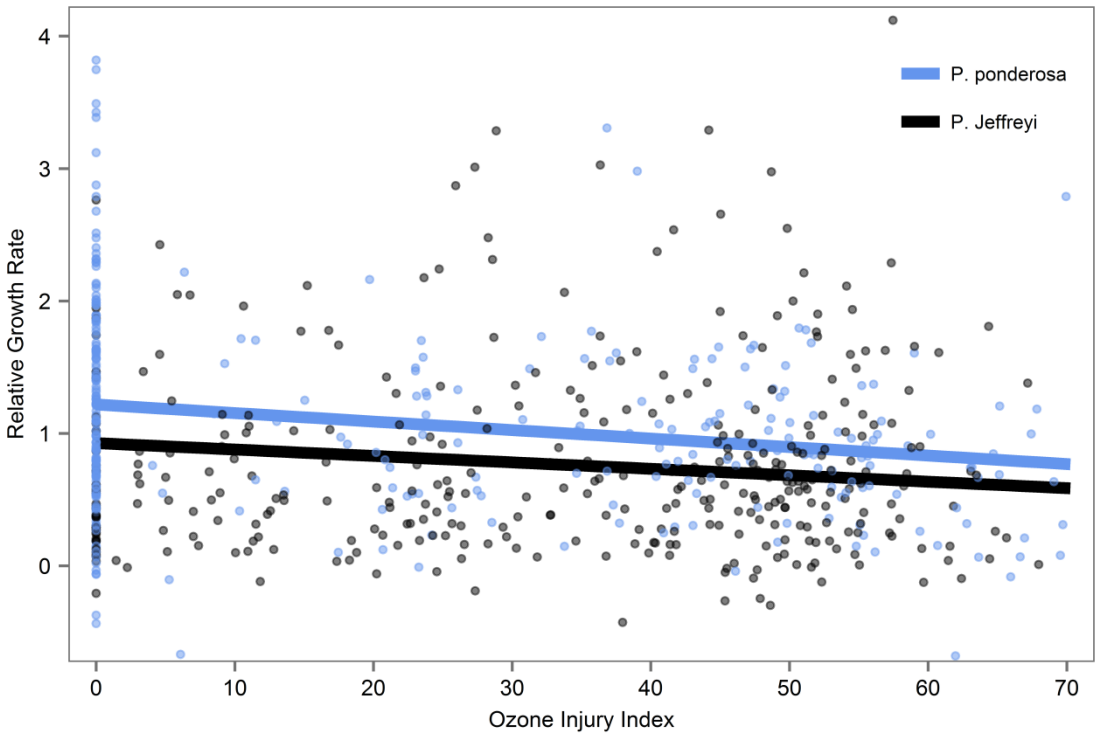

Figure 4
Linear mixed effects model of relative growth rate (RGR), percent DBH per year, as related to ozone injury index (OII). Lines represent overall model relationship for a tree of median diameter within each species. Points indicate individual trees in periods 1991-2000 and 2001-2012. Ponderosa pine grows more rapidly than Jeffrey pine and is also more negatively affected by O_3 injury. Equation summarizing the overall relationship is RGR = - 0.139 - 0.142 OII – 0.38(DBH) – 0.138(SPP) + 0.145(OII:SPP) ~ 1|ID

REFERENCES

Ainsworth, E. A., C. R. Yendrek, S. Sitch, W. J. Collins, and L. D. Emberson. 2012. The Effects of Tropospheric Ozone on Net Primary Productivity and Implications for Climate Change. Annual Review of Plant Biology **63**:637-661.

Arbaugh, M., P. Miller, J. Carroll, and B. Takemoto. 1998. Relationships of ozone exposure to pine injury in the Sierra Nevada and San Bernardino Mountains of California, USA. Environmental Pollution **101**:291-301.

Arbaugh, M. J., and A. Bytnerowicz. 2003. Introduction to a regional passive ozone sampler network in the Sierra Nevada. Pages 157-164 *in* A. Bytnerowicz, M. J. Arbaugh, and R. Alonso, editors. Ozone air pollution in the Sierra Nevada: distribution and effects on forests. Elsevier Science Ltd., Oxford.

Arbaugh, M. J., D. L. Peterson, and P. R. Miller. 1999. Air pollution effects on growth of ponderosa pine, Jeffrey pine, and bigcone Douglas-fir. Pages 179 - 207 *in* P. R. Miller and J. R. McBride, editors. Oxidant Air Pollution Impacts in the Montane Forests of Southern California: A Case Study of the San Bernardino Mountains. Springer, New York.

Battles, J. J., T. J. Fahey, C. T. Driscoll, J. D. Blum, and C. E. Johnson. 2014. Restoring Soil Calcium Reverses Forest Decline. Environmental Science & Technology Letters **1**:15-19.

Beaver, S., and A. Palazoglu. 2009. Influence of synoptic and mesoscale meteorology on ozone pollution potential for San Joaquin Valley of California. Atmospheric Environment **43**:1779-1788.

Beaver, S., S. Tanrikulu, A. Palazoglu, A. Singh, S. T. Soong, Y. Q. Jia, C. Tran, B. Ainslie, and D. G. Steyn. 2010. Pattern-Based Evaluation of Coupled Meteorological and Air Quality Models. Journal of Applied Meteorology and Climatology **49**:2077-2091.

Bormann, F. H. 1985. Air Pollution and Forests: An Ecosystem Perspective. BioScience **35**:434-441.

Braun, S., C. Schindler, and B. Rihm. 2014. Growth losses in Swiss forests caused by ozone: Epidemiological data analysis of stem increment of Fagus sylvatica L. and Picea abies Karst. Environmental Pollution **192**:129-138.

Burnham, K. P., and D. R. Anderson. 2002. Model Selection and Multimodel Inference: A Practical Information-Theoretic Approach. 2nd edition. Springer-Verlag.

Bytnerowicz, A., M. Arbaugh, and P. E. Padgett. 2004. Evaluation of Ozone and HNO_3 Vapor Distribution and Ozone Effects on Conifer Forests in the Lake Tahoe Basin and Eastern Sierra Nevada: Final Report. California Air Resources Board Contract No. 01-334.

Bytnerowicz, A., M. J. Arbaugh, and R. Alonso, editors. 2003. Ozone air pollution in the Sierra Nevada: distribution and effects on forests. . Elsevier Science Ltd.

Bytnerowicz, A., J. D. Burley, R. Cisneros, H. K. Preisler, S. Schilling, D. Schweizer, J. Ray, D. Dulen, C. Beck, and B. Auble. 2013a. Surface ozone at the Devils Postpile National Monument receptor site during low and high wildland fire years. Atmospheric Environment **65**:129-141.

Bytnerowicz, A., M. Fenn, S. McNulty, F. Yuan, A. Pourmokhtarian, C. Driscoll, and T. Meixner. 2013b. Interactive Effects of Air Pollution and Climate Change on Forest Ecosystems in the United States: Current Understanding and Future Scenarios. Pages 333-369 *in* R. Matyssek, N. Clarke, P. Cudlin, T. N. Mikkelsen, J. P. Tuovinen, G. Wieser, and E. Paoletti, editors. Developments in Environmental Science. Elsevier.

California Department of Finance. 2014. Report P-1 (County): State and County Total Population Projections, 2010-2060 (5-year increments). Sacramento, CA. [Available online: http://www.dof.ca.gov/research/demographic/reports/projections/P-1/].

California Environmental Protection Agency - Air Resources Board. 2015. Air Quality and Meteorological Information System. [Available online at: http://www.arb.ca.gov/aqmis2/aqdselect.php?tab=hourly].

Carroll, J., P. R. Miller, and J. Pronos. 2003. Historical perspectives on ambient ozone and its effects on the Sierra Nevada. In: Ozone air pollution in the Sierra Nevada: distribution and effects on forests. Bytnerowicz, A., Arbaugh, M.J., and Alonso, R., Eds. In: Developments in Environmental Science, Krupa, S.V., Ed. No. 2. Elsevier.

Carroll, J. J., and A. J. Dixon. 1993. Sierra Cooperative Ozone Impact Assessment Study: Year 3. Volumes 1 and 2. Final Report Contract No A132-188. Prepared for the California Air Resources Board, Research Division, October 1993.

Carroll, J. J., and A. J. Dixon. 1995. Sierra Cooperative Ozone Impact Assessment Study: Year 4. Volumes 1 and 2. Final Report Contract No 92-346. Prepared for the California Air Resources Board, Research Division, May 1995.

Chappelka, A. H., and L. J. Samuelson. 1998. Ambient ozone effects on forest trees of the eastern United States: a review. New Phytologist **139**:91-108.

Cisneros, R., A. Bytnerowicz, D. Schweizer, S. Zhong, S. Traina, and D. H. Bennett. 2010. Ozone, nitric acid, and ammonia air pollution is unhealthy for people and ecosystems in southern Sierra Nevada, California. Environmental Pollution **158**:3261-3271.

Constable, J. V. H., and G. E. Taylor, Jr. . 1997. Modeling the effects of elevated tropospheric O_3 on two varieties of Pinus ponderosa. Canadian Journal of Forest Research **27**:527-537.

Crawley, M. J. 2002. Statistical Computing: An Introduction to Data Analysis using S-Plus. Wiley, Hoboken, NJ, p. 772.

Das, A., J. Battles, N. Stephenson, and P. van Mantgem. 2007. The relationship between tree growth patterns and likelihood of mortality: a study of two tree species in the Sierra Nevada. Canadian Journal of Forest Research **37**:580-597.

de Bauer, M. d. L., and T. Hernández-Tejeda. 2007. A review of ozone-induced effects on the forests of central Mexico. Environmental Pollution **147**:446-453.

Duriscoe, D. M., and K. W. Stolte. 1990. Cruise survey of oxidant air pollution injury to Pinus ponderosa and Pinus jeffreyi in Saguaro National Monument, Yosemite National Park, and Sequoia and Kings Canyon National Parks. NPS/AQD-90/003,USDI National Park Service Air Quality Division, Denver, CO.

Eatough Jones, M., T. D. Paine, M. E. Fenn, and M. A. Poth. 2004. Influence of ozone and nitrogen deposition on bark beetle activity under drought conditions. Forest Ecology and Management **200**.

Eitzel, M. V., J. Battles, R. York, and P. de Valpine. 2015. Can't see the trees for the forest: complex factors influence tree survival in a temperate second growth forest. Ecosphere **6**:1-17.

Fay, M. P., and P. A. Shaw. 2010. Exact and Asymptotic Weighted Logrank Tests for Interval Censored Data: The interval R package. Journal of Statistical Software. http://www.jstatsoft.org/v36/ i02/. 36 (2):1-34.

Feng, Z., J. Sun, W. Wan, E. Hu, and V. Calatayud. 2014. Evidence of widespread ozone-induced visible injury on plants in Beijing, China. Environmental Pollution **193**:296-301.

Fenn, M. E., P. H. Dunn, and R. Wilborn. 1990. Black Stain Root Disease in Ozone-Stressed Ponderosa Pine. Plant Disease **74**:426-430.

Fenn, M. E., K. F. Lambert, T. F. Blett, D. A. Burns, L. H. Pardo, G. M. Lovett, R. A. Haeuber, D. C. Evers, C. T. Driscoll, and D. S. Jeffries. 2011. Setting Limits: Using Air Pollution Thresholds to Protect and Restore U.S. Ecosystems. Issues in Ecology:Published by the Ecological Society of America.

Flint, L. E., A. L. Flint, J. F. Thorne, and R. Boynton. 2013. Fine-scale hydrologic modeling for regional landscape applications: the California Basin Characterization Model development and performance. Ecological Processes **2**.

Forster, P., Ramaswamy, V., Artaxo, P., Berntsen, T., Betts, R., Fahey, D.W., Haywood, J., Lean, J., Lowe, D.C., Myhre, G., Nganga, J., Prinn, R., Raga, G., Schulz M., and Van Dorland, R.,. 2007. Changes in Atmospheric Constituents and in Radiative Forcing. . Climate Change 2007: The Physical Science Basis. Contribution of Working Group I to

the Fourth Assessment Report of the Intergovernmental Panel on Climate Change [Solomon, S., D. Qin, M. Manning, Z. Chen, M. Marquis, K.B. Averyt, M.Tignor and H.L. Miller (eds.)]. Cambridge University Press, Cambridge, United Kingdom and New York, NY, USA.

Fowler, D., J. Cape, M. Coyle, C. Flechard, J. Kuylenstierna, K. Hicks, D. Derwent, C. Johnson, and D. Stevenson. 1999. The global exposure of forests to air pollutants. Water Air and Soil Pollution **116**:5-32.

Franklin, J. F., H. H. Shugart, and M. E. Harmon. 1987. Tree death as an ecological process. BioScience **37**:550-556.

Gauss, M., G. Myhre, I. S. A. Isaksen, V. Grewe, G. Pitari, O. Wild, W. J. Collins, F. J. Dentener, K. Ellingsen, L. K. Gohar, D. A. Hauglustaine, D. Iachetti, F. Lamarque, E. Mancini, L. J. Mickley, M. J. Prather, J. A. Pyle, M. G. Sanderson, K. P. Shine, D. S. Stevenson, K. Sudo, S. Szopa, and G. Zeng. 2006. Radiative forcing since preindustrial times due to ozone change in the troposphere and the lower stratosphere. Atmos. Chem. Phys. **6**:575-599.

Grulke, N. E., R. Alonso, T. Nguyen, C. Cascio, and W. Dobrowolski. 2004. Stomata open at night in pole-sized and mature ponderosa pine: implications for O_3 exposure metrics. Tree Physiology **24**:1001-1010.

Grulke, N. E., and L. Balduman. 1999. Deciduous Conifers: High N Deposition and O_3 Exposure Effects on Growth and Biomass Allocation in Ponderosa Pine. Water, Air, and Soil Pollution **116**:235-248.

Grulke, N. E., R. Johnson, A. Esperanza, D. Jones, T. Nguyen, S. Posch, and M. Tausz. 2003. Canopy transpiration of Jeffrey pine in mesic and xeric microsites: O_3 uptake and injury response. Trees **17**:292-298.

Grulke, N. E., and P. R. Miller. 1994. Changes in gas exchange characteristics during the life span of giant sequoia: implications for response to current and future concentrations of atmospheric ozone. Tree Physiology **14**:659-668.

Grulke, N. E., Minnich, R.A., Paine, T.D., Seybold, S.J., Chavez, D.J., Fenn, M.E., Riggan, P.J., Dunn, A., . 2009. Air pollution increases forest susceptibility to wildfires: a case study in the San Bernardino Mountains in southern California. In: Bytnerowicz, A., Arbaugh, M.J., Riebau, A.R., Andersen, C. (Eds.), Wildland Fires and Air Pollution. Developments in Environmental Science, vol. 8. Elsevier, Amsterdam, pp. 365–403.

Grulke, N. E., E. Paoletti, and R. L. Heath. 2007. Comparison of calculated and measured foliar O_3 flux in crop and forest species. Environmental Pollution **146**:640-647.

Grulke, N. E., H. K. Preisler, C. Rose, J. Kirsch, and L. Balduman. 2002. O_3 uptake and drought stress effects on carbon acquisition of ponderosa pine in natural stands. New Phytologist **154**:621-631.

Heath, R. L. 1987. The Biochemistry of Ozone Attack on the Plasma Membrane of Plant Cells. Pages 29-54 *in* J. A. Saunders, L. Kosak-Channing, and E. E. Conn, editors. Phytochemical Effects of Environmental Compounds. Springer US.

Hogsett, W. E., D. T. Tingey, E. H. Lee, P. A. Beedlow, and C. P. Andersen. 2007. An Approach for Evaluating the Effectiveness of Various Ozone Air Quality Standards for Protecting Trees. Environmental Management **41**:937-948.

James, R. L., F. W. Cobb Jr., P. R. Miller, and J. R. Parmeter Jr. 1980. Effects of Oxidant Air Pollution on Susceptibility of Pine Roots to *Fomes annosus*. Phytopathology **70**:560-563.

Juknys, R., A. Augustaitis, J. Venclovienė, A. Kliučius, A. Vitas, E. Bartkevičius, and N. Jurkonis. 2014. Dynamic response of tree growth to changing environmental pollution. European Journal of Forest Research **133**:713-724.

Kaplan, E. L., and P. Meier. 1958. Nonparametric-Estimation from Incomplete Observations. Journal of the American Statistical Association **53**:457-481.

Karnosky, D. F., J. M. Skelly, K. E. Percy, and A. H. Chappelka. 2007. Perspectives regarding 50 years of research on effects of tropospheric ozone air pollution on US forests. Environmental Pollution **147**:489-506.

Keane, R. E., M. Austin, C. Field, A. Huth, M. Lexer, D. Peters, A. Solomon, and P. Wyckoff. 2001. Tree mortality in gap models: application to climate change. Climatic Change **51**:509-540.

Kefauver, S. C., J. Penuelas, and S. L. Ustin. 2012. Improving assessments of tropospheric ozone injury to Mediterranean montane conifer forests in California (USA) and Catalonia (Spain) with GIS models related to plant water relations. Atmospheric Environment **62**:41-49.

Kellomäki, S., and K. Y. Wang. 1997. Effects of elevated O_3 and CO_2 concentrations on photosynthesis and stomatal conductance in Scots pine. Plant, Cell & Environment **20**:995-1006.

King, J. S., M. E. Kubiske, K. S. Pregitzer, G. R. Hendrey, E. P. McDonald, C. P. Giardina, V. S. Quinn, and D. F. Karnosky. 2005. Tropospheric O_3 compromises net primary production in young stands of trembling aspen, paper birch and sugar maple in response to elevated atmospheric CO_2. New Phytologist **168**:623-636.

Kolb, T., and R. Matyssek. 2001. Limitations and perspectives about scaling ozone impacts in trees. Environmental Pollution **115**:373-392.

Krupa, S., M. McGrath, C. Andersen, F. Booker, K. Burkey, A. Chappelka, B. Chevone, E. Pell, and B. Zilinskas. 2001. Ambient ozone and plant health. Plant Disease **85**:4-12.

Lefohn, A. S., and V. C. Runeckles. 1987. Establishing standards to protect vegetation—ozone exposure/dose considerations. Atmospheric Environment **21**:561-568.

Likens, G. E., C. T. Driscoll, and D. C. Buso. 1996. Long-Term Effects of Acid Rain: Response and Recovery of a Forest Ecosystem. Science **272**:244-246.

Massman, W. J. 2004. Toward an ozone standard to protect vegetation based on effective dose: a review of deposition resistances and a possible metric. Atmospheric Environment **38**:2323-2337.

Matyssek, R., D. F. Karnosky, G. Wieser, K. Percy, E. Oksanen, T. E. Grams, M. Kubiske, D. Hanke, and H. Pretzsch. 2010. Advances in understanding ozone impact on forest trees: messages from novel phytotron and free-air fumigation studies. Environ Pollut **158**:1990-2006.

Matyssek, R., H. Sandermann, K. Esser, U. Lüttge, W. Beyschlag, and F. Hellwig. 2003. Impact of Ozone on Trees: an Ecophysiological Perspective. Pages 349-404 *in* U. Lüttge, W. Beyschlag, B. Büdel, and D. Francis, editors. Progress in Botany. Springer.

Matyssek, R., G. Wieser, C. Calfapietra, W. de Vries, P. Dizengremel, D. Ernst, Y. Jolivet, T. N. Mikkelsen, G. M. J. Mohren, D. Le Thiec, J. P. Tuovinen, A. Weatherall, and E. Paoletti. 2012. Forests under climate change and air pollution: Gaps in understanding and future directions for research. Environmental Pollution **160**:57-65.

McBride, J., V. Semion, and P. Miller. 1975. Impact of air pollution on the growth of ponderosa pine. California Agriculture **29**.

Miller, P., K. Stolte, D. M. Duriscoe, and J. Pronos. 1996. Evaluating Ozone Air Pollution Effects on Pines in the Western United States. USDA Forest Service General Technical Report PSW-155:1-87.

Miller, P. A., O. C. Taylor, and R. G. Wilhour. 1982. Oxidant Air Pollution Effects on a Western Coniferous Forest Ecosystem. Environmental Protection Agency, Research and Development. Environmental Research Laboratory Corvallis, OR. EPA-600/D-82-276

Miller, P. R., G. J. Longbotham, and C. R. Longbotham. 1983. Sensitivity of Selected Western Conifers to Ozone. Plant Disease **67**:1113-1115.

Miller, P. R., M. H. McCutchan, and H. P. Milligan. 1972. Oxidant air pollution in the Central Valley, Sierra Nevada foothills, and Mineral King Valley of California. Atmospheric Environment **6**:623-633.

Miller, P. R., and A. A. Millecan. 1971. Extent of oxidant air pollution damage to some pines and other conifers in California. Plant Disease Reporter **55**:555-559.

Miller, P. R., J. R. Parmeter Jr, O. C. Taylor, and E. A. Cardiff. 1963. Ozone injury to the foliage of Pinus ponderosa. Phytopathology **53**:1072-1076.

Momen, B., P. D. Anderson, J. A. Helms, and J. L. J. Houpis. 1997. Acid Rain and Ozone Effects on Gas Exchange of Pinus ponderosa: A Comparison between Trees and Seedlings. International Journal of Plant Sciences **158**:617-621.

Munz, P. A., and D. D. Keck. 1973. A California Flora and Supplement. University of California Press, Berkeley, CA.

Musselman, R. C., A. S. Lefohn, W. J. Massman, and R. L. Heath. 2006. A critical review and analysis of the use of exposure- and flux-based ozone indices for predicting vegetation effects. Atmospheric Environment **40**:1869-1888.

Musselman, R. C., and T. J. Minnick. 2000. Nocturnal stomatal conductance and ambient air quality standards for ozone. Atmospheric Environment **34**:719-733.

National Park Service - Air Resources Division. 2013. Air quality in national parks: trends (2000–2009) and conditions (2005–2009). Natural Resource Report NPS/NRSS/ARD/NRR—2013/683. National Park Service, Denver, Colorado.

National Park Service - Air Resources Division. 2015. NPS Gaseous Pollutant and Meteorological Data, Sequoia and Kings Canyon National Park. Gaseous Pollutant Monitoring Program, Denver, CO. Distributed by Air Resource Specialists, Inc. [Available online: http://ard-request.air-resource.com/] Denver, CO.

Panek, J., D. Saah, A. Esperanza, A. Bytnerowicz, W. Fraczek, and R. Cisneros. 2013a. Ozone distribution in remote ecologically vulnerable terrain of the southern Sierra Nevada, CA. Environmental Pollution **182**:343-356.

Panek, J. A. 2004. Ozone uptake, water loss and carbon exchange dynamics in annually drought-stressed Pinus ponderosa forests: measured trends and parameters for uptake modeling. Tree Physiology **24**:277.

Panek, J. A., M. R. Kurpius, and A. H. Goldstein. 2002. An evaluation of ozone exposure metrics for a seasonally drought-stressed ponderosa pine ecosystem. Environmental Pollution **117**:93-100.

Panek, J. A., D. Saah, and A. Esperanza. 2013b. A natural resource condition assessment for Sequoia and Kings Canyon National Parks: Appendix 2. Air Quality. Air Quality, 2013, National Park Service; Fort Collins, Colorado, National Park Service, Natural Resource Report. NPS/SEKI/NRRd2013/665.2.

Paoletti, E. 2006. Impact of ozone on Mediterranean forests: A review. Environmental Pollution **144**:463-474.

Paoletti, E., and W. J. Manning. 2007. Toward a biologically significant and usable standard for ozone that will also protect plants. Environmental Pollution **150**:85-95.

Patterson, M. T., and P. W. Rundel. 1989. Ozone impacts on photosynthetic capacity of Jeffrey pine in Sequoia National Park. Final Report, Project PX-001-7-1152; Denver, Colorado, Air Quality Division, USDI National Park Service; 34 pp.

Pedersen, B. S. 1998. Modeling tree mortality in response to short- and long-term environmental stresses. Ecological Modelling **105**:347-351.

Perry, F. N., and Next10.org. 2015. California Green Innovation Index: International Edition. Next 10, San Francisco, CA. [Available online: http://next10.org/international].

Peterson, D., M. Arbaugh, and L. Robinson. 1991. Regional growth changes in ozone-stressed ponderosa pine (Pinus ponderosa) in the Sierra Nevada, California, USA. The Holocene **1**:50.

Peterson, D. L., and M. J. Arbaugh. 1988. An Evaluation of the Effects of Ozone Injury on Radial Growth of Ponderosa Pine (Pinus ponderosa) in the Southern Sierra Nevada. Journal of the Air Pollution Control Association **38**:921-927.

Peterson, D. L., M. J. Arbaugh, V. A. Wakefield, and P. R. Miller. 1987. Evidence of Growth Reduction in Ozone-Injured Jeffrey Pine (*Pinus jeffreyi* Grev. and Balf.) in Sequoia and Kings Canyon National Parks. Journal of the Air Pollution Control Association **37**:906-912.

Pinheiro, J., D. Bates, S. DebRoy, and D. Sarkar. 2014. Package 'nlme', Linear and Nonlinear Mixed Effects Models. Documentation: http://cran.r-project.org/web/packages/nlme/nlme.pdf.

Pretzsch, H., J. Dieler, R. Matyssek, and P. Wipfler. 2010. Tree and stand growth of mature Norway spruce and European beech under long-term ozone fumigation. Environmental Pollution **158**:1061-1070.

R Core Team. 2016. R: A language and environment for statistical computing. R Foundation for Statistical Computing, Vienna, Austria. URL https://www.R-project.org/.

Reich, P. B. 1987. Quantifying plant response to ozone: a unifying theory. Tree Physiology **3**:63-91.

Reich, P. B., and R. G. Amundson. 1985. Ambient Levels of Ozone Reduce Net Photosynthesis in Tree and Crop Species. Science **230**:566-570.

Salardino, D. H., and J. J. Carroll. 1998. Correlation between ozone exposure and visible foliar injury in ponderosa and Jeffrey pines. Atmospheric Environment **32**:3001-3010.

Samuelson, L., and J. Kelly. 2001. Scaling ozone effects from seedlings to forest trees. New Phytologist.

San Joaquin Valley Air Pollution Control District. 2007. 2007 Ozone Plan.

San Joaquin Valley Air Pollution Control District. 2010. 2010 Ozone Mid-Course Review. Fresno, California June 2010. .

Sheil, D., and R. M. May. 1996. Mortality and Recruitment Rate Evaluations in Heterogeneous Tropical Forests. Journal of Ecology **84**:91-100.

Sitch, S., P. M. Cox, W. J. Collins, and C. Huntingford. 2007. Indirect radiative forcing of climate change through ozone effects on the land-carbon sink. Nature **448**:791-794.

Smith, M. D., A. K. Knapp, and S. L. Collins. 2009. A framework for assessing ecosystem dynamics in response to chronic resource alterations induced by global change. Ecology **90**:3279-3289.

Steiner, A. L., S. Tonse, R. C. Cohen, A. H. Goldstein, and R. A. Harley. 2006. Influence of future climate and emissions on regional air quality in California. Journal of Geophysical Research: Atmospheres **111**:n/a-n/a.

Stephenson, N. L. 1988. Climatic control of vegetation distribution: the role of the water balance with examples from North America and Sequoia National Park, California. Cornell University, Ithaca, NY.

Stephenson, N. L. 1998. Actual evapotranspiration and deficit: biologically meaningful correlates of vegetation distribution across spatial scales. Journal of Biogeography **25**:855-870.

Sun, G. E., S. B. McLaughlin, J. H. Porter, J. Uddling, P. J. Mulholland, M. B. Adams, and N. Pederson. 2012. Interactive influences of ozone and climate on streamflow of forested watersheds. Global Change Biology **18**:3395-3409.

Temple, P., and P. Miller. 1994. Foliar ozone injury and radial growth of ponderosa pine. Canadian Journal of Forest Research **24**:1877-1882.

The Royal Society. 2008. Ground-level Ozone in the 21st century: Future Trends, Impacts, and Policy Implications. Royal Society Science Policy Report 15/08, RS1276, 2008; https://royalsociety.org/~/media/Royal_Society_Content/policy/publications/2008/7925.pdf.

Therneau, T. 2015. A Package for Survival Analysis in S. version 2.38, http://CRAN.R-project.org/package=survival.

Thomas, R. B., S. E. Spal, K. R. Smith, and J. B. Nippert. 2013. Evidence of recovery of Juniperus virginiana trees from sulfur pollution after the Clean Air Act. Proceedings of the National Academy of Sciences **110**:15319-15324.

U.S. Environmental Protection Agency. 2007. Technical Report on Ozone Exposure, Risk, and Impact Assessments for Vegetation. Office of Air Quality Planning and Standards, Health and Environmental Impacts Division, Research Triangle Park, NC. Page Online: http://www.epa.gov/ttn/naaqs/standards/ozone/data/2007_2001_environmental_tsd.pdf.

U.S. Environmental Protection Agency. 2013. Integrated Science Assessment for Ozone and Related Photochemical Oxidants. Office of Research and Development, National Center for Environmental Assessment. Research Triangle Park, NC.

U.S. Environmental Protection Agency. 2014. Welfare Risk and Exposure Assessment for Ozone.*in* O. o. A. a. Radiation, editor., Office of Air Quality Planning and Standards; Health and Environmental Impacts Division; Risk and Benefits Group Research Triangle Park, NC. Publication No. EPA-452/R-14-005a.

U.S. Environmental Protection Agency. 2015. National Ambient Air Quality Standards for Ozone; Final Rule. Federal Register Vol. 80, No. 206 October 26, 2015. Rules and Regulations 40 CFR Parts 50, 51, 52, 53, and 58. United States Government Printing Office, Washington, D.C. Pages 65292-65468.

U.S. Forest Service, National Park Service, and U.S. Fish and Wildlife Service. Federal land managers' air quality related values work group (FLAG): phase I report—revised (2010). Natural Resource Report NPS/NRPC/NRR—2010/232. 2010. National Park Service, Denver, Colorado.

Van Dingenen, R., F. J. Dentener, F. Raes, M. C. Krol, L. Emberson, and J. Cofala. 2009. The global impact of ozone on agricultural crop yields under current and future air quality legislation. Atmospheric Environment **43**:604-618.

van Mantgem, P. J., and N. L. Stephenson. 2007. Apparent climatically induced increase of tree mortality rates in a temperate forest. Ecology Letters **10**:909-916.

van Mantgem, P. J., N. L. Stephenson, J. C. Byrne, L. D. Daniels, J. F. Franklin, P. Z. Fule, M. E. Harmon, A. J. Larson, J. M. Smith, A. H. Taylor, and T. T. Veblen. 2009. Widespread Increase of Tree Mortality Rates in the Western United States. Science **323**:521-524.

Volz, A., and D. Kley. 1988. Evaluation of the Montsouris series of ozone measurements made in the nineteenth century. Nature **332**:240-242.

Wan, W., W. J. Manning, X. Wang, H. Zhang, X. Sun, and Q. Zhang. 2014. Ozone and ozone injury on plants in and around Beijing, China. Environmental Pollution **191**:215-222.

Western Regional Climate Center. 2015. Cooperative climatalogical data summaries. US Cooperative Observer Program, NOAA-NWS. [Available online at: http://www.wrcc.dri.edu/coopmap/].

Wittig, V. E., E. A. Ainsworth, and S. P. Long. 2007. To what extent do current and projected increases in surface ozone affect photosynthesis and stomatal conductance of trees? A meta-analytic review of the last 3 decades of experiments. Plant, Cell & Environment **30**:1150-1162.

Wittig, V. E., E. A. Ainsworth, S. L. Naidu, D. F. Karnosky, and S. P. Long. 2009. Quantifying the impact of current and future tropospheric ozone on tree biomass, growth, physiology and biochemistry: a quantitative meta-analysis. Global Change Biology **15**:396-424.

Zhao, Z., S.-H. Chen, M. J. Kleeman, and A. Mahmud. 2011. The Impact of Climate Change on Air Quality–Related Meteorological Conditions in California. Part II: Present versus Future Time Simulation Analysis. Journal of Climate **24**:3362-3376.

Chapter 2 Appendix A

Contents

1. Research Site Details

Each of the long term study sites (Giant Forest, Grant Grove, and Shaver Lake) includes 150 trees in three 2 hectare plots of 50 trees each. Short term sites are arranged as either three 0.5-1.5 ha plots of 20-30 canopy trees, or as a larger single plot with 50 canopy trees. Each air quality monitoring site is co-located with a forest monitoring sites, except at Sugarloaf Basin, which relies on air quality monitors at nearby Giant Forest. Coordinates and additional information on ozone monitoring is provided in Table SI-1. Injury surveys include 300 trees at high O_3 exposure (Grant Grove, Giant Forest), 200 at moderate exposure (Shaver Lake, Snow Corral) and 253 at low exposure (Atwell Mill, Huntington Lake, Florence Lake, and Sugarloaf Basin). Diurnal variation in O_3 concentrations for the long term sites is described in Van Ooy and Carroll (1995). The study region includes 5849 km^2 within Class I designations, areas subject to stringent limits on air quality degradation.

Recent estimates of total wet and dry deposition of nitrogen in the southern Sierra Nevada range from 1.4-5.5 kg N/ha/year (Panek et al 2013). Deposition is approximately one third each of N O_3-N, precipitation NH_4-N, and HN O_3-N. The total deposition is elevated above background levels, particularly in locations south of this study area on the western slope. However, these research sites do not exceed 17 kg N/ ha/year, the critical load for nitrate leaching and tree root biomass loss in California mixed conifer forests. In some years, deposition may exceed 5 kg N/ha/year, the deposition rate that is a critical load threshold for sensitive lichen communities (Fenn et. Al. 2010).

The surveyed forest plots are dominated by *P. ponderosa* and *P. Jeffreyi*. Forest soils are sandy loams derived from granitic parent material, and are generally less than a meter in depth to bedrock. Understory vegetation is a mix of montane shrubs, primarily pinemat manzanita (*Arctostaphylos nevadensis* A. Gray), mountain whitethorn (*Ceanothus cordulatus* Kellogg), and bush chinquapin (*Chrysolepis sempervirens* Hjelmq.), at 30-70% cover.

Chapter 2 Appendix A

2. Measuring O_3 exposure

A. Air Quality Monitoring

Ozone concentrations of ambient air were measured via UV absorption. Instruments included the Dasibi models 1003AH and 1008AH, 2B Technologies model 202, and Thermo Scientific model 49C. In this method, air generally enters a sample inlet and is divided into two parts. The first is scrubbed, becoming the reference gas. The second part is not scrubbed and becomes the sample of ambient air. The intensity of UV light in each portion of air is measured by a detector. Then, the analyzer calculates O_3 concentration on the basis of comparative UV adsorption of the reference and the sample. Within a time period dependent on the instrument, each air path is re-measured, and the paths switched within the instrument so that they are measured by each detector. The resulting average concentration for the time period is then recorded.

B. W126 Index

The W126 index is a cumulative, concentration-weighted index of O_3 exposure that gives higher concentrations of O_3 greater emphasis. In keeping with observations of effects on vegetation, concentrations over 70 parts per billion by volume are given more importance than low concentrations. The weights are applied to hourly concentrations during calculation of the index using a sigmoidal curve (1)(Lefohn and Runekcles 1987):

(1) $$W126 = O_3 * \left(\frac{1}{1+\left(4403 * e^{-126 * O_3}\right)} \right)$$

The resulting weighted values, expressed in ppm-hours, are summed for each day. This sum may apply to either daylight hours (08:00 – 20:00, $W126_{12}$) or the full 24- hour day ($W126_{24}$). Cumulative sums of the daily totals form the index for each three-month period. The annual W126 index is identified either by a designated season (usually that with peak O_3 concentrations for the region) or by the maximum 3-month index within each year. Three-year mean W126 indices are also commonly reported.

In this study, we express O_3 exposure using both $W126_{12}$ and $W126_{24}$, for ease of comparison to existing studies that use one or both approaches. The rationale for using 24 hour days in the index is that many plant species, including *P. ponderosa* and *P. Jeffreyi*, have significant nighttime stomatal conductance and resultant O_3 uptake. Therefore, following the recommendations of the Federal Land Managers Air Quality Related Values Work Group (USFS et. al. 2010), we have conducted key analyses using $W126_{24}$.

The US Environmental Protection Agency (EPA) strengthened the primary and secondary National Ambient Air Quality Standards (NAAQS) for O_3 to 70 parts per billion in October 2015. This limit was set following extensive analysis of the environmental impacts expected from $W126_{12}$ at 7, 11, and 15 ppm-hours. The establishment of a stronger secondary standard based on a cumulative index was also supported by the National Park Service as the basis for protecting sensitive vegetation. Although the EPA determined that "a cumulative, seasonal index was the most biologically relevant way to relate exposure to plant growth response," due to other considerations the W126 metric was not used for the new NAAQS (US EPA 2015). The 70 ppb

limit is expected to provide ecosystem protections that are equivalent to a 3-year W126 index of 17 ppm-hours.

3. OII/Ozone Injury Index

Injury of trees was assessed in the field following the Ozone Injury Index (OII) method (Miller et. al. 1996). The OII score for each tree combines four weighted parts: 1) proportion of leaf area with visible chlorotic mottle (Figure 1A, 40%), 2) retention of annual needle groups, known as whorls (40%), 3) percent live crown (10%) and 4) average needle length (10%)(Schilling and Duriscoe, 1996). Mottle on needles less than five years old and whorl retention are given greater emphasis based on their importance in photosynthesis physiology (Patterson and Rundel 1989). The highest possible OII is 100. OII=100 corresponds to a severely injured tree, with over 40% of leaf area affected by chlorotic mottle. OII=0 corresponds to an asymptomatic tree (no chlorotic mottle present). Observation of chlorotic mottle is required to generate any OII above zero. Therefore, no damage is attributed to pollution without the characteristic foliar symptoms also present%) (Schilling and Duriscoe, 1996). A tree's OII score is based on measurement of five branchlets, each of which may retain needles originating 1-10 years prior. In long term plots, OII was repeatedly assessed in tagged trees (n = 450) six or more times from 1991 to 2013. Trees in short term plots were surveyed once in 2011, 2012, or 2013 (n = 245). Personnel varied in each summer field season; to ensure consistent application of the OII technique a developer of this method led field surveys in 1991-1994 and also provided technician training in 2011-2012.

. **Table A1 Site Monitoring Details**

Site	Years	Type/ frequency	Instrument	Latitude	Longitude	Elevation (meters)	Operator/ reference	Monitoring site also known as
Giant Forest	1991-2013	Active/ hourly	Thermo Scientific 49C	36.566	-118.777	1890	NPS Air Resources Division/10	NPS Lower Kaweah
Grant Grove	1990-1995	Active/ hourly	Dasibi 1008AH	36.737	-118.957	2012	NPS Air Resources Division/10, CA ARB/11	Wilsonia
Grant Grove	2007-2013	Active/ hourly	2B Technologies Model 202	36.697	-119.019	1246	USFS Region 5 Air Program	Pinehurst
Shaver Lake	1995-2002	Active/ hourly	Dasibi 1003 AH	37.138	-119.269	1755	California ARB/11	Shaver Lake Perimeter Rd ARB
Shaver Lake	1991-1994; 2003-2005; 2007; 2011; 2013	Active/ hourly	Dasibi 1008AH	37.137	-119.261	1720	USFS Region 5 Air Program, SCOIAS/12,13	Shaver Lake USFS-SCOIAS
Atwell Mill	1992-1993; 1997-2004	Active/ hourly	Thermo Scientific 49C	36.429	-118.763	1225	NPS Air Resources Division/10	NPS Lookout Point
Snow Corral	2003-2005; 2007	Active/ hourly	2B Technologies Model 202	36.961	-119.175	1464	USFS Region 5 Air Program	Fence Meadow
Huntington Lake	2011	Active/ hourly	2B Technologies Model 202	37.255	-119.161	2134	USFS Region 5 Air Program	Huntington 2
Huntington Lake	2012-2013	Active/ hourly	2B Technologies Model 202	37.271	-119.124	2588	USFS Region 5 Air Program	Huntington 1
Florence Lake	2011-2013	Active/ hourly	2B Technologies Model 202	37.278	-118.975	2280	USFS Region 5 Air Program	Florence Lake

Chapter 2 Appendix A

Table A2 Ozone Exposure

Year	Site	$W126_{24}$ ppm-hours	$W126_{24}$ 3 year mean	$W126_{12}$ ppm-hours	$W126_{12}$ 3 year mean
1989	GF	79.67	75.33	46.04	44.27
1990	GF	80.06	83.65	40.19	46.58
1991	GF	82.21	80.65	51.73	45.98
1992	GF	97.50	86.59	55.87	49.26
1993	GF	112.12	97.27	63.38	57.00
1994	GF	104.03	104.55	51.36	56.87
1995	GF	61.02	92.39	41.91	52.22
1996	GF	100.93	88.66	53.93	49.07
1997	GF	64.89	75.61	36.27	44.04
1998	GF	61.12	75.65	42.24	44.15
1999	GF	72.79	66.27	45.32	41.28
2000	GF	48.95	60.95	23.04	36.87
2001	GF	89.85	70.53	48.85	39.07
2002	GF	134.25	91.02	69.02	46.97
2003	GF	81.57	101.89	37.09	51.65
2004	GF	72.53	96.12	41.90	49.34
2005	GF	79.39	77.83	47.30	42.09
2006	GF	83.62	78.51	45.60	44.93
2007	GF	90.07	84.36	45.98	46.29
2008	GF	95.51	89.74	49.10	46.89
2009	GF	45.28	76.96	28.75	41.27
2010	GF	42.47	61.09	26.54	34.80
2011	GF	55.42	47.72	33.41	29.57
2012	GF	70.80	56.23	40.75	33.57
2013	GF	65.62	63.95	34.38	36.18
1990	GG	79.12	NA	42.93	NA
1991	GG	76.40	NA	45.67	NA
1992	GG	89.51	81.68	47.18	45.26

Chapter 2 Appendix A

Year	Site	$W126_{24}$ ppm-hours	$W126_{24}$ 3 year mean	$W126_{12}$ ppm-hours	$W126_{12}$ 3 year mean
1993	GG	82.30	82.74	47.53	46.79
1994	GG	113.40	95.07	60.96	51.89
1995	GG	66.17	87.29	40.50	49.66
2007	GG	71.39	NA	35.86	NA
2008	GG	65.51	NA	31.29	NA
2009	GG	30.54	55.81	21.10	29.42
2010	GG	45.53	47.19	25.62	26.00
2011	GG	72.58	49.55	42.85	29.86
2012	GG	98.83	72.31	52.44	40.30
2013	GG	66.13	79.18	33.44	42.91
1991	SL	46.51	NA	42.70	NA
1992	SL	59.28	NA	39.43	NA
1993	SL	60.25	55.35	48.31	43.48
1994	SL	78.76	66.10	59.96	49.23
1995	SL	10.68	49.90	10.23	39.50
1996	SL	66.26	51.90	47.98	39.39
1997	SL	45.58	40.84	33.09	30.43
1998	SL	46.12	52.66	38.05	39.70
1999	SL	50.58	47.43	38.03	36.39
2000	SL	49.98	48.89	36.26	37.45
2001	SL	50.80	50.45	38.01	37.43
2002	SL	68.11	56.30	50.48	41.58
2003	SL	17.31	45.41	16.72	35.07
2004	SL	29.62	38.35	26.85	31.35
2005	SL	1.62	16.18	1.53	15.03
2007	SL	29.18	20.14	19.45	15.94
2011	SL	15.72	NA	15.19	NA
2013	SL	47.24	NA	23.40	NA
1992	AT	95.17	NA	50.58	NA
1993	AT	54.29	NA	38.97	NA
1997	AT	78.51	NA	51.91	NA

Chapter 2 Appendix A

Year	Site	$W126_{24}$ ppm-hours	$W126_{24}$ 3 year mean	$W126_{12}$ ppm-hours	$W126_{12}$ 3 year mean
1998	AT	64.81	NA	47.78	NA
1999	AT	102.24	81.86	60.33	53.34
2000	AT	89.98	85.68	53.19	53.77
2001	AT	90.64	94.29	49.63	54.38
2002	AT	125.91	102.17	67.65	56.82
2003	AT	74.92	97.16	40.81	52.70
2004	AT	97.86	99.56	56.30	54.92
2011	FL	7.61	NA	5.88	NA
2012	FL	19.06	NA	13.11	NA
2013	FL	23.84	16.84	16.53	11.84
2011	HL	2.16	NA	2.13	NA
2012	HL	8.91	NA	6.03	NA
2013	HL	27.09	12.72	13.05	7.07
2003	SC	37.69	NA	19.84	NA
2004	SC	80.95	NA	34.54	NA
2005	SC	1.97	40.20	1.14	18.51
2007	SC	66.63	NA	27.06	NA

GF: Giant Forest; GG: Grant Grove; SL: Shaver Lake; AT: Atwell Mill; FL: Florence Lake; HL: Huntington Lake; SC: Snow Corral.

Chapter 2 Appendix A

Table A3 Tree Injury, 1991-2013

Year	Site	Mean OII	Standard Error OII	Trees surveyed	Symptomatic trees	Proportion symptomatic
1991	Giant Forest	44.66	1.33	150	139	0.93
1992	Giant Forest	41.74	1.55	150	136	0.91
1993	Giant Forest	39.56	1.65	145	129	0.89
1994	Giant Forest	43.94	1.37	143	139	0.97
2000	Giant Forest	46.60	1.49	130	118	0.91
2011	Giant Forest	33.86	2.01	92	79	0.86
2012	Giant Forest	28.86	2.14	89	69	0.78
1991	Grant Grove	40.84	1.52	150	142	0.95
1992	Grant Grove	40.53	1.59	150	143	0.95
1993	Grant Grove	38.96	1.60	149	136	0.91
1994	Grant Grove	38.20	1.52	147	138	0.94
2000	Grant Grove	38.53	1.60	135	125	0.93
2011	Grant Grove	23.55	1.83	103	91	0.88
2012	Grant Grove	19.53	1.85	103	76	0.74
1991	Shaver Lake	19.26	1.71	149	76	0.51
1992	Shaver Lake	19.49	1.79	150	71	0.47
1993	Shaver Lake	21.07	1.63	142	93	0.66
1994	Shaver Lake	8.48	1.44	145	31	0.21
2001	Shaver Lake	11.29	1.64	144	39	0.27
2011	Shaver Lake	10.67	1.79	81	29	0.36
2012	Atwell Mill	8.34	1.88	45	22	0.49
2013	Atwell Mill	12.44	2.66	30	19	0.63
2011	Huntington Lake	3.19	0.85	50	13	0.26
2011	Snow Corral	7.22	2.04	50	12	0.24
2012	Sugarloaf Basin	0.30	0.23	38	2	0.05
2011	Florence Lake	0.00	0.00	38	0	0.00

Chapter 2 Appendix A

Table A4 Probability of Survival

	Giant Forest	Grant Grove	Shaver Lake
1991	1	1	1
1994	0.973	0.922	0.991
2002	0.874	0.969	0.980
2012	0.847	0.891	0.971

Kaplan-Meier survival probabilities for long term study sites.

Chapter 2 Appendix A

REFERENCES for Appendix A

California Environmental Protection Agency - Air Resources Board. 2015. Air Quality and Meteorological Information System. [Available online at: http://www.arb.ca.gov/aqmis2/aqdselect.php?tab=hourly].

Carroll, J. J. and Dixon, A. J. 1993. Sierra Cooperative Ozone Impact Assessment Study: Year 3. Volumes 1 and 2. Final Report Contract No A132-188. Prepared for the California Air Resources Board, Research Division, October 1993.

Carroll, J. J. and Dixon, A. J., 1995. Sierra Cooperative Ozone Impact Assessment Study: Year 4. Volumes 1 and 2. Final Report Contract No 92-346. Prepared for the California Air Resources Board, Research Division, May 1995.

Fenn, M. E., E. B. Allen, S. B. Weiss, S. Jovan, L. H. Geiser, G. S. Tonnesen, R. F. Johnson, L. E. Rao, B. S. Gimeno, F. Yuan, T. Meixner, and A. Bytnerowicz. 2010. Nitrogen critical loads and management alternatives for N-impacted ecosystems in California. Journal of Environmental Management 91:2404-2423.

Lefohn, A. S., and V. C. Runeckles. 1987. Establishing standards to protect vegetation—ozone exposure/dose considerations. Atmospheric Environment 21:561-568.

Miller, P., K. Stolte, D. M. Duriscoe, and J. Pronos. 1996. Evaluating Ozone Air Pollution Effects on Pines in the Western United States. USDA Forest Service General Technical Report PSW-155:1-87.

National Park Service - Air Resources Division, 2015. NPS Gaseous Pollutant and Meteorological Data, Sequoia and Kings Canyon National Park. Gaseous Pollutant Monitoring Program, Denver, Colorado. Distributed by Air Resource Specialists, Inc. [Available online: http://ard-request.air-resource.com/] Denver, Colorado.

Patterson, M. T., and P. W. Rundel. 1989. Ozone impacts on photosynthetic capacity of Jeffrey pine in Sequoia National Park. Final Report, Project PX-001-7-1152; Denver, Colorado, Air Quality Division, USDI National Park Service; 34 pp.

Panek, J. A.; Saah, D.; Esperanza, A., 2013. A natural resource condition assessment for Sequoia and Kings Canyon National Parks: Appendix 2. Air Quality. Air Quality, 2013, National Park Service; Fort Collins, Colorado, National Park Service, Natural Resource Report. NPS/SEKI/NRRd2013/665.2. **2013.**

Schilling, S., and D. Duriscoe. 1996. Data Managementand Analysis of Ozone Injury to Pines. In: Evaluating Ozone Air Pollution Effects on Pines in the Western United States,. USDA Forest Service General Technical Report PSW-GTR-155; Miller, P. R.; Stolte, K. W.; Duriscoe, D. M.; Pronos, J., technical coordinators.

Chapter 2 Appendix A

U.S. Forest Service; National Park Service; U.S. Fish and Wildlife Service, 2010. Federal land managers' air quality related values work group (FLAG): phase I report—revised (2010). Natural Resource Report NPS/NRPC/NRR—2010/232. National Park Service, Denver, Colorado.

U.S. Environmental Protection Agency, 2015. National Ambient Air Quality Standards for Ozone; Final Rule. Federal Register Vol. 80, No. 206 October 26, 2015. Rules and Regulations 40 CFR Parts 50, 51, 52, 53, and 58. United States Government Printing Office, Washington, D.C. **2015**; pp 65292-65468.

Van Ooy, D. J., and J. J. Carroll. 1995. The spatial variation of ozone climatology on the Western slope of the Sierra Nevada. Atmospheric Environment 29:1319-1330.

CHAPTER 3 | Forest ecosystem response to chronic stress: interacting effects of air pollution and climate on tree growth

1. INTRODUCTION

Forest ecosystems face a vast array of environmental stressors. Trees, long-lived and characteristically immobile, cope with stressors that ranges from the natural variation in weather and climate to large scale human alteration of atmospheric conditions (Aber et al. 2001, Allen et al. 2010). In order to understand the importance of environmental stressors to ecosystem processes, we must understand how trees respond to them alone and in combination, under realistic field conditions, and on meaningful time scales (Franklin et al. 1987). Characterizing responses to multiple stressors is essential because interactions among stressors are poorly quantified but can be powerful drivers of ecosystem change (Côté et al. 2016, Paine et al. 1998). In this study, we describe long term tree growth response to climatic conditions and ozone pollution exposure, conditions that impact forested ecosystems in California's Sierra Nevada both individually and interactively.

1.1 Forest growth responses to stress

Growth is a key indicator of tree vitality and forest ecosystem condition. Because resource allocation in plants prioritizes primary growth, tree secondary growth is responsive to events and environmental factors that reduce tree vigor (Dobbertin 2005, Waring 1987). Variations in the tree ring record accurately reflect variations in net ecosystem productivity and carbon uptake by forests (Babst et al. 2013). Growth patterns are a direct product of photosynthesis, a fundamental ecological process, integrated over time in a measurable way (Clark et al. 2001, Schweingruber 1996). Quantifying growth patterns in individuals can reveal emergent community-scale processes that are otherwise difficult to assess. This is especially true for long-lived tree species and the forest processes they shape. The degree and temporal distribution of changes to tree growth depends upon the stressor and its form of action (Fritts 1976). Ecosystem perturbations including stressors are often described as either pulse, a fast-acting and short lived change in conditions, or press, a sustained alteration of the environment (Bender et al. 1984, Ives and Carpenter 2007). Tree growth responses to pulse stressors are typically realized over one or a few growth rings. Successive pulse events can also contribute to accumulated declines over time. In contrast, the impact of press disturbances is more subtle, but persistent and often accumulating over the course of many years (Pedersen 1998a). Environmental stressors and growth losses predispose trees to damaging attacks by insects and pathogens and put affected trees at a competitive disadvantage (Manion 1991, Dobbertin 2005). Plant resources allocated to defense may also increase, further reducing labile carbon available for diameter growth. Ultimately, growth declines reduce tree vigor and contribute to mortality (Pedersen 1998a, Das et al. 2007).

1.2 Compound environmental stress

Myriad factors contribute to growth declines, and rare is the ecosystem stressor that acts in isolation. Simultaneous and successive stressors are a common occurrence: this pattern is

increasingly true for ubiquitous anthropogenic stressors like air pollution (Manion 1991, Niinemets 2010). In some systems, the compound effects of simultaneous and/or successive stressors cause dramatic shifts in community composition, trophic linkages, and overall ecosystem function, termed “ecological surprises” (Paine et al. 1998). Stressors can be defined as any natural or anthropogenic pressure that causes a quantifiable positive or negative biological response (Boyd and Hutchins 2012, Côté et al. 2016; Figure 1). Ecologists describe interactions among stressors as additive, antagonistic, or synergistic (Folt et al 1999). In a classic scenario where two effects are negative, an additive relationship is represented by simple linear addition of the isolated effects. Synergistic interactions are those in which the net effect is greater than the sum of its parts, and antagonistic interactions are those in which one factor negates the effects of another. Ecophysiological studies suggest that an antagonistic interaction may play out among forest stressors in the southern Sierra Nevada: late summer water limitation, triggering stomatal closure, prohibits uptake of ozone and precludes air pollution uptake, at least over short time scales (Bauer et al. 2000, Panek 2004). While detection and attribution of organismal responses to stressors are complex problems, describing these relationships reveals the realities of ecosystem function. The foundation for this understanding is the underlying response to each stressor.

1.3 Influence of water limitation and related climatic conditions

Water availability exerts strong controls on the growth and survival of trees. Increasingly warm and dry conditions have recently fostered die-off events across the North American West and in forests worldwide (Allen et al. 2010, Anderegg et al. 2015, Hicke et al. 2012). Water limitation is also a key driver in ongoing catastrophic forest mortality in California (Asner et al. 2016). Although species are adapted to the range of conditions in their native environment, deficits can lead to changes in growth, shifts in composition and structure, and altered forest function (Clark et al. 2016). Drought conditions arise as a consequence of higher than average temperature, lower than average precipitation, or both. High temperatures are a strong driver of water limitation in ecosystems; changes in temperature reflect modified growing season length, changes in water storage in soil and snow, and increased plant demand for water (Adams et al. 2009, Williams et al. 2013). The timing and quantity of precipitation also shapes the magnitude and timing of tree growth. Climatic water deficit is a biologically relevant expression of plant water availability that quantifies unmet evaporative demand. Deficits, more so than merely temperature or precipitation alone, are well correlated with local forest type, particularly in the southern Sierra Nevada (Stephenson 1998, Lutz et al. 2010). Annual deficit has also been shown to be a key predictor of major growth declines in Douglas-fir and whitebark pine (*Pseudotsuga menziesii, Pinus albicaulus;* Littel et al. 2008, Millar et al. 2012). Recent developments in fine-scale hydrologic modeling enable estimates of deficit and other climatic conditions at fine spatial resolution (270m pixels) throughout California (Flint et al. 2013), offering new possibilities in understanding growth responses to local climate.

The stress of recurrent water shortages can permanently change growth trajectories and modify climate-growth relationships (Pedersen 1998b, Macalady and Bugmann 2014). Tree growth in climatic regions with well-defined annual droughts responds to prevailing conditions in earlier seasons. For example, trees in Mediterranean climates need access to soil water through hot, dry summers, and therefore rely on precipitation from the previous winter and earlier. In Sierra Nevada conifers, growth is typically dependent on winter precipitation and summer temperatures

during previous and current years; the specific timing varies within this extensive ecoregion (Yeh and Wensel 2000, Hurteau et al. 2007). A key determinant of water availability for the Sierra Nevada is forest density. Mixed conifer and low elevation pine forests have greater tree density and canopy cover than their historic analogs, driving greater demand for finite water resources (Stephens et al. 2015).

1.4 Ozone pollution in forests

Ozone is a secondary air pollutant that causes oxidative damage to plant tissues, disrupting the structures and mechanisms of photosynthesis (Matyssek et al. 2003). Across many species, trees exposed to elevated ozone demonstrate reduced carbon assimilation, lower root biomass, early leaf senescence, and loss of stomatal control (Ainsworth et al. 2012). Tropospheric ozone has increased about 200% within the last century, with forest damage documented across southern Europe, eastern China, Mexico, California, and the eastern U.S. (Braun et al. 2014, de Bauer and Hernández-Tejeda 2007, Feng et al. 2014, Karnosky et al. 2007). Concentrations are expected to climb to phytotoxic levels in the majority of global forests within the next century (The Royal Society 2008). The diagnostic response to ozone pollution in ponderosa and Jeffrey pines (*Pinus ponderosa* Dougl ex. Laws, *Pinus jeffreyi* Balfour) is a pattern of damaged and yellowing leaf tissue called chlorotic mottle (Figure 2). Other symptoms include shortened needle retention time, shorter average needle length, fewer annual whorls per branch, and decreased crown density (Kellomäki and Wang 1997, Grulke and Balduman 1999). In earlier work (Chapter 2), we observed annual relative growth losses of 12-25% in ponderosa and Jeffrey pines growing in severely polluted parts of the Sierra Nevada range. These forests experienced severe ozone exposure as early as 1970, and foliar injury was observed in the region shortly thereafter (Bytnerowicz et al 1999). Like other stressors, ozone can weaken trees and predispose them to damage by insects, and disease, and drought (USEPA 1980, Miller and McBride 1999, Allen and Brashears 2009). Individual tree responses integrate into transformative impacts on forest ecosystems, where they facilitate insect attack, increase fire risk, and suppress net primary productivity (Aber et al. 2001, Ainsworth et al. 2012, Bytnerowicz et al. 2003).

Ozone originates from the reaction of nitrogen oxides and oxygen in the presence of sunlight and heat. Peak concentrations in the southern Sierra Nevada of over 120 parts per billion (ppb) occur in mid to late summer, while elevated levels sufficient to damage plant tissues (> 40 ppb) are present as early as May and sometimes into November. High summer temperatures, common in the San Joaquin valley, drive formation of ozone in the region while simultaneously driving water limitation in forests. Both ozone and water availability act directly upon plant growth mechanisms, and have the potential to propagate impacts to ecosystem scales (Ainsworth et al. 2012, Allen and Breshears 1998). Yet, because they are linked through water, these two stressors have the potential to antagonistically interact at ecosystem scales. At the physiological level, measurements of gas exchange and photosynthesis have established that peak ambient ozone concentrations on the western slope of the Sierra Nevada do not correspond with peak ozone uptake through the stomata (Bauer et al. 2000, Panek 2004, Grulke et al. 2003). The divergence is attributable to patterns in stomatal closure triggered by seasonal and daily water limitation (Panek and Goldstein 2001). However, it is unknown whether the implications of lower ozone flux are evident in annual or long term growth, and also unclear if the effects are consistent across the landscape (Grulke et al 2002). These ecophysiological observations lead to a

compelling question: Does the annual summer drought in Sierra Nevada forests limit damage to the ecosystem from ozone pollution?

1.5 Purpose & Hypotheses

The goal of this study is to quantify tree growth responses to climatic stressors and chronic ozone exposure, both individually and interactively. These environmental stressors each separately influence Sierra Nevada forests, but in distinct and potentially interacting ways. We relied on annual growth records obtained from tree rings of Jeffrey pine trees sampled across a pollution gradient to document tree growth responses. We expected to observe lower relative growth rates in warm and dry years, expressed by both water availability and demand. Because water deficits in the region are strongly influenced by winter precipitation and soil water availability, we predicted that the climate-growth relationship would rely on prevailing conditions in both the early growing season and the previous year. A gradient of pollution exposure enabled our comparison of tree growth under minimum and elevated ozone levels, across sites with shared climatic conditions. Tree growth response to ozone is expected to be negative overall. Finally, tree growth response to the combined effects of climate and ozone pollution may be complex, as late summer water limitation can preclude ozone uptake at the leaf level. We expected that at a regional scale, the combined effects of these environmental stressors would be antagonistic, as opposed to additive or synergistic.

2. METHODS

2.1 Experimental design and study setting

Our region-wide study was based on a network of sites stratified across a gradient of ozone exposure, with coupled assessments of air quality and forest conditions at each location. The network was designed as a natural experiment to assess forest response to air pollution, using patterns at sites where pollution has little influence to inform our understanding of sites where ozone pollution is a major ecosystem stressor (Figures 3-4). Ozone concentrations on the western slope of the southern Sierra Nevada range from summer averages well over 60 ppb, to low, background exposure levels of less than 30 ppb, not considered hazardous to vegetation (Panek et al. 2013a, Cisneros et al. 2010). Formation of the pollution gradient is driven by distance from emissions sources, diurnal mixing of upslope and downslope air parcels in the mountainous terrain, and breakdown of ozone molecules over time (Bytnerowicz et al. 2003). Montane conifer forests in the southern Sierra Nevada experience a Mediterranean climate with hot, dry summers and mild wet winters. Across the seven-site study, precipitation totals 930-1100 mm annually, with 30-60% falling as snow (Stephenson 1988, Western Regional Climate Center 2015). Ninety-five percent of rain and snow falls from October through May (Flint et al. 2013). Elevations span 1900 to 2300 m.

Research locations were selected on the basis of the dominance and density of ozone sensitive pine species, shared annual exposure to climatic water deficits among all sites, and proximity to existing air quality monitoring infrastructure. Study sites were mixed conifer forests dominated by Jeffrey pine, with white fir (*Abies concolor* Lindley), incense-cedar (*Calocedrus decurrens* Florin), sugar pine (*P. lambertiana* Doug.), and black oak (*Quercus kelloggii* Newb.) also present (Figure 4). At Giant Forest and Grant Grove, study sites encompassed trees within a

research network active 1991-2001 that was established to study the long term effects of pollution on forests (Bytnerowicz et al. 2003, Arbaugh and Bytnerowicz 2003). Our research extended the sampling regime and spatial coverage of this work. Within sites, targeted study trees were mature pines over 20 cm diameter at breast height (DBH) from dominant, codominant, and open grown canopy classes. For both increment core collection and ozone injury monitoring, only trees lacking major pests, pathogens, and physical damage (exclusive of ozone injury) were sampled, according to established procedures for long term pollution monitoring (Miller et al. 1996). Each site consisted of 50-150 trees arranged in 1-3 plots. The forests are managed primarily as natural and recreational landscapes, with no record of timber harvest within the last 80 years. Low-severity fires have occurred within the past 20 years in portions of the Grant Grove, Sugarloaf Basin, and Atwell Mill sites, with limited physical impacts on the health of trees in the survey (Chapter 2 Appendix A-1).

2.2 Field and laboratory methods

2.2.1 Air quality monitoring and exposure index

Ozone exposure was measured via ultraviolet absorption at six of the sites in our regional network. From 1984-2012, summer air quality monitoring was continuous at Giant Forest, active in more than 10 years at Grant Grove, Shaver Lake and Atwell Mill, and episodic elsewhere. At the sites with highest ozone exposures, monitors are on average within1 km of study plots (Chapter 2 Table A1). Exposure is calculated from 24-hour ppb measurements by the cumulative W126 index, which is weighted to emphasize known biological impacts at high concentrations (above 70 ppb; Lefohn and Runeckles 1987). The W126 exposure index is intended as proxy for effective flux, and thus the physiological drivers of ozone injury to vegetation (Musselman et al. 2006). Previous studies in the southern Sierra Nevada have established that W126 is a strong predictor of injury to pines (Chapter 2; Arbaugh et al. 1998). The US National Ambient Air Quality Standard (NAAQS) for ozone sets a W126 limit of 17 parts per million hours (ppm-hours; averaged over 3 years) for protection of ecosystems (U.S. Environmental Protection Agency 2015). Grant Grove and Giant Forest regularly exceed this standard, averaging over 70 ppm-hours for the duration of this study. Plots at Atwell Mill and Snow Corral sites have lower exposure, but exceed 17 ppm-hours on a regular basis. The sites with best air quality are Huntington Lake, Florence Lake, and Sugarloaf Basin, with average summer ozone exposure below 17 ppm-hours.

2.2.2 Dendroecological collections and preparation

At all sites, we identified trees that were suitable for both foliar injury surveys and core collection (canopy <10 m from ground level, no major disease damage or physical injuries). A minimum of 30 dominant, codominant, and open grown Jeffrey pines were cored at each site. Trees not limited by light are most responsive to climate variation (Clark et al. 2014). Typically, two 5.15mm diameter cores were obtained from each tree at breast height; one core per tree was collected from the sites sampled in 2011. All cores were collected in late summer from 2011-2013, and sampling-year growth was excluded from chronology development. In sites established through earlier studies (Giant Forest and Grant Grove), all live trees included in the ozone injury study were cored.

Preparation and measurement of increment cores followed the current best practices for dendrochronology. First, cores were dried and mounted for measurement, then prepared for

viewing with progressively finer grit sandpaper and polishing paper (150 grit through 600-1500 grit), according to the methods developed by Stokes and Smiley (1968) and Fritts (1976). Rings were then counted and measured to 0.01 mm resolution using a dissecting microscope and sliding stage micrometer (Velmex Measuring System, Bloomfield, NY; Acu-rite encoder Heidenhain 178 Corp, Shaumberg, IL). All ring counts were checked independently by a second person, and every fifth core was fully remeasured by a second person. These repeated measures were used to assure that the overall error was less than 5% of the standard deviation of ring widths. With the aid of the computer program COFECHA (Holmes 1983, Grissino-Mayer 2001), we then constructed species-specific chronologies from the dominant, codominant, and open grown trees at each site. All cores were crossdated using these chronologies as a reference and COFECHA to help identify missing or misdated rings. The few trees from suppressed and intermediate canopy classes that were monitored for ozone injury were excluded from site-specific chronologies. In trees with more than one increment core (the majority of individuals), the series were averaged.

2.3 Analytical methods

2.3.1 Chronology development

From the site-specific chronologies, we developed two distinct regional chronologies: 1) a growth chronology from sites with the least ozone pollution (*minimum ozone chronology*); and 2) a growth chronology for all trees at all sites (*all sites chronology*). The minimum ozone chronology was needed to establish climate dependency while minimizing the impact of ozone exposure. It included only individuals found at minimum ozone sites defined as having predicted summer mean ozone exposure << 45 ppb, as compared to > 60 ppb in excluded locations (Panek et al. 2013a). In the minimum ozone chronology tree growth was expressed as ring width indices (RWI). The all sites chronology was used to quantify ozone exposure dependency. It included all trees from across the ozone pollution gradient and annual tree growth was expressed as relative basal area increment (rBAI). After analysis of the chronology itself, data from individual trees was used for development of the growth model.

Chronology development: minimum ozone

After crossdating, cores with an overall shared correlation coefficient > 0.45 were used to develop chronologies. The resulting ring width series were then detrended to reduce the effects of age and endogenous disturbances prevalent among one or a few trees, but not expected to affect the whole region. We used ARSTAN software to standardize ring width measurements and minimize these trends within each series, applying a 50% frequency cutoff smoothing spline at 0.67% of total series length (Cook and Kairiukstis 1990). The chronologies used biweight robust mean estimation, giving large and small outliers the same statistical treatment. Rbar-weighted variance stabilization was applied to reduce bias related to changing sample sizes (Osborn et al. 1997). The minimum ozone chronology has minimum sample size of n=10 individuals to avoid potential variance bias in small samples.

Chronology development: all sites

After the crossdating procedures described above, a chronology of relative growth (rBAI) was developed from raw ring width measurements. BAI (mm^2/year) was calculated assuming on a circular stem, with diameter inside bark calculated from outside bark DBH in the year cored, as in Equation 1: (Dolph 1984),

1) $$BAI = \pi({r_n}^2 - {r_{n-1}}^2)$$

when r is tree radius at the end of growth in year n (Biondi and Qeadan 2008). A mean chronology was calculated with biweight means in the Dendrochronology Program Library in R (Biondi and Qeadan 2008, Bunn et al. 2016). Because growth is strongly influenced by tree size, rBAI chronologies are applied in this analysis to eliminate age-related growth patterns while preserving episodic growth trends, which could be potentially tied to climate or pollution (Innes and Cook 1989, Bowman et al. 2013). To prevent negative BAI estimates, outer diameter calculations that resulted in negative juvenile growth were replaced with measurements beginning from pith (Rollinson et al. 2016). Relative BAI was calculated for each individual in each year by averaging annual increment of each tree and dividing by the basal area of the previous year. Equation 2:

2) $$rBAI = BAI_n \div \pi(r_{n-1})^2$$

2.3.2 Growth-climate linkages

Growth responses were quantified in a two-step analytical process. First, we described growth dependence on climate using minimum ozone chronology. Next, we joined this climate model with information on ozone exposure and late-season water limitation, as well as site and tree characteristics, to understand the influence of pollution and its interactions in climate context using the all sites chronology. An overview of these analytical steps is provided in Figure 5.

Growth response to climate

To characterize climatic influence on growth, we first selected climatic variables and examined their influence on growth in the region (Figure 5). This information was then used to form a suite of candidate models, which were vetted using an information theoretic approach. Monthly climate variables – precipitation, deficit, and maximum temperature – were selected a priori given their previously observed importance for tree growth generally (Cook and Kairiukstis 1990) and specifically in this region (Royce and Barbour 2001b, Hurteau et al. 2007). Deficit, or total potential evapotranspiration minus actual evapotranspiration, is an expression of plant water stress and is known to predict vegetation distribution (Stephenson 1998). We included it to evaluate its utility for further understanding annual tree growth. Climate variables specific to each site were obtained from the monthly historic values (1896-2012) within the Basin Characterization Model, a biophysical model of monthly regional water balance (Flint et al. 2013). Maximum temperatures are daily maximum values averaged over all days in the month (°C). Precipitation values are totals for the month (mm). The climate data is specific to 270 x 270 m pixels; and site-based climate values are calculated as the average of plot values within each site.

Using precipitation, temperature, deficit, and the minimum ozone chronology, we then examined the timing and variables that best describe climate dependency through a diagnostic correlation analysis. We applied the *Seascorr* tool to test correlations between tree rings and sets of two monthly climate variables, integrated over periods of variable length (1-9 months). Significance of climate correlations was assessed using a Monte Carlo approach and 99% confidence limits (Zang and Biondi 2015, Meko et al. 2011). Then, we constructed candidate models of growth: for each climate input variable in the diagnostic correlation analysis, we identified the three multi-month periods (“seasons”) with the greatest influence. Two are maximum correlations, and

one represents the longest duration of significant influence. Climate variables were summarized as means (deficit, temperature) or cumulative sums (precipitation). All combinations of these seasons, some overlapping, resulted in 20 candidate models. We compared model performance using Akaike's Information Criterion (AIC); among the highly ranked with equivalent AIC, the model with highest overall R^2 was selected (Johnson and Omland 2004). This statistical analysis was carried out using package *treeclim* and specifically the *Seascorr* diagnostic routine (R Core Team 2016, Zang and Biondi 2015).

2.3.3 Describing growth-ozone linkages

Growth response to ozone exposure in local climate context

In the second step of growth analysis, we examined response of tree growth to ozone pollution in the context of regional climate using a linear mixed effects approach (Figure 5). Mixed effects models are well suited for describing the factors affecting growth within this regional network, as random effects can statistically control for the expected variation among trees and sites (Crawley 2002). In each of the candidate models, relative growth from each tree included in the all sites chronology was the response variable, and the climate predictors identified in the first step served as fixed effects. To evaluate the influence of ozone, we employed ozone exposure parameters in all their possible combinations. These are: 1) ozone exposure (June-September W126 index), which describes concentration over time, 2) a proxy for late summer water availability (either deficit or maximum temperature, both June-September), and 3) a term describing the interaction between ozone and summer water availability. Either maximum temperature or deficit represents water availability in the candidate models because both closely predict dry season water potentials (Urban et al. 2000, Royce and Barbour 2001a). Evapo-transpiration from mid-elevation Sierra Nevada forests is tightly coupled to summer temperature, a key component of deficit (Goldstein et al. 2000, Goulden et al. 2012, Stephenson 1998). The ozone exposure parameters are specific to June-September in the year of growth because this period, specifically the latter part, encompasses the disparity between ozone flux and uptake (Panek and Goldstein 2001, Panek 2004). Tree size and year of growth are the remaining fixed parameters in the model, included to capture the influence of size and autocorrelation in growth. The variation among trees and sites was accounted for with nested (trees within sites) random intercepts. Because annual ozone exposure data is first available in 1984, the mixed effects analysis examined annual growth from 1984-2012. All predictor variables were scaled (mean = 0, variance =1) before model fitting. Parameter estimates were calculated using restricted maximum log-likelihood (REML, Bates et al. 2015). As before, we used the ΔAIC to select the best model among the candidates (Johnson and Omland 2004).

Performance of the final growth response model was assessed using the variance explained and a comparison of predicted versus observed annual growth. We assessed marginal and conditional R^2, or the expression of the variance explained by the fixed effects and by the fixed and random effects together (Nakagawa and Schielzeth 2013). We further diagnosed model fit by comparing the observed and model-predicted relative growth, as well as the distribution of these differences. We assessed the importance of key parameters and interactions within the growth response model using likelihood ratio tests. Likelihood estimates were calculated using REML, and p-values for each effect were obtained by likelihood ratio tests of the final growth response model with and without the parameter of interest (Pinheiro and Bates 2000). We quantified the growth

impact of parameters in terms of unscaled relative growth (percent rBAI per year) under median conditions of all other predictors. Using results of these analyses, we then explored the implications of our findings by hindcasting tree growth responses to contrasting air quality scenarios.

2.3.4 Interaction of ozone with summer water limitation

To investigate the potential influence of ozone and summer water availability in interaction, we began with the likelihood ratio test described above. We then examined the response's patterns in the context of covarying environmental conditions. We compared the observed magnitude and direction of growth response to a null model containing an additive response to the effects of ozone and summer temperatures (the selected proxy for water availability). The goal of this analysis was to specify the growth impacts of the ozone – water limitation interaction, and to describe whether the relationship has an additive, antagonistic, or synergistic effect on tree growth. Expected combined effects were based on the sum of stressor effects in isolation, with significant departures from the (null) additive effect representing antagonistic or synergistic interactions (Darling and Côté 2008). Effect size was calculated by varying each of the stressors independently by one standard deviation, keeping all other predictors at median values. The null model, an additive response, was computed from the sum of main effects in isolation (Gurevitch et al. 1992). Estimates for single and combined parameters were derived from REML estimates of the growth response model, with 95% confidence intervals computed from their likelihood profiles (Pinheiro and Bates 2000). Effect sizes were rescaled to the observed values for the purposes of visualization. All statistical analysis with the exception of chronology development, as noted, was carried out in the R statistical computing environment version 3.3.0 (R Core Team 2016).

3. RESULTS

3.1 Climatic influence on growth

3.1.1 Tree growth and regional climate

The overall series intercorrelation for the minimum ozone chronology was 0.51, with a mean length of 83 years (Table 1). Seventy-seven individuals make up the chronology; sample depth at the start of climate data availability (1897) is n=10 trees. Across the five mid-elevation sites included in this analysis, canopy Jeffrey pines demonstrated a significant and shared response to climate over the last century. Climatic patterns showcased the strong annual summer drought (Figure 6). High precipitation years were driven by December-March rain and snow; summer temperatures and deficits peak in July and August. Responses to California's 1976-77 drought (largest growth decline) and 1982 El Nino-driven rainy season (largest growth increase) were among the clearest patterns in the chronology (Figures 7 and 8). Variation across sites (selected for their shared climatic conditions) was limited as measured by annual totals (precipitation, deficit) or average maximum temperature (Appendix A, Figure A2). The frequency of "warm drought" years, defined as with years with both hot and dry conditions (> 0.5 SD temperature and precipitation) was 17% in the last 29 years (1984-2012), compared to 5.7% from 1897-1983.

3.1.2 Seasonality of growth response to climate

Using the Jeffrey pine minimum ozone chronology, we examined seasonal response to climate over periods of 1, 3, 5, 7 and 9 months, 1897-2012. In this diagnostic correlation analysis, we found that annual growth indices were consistently positively correlated with precipitation and negatively correlated with deficit and maximum temperature ($\alpha = 0.01$). Temperature was significantly correlated in single-month windows; temperature and precipitation in 3-month windows, and all three climate variables seasons in longer than 5 months. For each of these variables, the number of significant periods increased with season length, and 9 month seasons had both the longest consecutive significant responses and the largest coefficients (Figure 9). Precipitation and deficit had similar overall timing in their influence on growth index. The strongest responses were in periods 7-9 months long, with highest correlations from the previous June through February of the calendar growth year. Temperature was also significantly correlated in summer and fall of the previous year, but for fewer consecutive periods. Using candidate models parameterized with the best primary correlations, we evaluated competing linear models of tree growth. Four models, all including summed June-February precipitation as a predictor, exceeded the performance of all others (ΔAIC to next best = 4.9, ΔAIC to first model including deficit in place of precipitation = 19.5). As these four were not differentiable in terms of AIC ($\Delta AIC < 2$), we selected the model with the greatest variance explained (adjusted R^2= 0.29; Figure 10). The model form is:

3: $RWI \sim 0.99 + (0.06 \times Ppt) + (-0.06 \times Temp) + (-0.01 \times (Ppt*Temp)) + \varepsilon$

for precipitation summed from the previous June through February and mean temperature from March through September of the previous year (Appendix A, Figure A3). Higher precipitation in the previous summer through winter was tied to larger ring width index, and higher temperatures in the previous year had the reverse effect. Specifically, the best climate model of annual ring width increment in 2012 depends on the total precipitation from June 2011 through February 2012 and average maximum temperature from March 2011 through September 2011. Precipitation and temperature were significant ($p << 0.01$); although the interaction of precipitation and temperature was not a significant predictor on its own, it was ultimately included in the selected model on the basis of overall model AIC. Variation in relative growth predicted by the model increased above about 20°C maximum temperature (Figure 10).

3.2 Ozone impacts on growth

3.2.1 Growth model selection and performance

The chronology from all seven sites across a regional gradient of pollution severity encompasses 323 trees and spans 1984-2012, overlapping the ozone exposure record (Figure 11, Table 1). The linear mixed effects model that best explained relative growth response in the all sites chronology included the climatic variables selected above, ozone exposure, growing season summer temperature as a proxy for water availability, and the interaction of ozone exposure with growing-season summer temperature (Table 2). The covariables of tree size (DBH) and timing (year) were also included in the selected model. Total variance explained (conditional R^2) for the selected model was 0.78; variance explained by fixed effects only (marginal R^2) was 0.37 (Appendix A Table A1). The model showed some inflation of variance with increasing relative growth, but otherwise met assumptions of normality in error distribution (Appendix A Figure A4). In examining model fit, we found that the distribution of predicted relative growth values

was not differentiable from those observed. The ΔrBAI, or difference between observed and predicted relative growth, was also centered at zero (Figure 12).

3.2.2 Influence of individual stressors and environmental conditions

The separate influence of each parameter on total relative growth was determined using a series of likelihood ratio tests (Table 3). In our model of tree growth, tree size was the most important fixed effect, with a likelihood estimate (-0.48) almost double that of the nearest predictors, ozone exposure and year (-0.24). Stressors specified in the model were climate (precipitation and temperature), ozone exposure, and growing season summer temperature. Ozone had the largest negative impact on growth, followed by previous year temperature (Figure 13, Table 3). Precipitation had a comparatively smaller and positive impact on growth (0.03). Both growing season summer temperature and its interaction with ozone were also significant and positive predictors of relative growth, although summer temperatures in their own right were not a significant influence in the regional climate response model (above). Of the random factors, the influence of variation among individuals was greater than that among sites.

3.3 Interacting stressors: summer ozone and summer temperatures

Initial likelihood ratio tests confirmed that both summer maximum temperatures and their interaction with ozone exposure were important predictors of relative growth ($p<0.0001$). The model indicates a changing response to ozone with increasing summer temperatures. Below average temperatures elicit moderate growth declines in response to ozone exposure (Figure 14, negative slope). For above average temperatures, growth has the opposite response, increasing with ozone exposure in a strong positive relationship (Figure 14, positive slope). This type of shift in response is diagnostic of interacting predictors.

We described the type of interaction by comparing the observed growth response to a model with a linearly additive growth response, as in Figure 1, part B. The relative growth rate at an ozone exposure of +1 standard deviation above the median, (81.2 ppm-hours), was 1.96% yr^{-1} ± 0.08%. Growth in response to +1 standard deviation increase in summer high temperatures (28.6 °C) alone was higher than typical growth, at 2.55± 0.05%. This is consistent with the definition of stressor as a driver with negative or positive impact (Boyd and Hutchins 2012, Côté et al. 2016). The predicted annual growth response with ozone and temperature interacting was 2.26 ± 0.16%. This was a significantly higher growth rate than expected from the sum of individual ozone exposure and summer temperature responses. The direction and magnitude of this departure from the expected additive response indicated that an antagonistic interaction takes place between ozone exposure and water limitation (Figure 15).

4. DISCUSSION

4.1 Key outcomes

Our evidence supports the contention that California's summer drought limits the negative impact of ozone pollution on the growth of Jeffrey pine trees. The design of our field study in the southern Sierra Nevada allowed us to isolate the common climatic drivers of tree growth from the effects of air pollution. We found that growth in mature Jeffrey pines is dependent on precipitation and spring-summer temperatures in the previous year. Importantly, trees exposed to elevated ozone also demonstrated lower relative growth rates when their typical growth

responses to climate were accounted for. These growth losses, attributable to a chronic anthropogenic stressor and modified by prevailing environmental conditions, may facilitate further changes to forest processes.

4.2 Implications and mechanism of the ozone-water limitation interaction

4.2.1 Implications

As ecologists, we often are concerned about the possibility of synergies amongst interacting stressors because such interactions can cause unpredictable outcomes, with tremendous potential to degrade ecosystems (Côté et al. 2016, Paine et al. 1998). However, antagonistic interactions amongst ecological actors are a more common case, and they too have widespread ecosystem implications – sometimes just as surprising (Darling and Côté 2008). Particularly with respect to global change agents, antagonistic relationships such as the one observed here have the potential to alter expected response to stressors, with widespread implications – for example, higher than expected annual growth rates in trees. Accounting for interactions and understanding the mechanisms driving these relationships will help more accurately predict their ecological responses (Rollinson et al. 2016).

4.2.2 Mechanisms and patterns of antagonistic interaction

Antagonistic interactions between ozone and prevailing climatic conditions led to a lessened overall growth impact from this common pollutant (Figure 15). Detailed physiological and atmospheric observations in ponderosa and Jeffrey pine stands show that water limitation, and specifically, stomatal closure, is the probable mechanism for this interaction (Bauer et al. 2000, Panek 2004, Ustin 2004). There is a clear divergence between ozone flux to needles and ambient concentration in water limited conditions, particularly during late summer (Panek and Goldstein 2001, Fares et al. 2013). Stomatal conductance is tightly controlled by leaf water potential, and stomatal resistance is the major influence on the transfer of any gas, including ozone, to vegetation (Baldocchi et al. 1987, Panek 2004). Jeffrey pine conductance and cambial growth largely stops when predawn water potentials surpass -0.7 MPa (Royce and Barbour 2001b). Accordingly, summer ozone uptake parallels canopy conductance: as water potentials reach this threshold, on average around Julian date 200 (mid-July), stomatal closure reduces ozone flux. Therefore, the tight link between summer maximum temperature and water availability results in the observed interaction between temperature and growth impacts from ozone.

The consequences on tree growth of this interaction will vary on the landscape according to local water availability and diurnal patterns in ozone concentration and uptake. Importantly, trees in mesic sites or with access to deep water may not experience the drop in ozone flux brought on by stomatal closure. Under dry conditions these individuals would continue photosynthesis, at the cost of additional pollution damage (Grulke et al. 2003). Ozone flux and concentration are also decoupled diurnally, with lower fluxes than concentrations beginning in late afternoon and lasting into evening (Bauer et al. 2000). The impact of this daily difference will vary depending on the diurnal pattern in ambient ozone concentration at a given site and the daily and seasonal timing of ozone flux (Kurpius and Goldstein 2003, Van Ooy and Carroll 1995).

However, in other ecosystems the interaction of ozone exposure and water use plays out much differently: Sun and others (Sun et al. 2012) observed watershed-scale increases in water use in polluted forests, facilitated by loss of stomatal control and runaway transpiration. “Sluggish”

stomatal control is caused by physical breakdown in the guard cells and membranes that grant osmotic control of the stomatal pore. This type of response to oxidative damage is more often prevalent in angiosperms than gymnosperms (Heath et al. 1997, Karnosky et al. 2007, Matyssek et al. 2003; cf. Kellomäki and Wang 1997). While Sierra Nevada forests will sustain greater pollution impacts when water is not limiting, Appalachian hardwood forests sustain greater pollution impacts in years of drought (McLaughlin et al. 2007). The relationship between climate, ozone, and growth is clearly context dependent. Thus characterizing the ecosystem-specific implications of interacting stressors is essential for understanding the full complexity of responses to compound stress and also for reducing uncertainty in dynamic vegetation models.

4.3 Climatic controls on tree growth

4.3.1 Precipitation and temperature

Growth in Jeffrey pines is dependent on climate of the previous year and preceding wet season, a common pattern in trees of Mediterranean climates generally and of Sierra Nevada forests specifically (Andreu et al. 2007, Fritts 1976, Yeh and Wensel 2000). The influence of rain and snow on growth is most evident from June of the previous year through February. Fall and winter precipitation clearly form the bulk of this supply: water stored in soil and bedrock fissures is an essential resource during the following growing season (Hubbert et al. 2001, Holbrook et al. 2014). The importance of previous summer rains to growth is likely manifested via water available for late-season bud formation and storage of non-structural carbohydrates, which facilitate rapid growth in the following spring (Kozlowski et al. 2012). Temperatures are most influential spanning March through September of the previous year, with higher spring and summer temperatures driving lower growth rates in the following year. In this water-limited system, the importance of temperature to growth similarly reflects water availability. Cool and moderate temperatures enable lower transpiration rates, longer growing seasons, and storage of carbon, resources utilized for rapid post-snowmelt growth the following year (Royce and Barbour 2001b). Under the warmest spring and summer conditions, water is limiting to late-season storage and growth in the following year reduced. Though the timing of growth shifts as elevation increases, directional relationships with precipitation and temperature are consistent within the mixed conifer forest type (Fowells 1941,Yeh and Wensel 2000).

4.3.2 Climatic water deficit

Although climatic water deficit did influence annual tree growth (Appendix A Figure A1), at these sites we found that cumulative seasonal deficits did not explain as much variation as mean temperature or cumulative precipitation. Yet, deficit is a strong predictor of mortality and of patterns in vegetation distribution (Das et al. 2013, Lutz et al. 2010). We attributed the comparatively lower importance of deficit to two possible factors. First, our research sites were intentionally selected to have similar average deficits across the regional network. This design choice facilitated comparison of trees across the region on the basis of their shared response to climate. Unavoidably, it also muted variation in deficit amongst sites and trees. A second explanation is that deficit indexes evaporative demand that is not met by available water, integrating both water storage and demand (Stephenson 1998). While storage at the ecosystem scale is effectively captured in deficit calculations (Flint et al. 2013), fine-scale storage relevant to individual trees is shaped by local factors, including soil thickness (Meyer et al. 2007). Local

exceptions to deficit not captured in deficit calculations – for example, trees with access to late-season water or locally deep soils – may also foster insensitivity to this climatic indicator.

4.3.3 Growing season summer temperature

Growing season summer temperature, a factor included because of its potential interaction with ozone, has an influence on growth distinct from the influence of previous year temperature. We found that higher maximum summer temperatures had a small positive influence on relative growth (Figure 14, Table 3), a pattern also apparent in previous work on Jeffrey pine (Royce and Barbour 2001b). Response to summer temperatures likely reflects growing season length; with available water, trees typically continue some growth into late summer and fall. Since apical growth and internode number depend on conditions when primordia are formed, previous March-September temperatures have a larger negative effect than the positive one seen in the current summer (Kozlowski et al. 2012, Pavlik and Barbour 1991, Royce and Barbour 2001b, Williams et al. 2013). To be clear, growth of tree rings takes place predominantly in spring and early summer. Therefore, previous year temperatures and winter precipitation, which are the major influences on supply of water and resources for formation of primordia, have the strongest climatic influence on growth. Secondarily, summer temperatures within the dwindling growing season drive evapotranspiration and indicate the onset of stomatal closure. It is as a proxy for late-season water potential that we are interested in the interaction of temperature with ozone exposure.

4.4 Growth response to ozone

4.4.1 Quantifying growth response

We observed an overall negative impact of ozone pollution on tree growth under field conditions in the southern Sierra Nevada, even when antagonistically interacting with high summer temperatures. In our growth model, predicted growth at zero ozone exposure (0 ppm-hours), with all other conditions at their observed median, is 3.25% annually (Figure 13). By contrast, growth in high ozone conditions, (+1 SD, 81.2 ppm-hours), corresponds to relative growth rates of 2.27% annually, a difference of 30%. We see similar growth differences in a simulated scenario of compliance with the current NAAQS for ozone. Jeffrey pines at Giant Forest and Grant Grove, two severely impacted sites in Sequoia and Kings Canyon National Parks, have average observed growth rates of 1.38% per year from 1984-2012, with typical ozone exposure of 75.5 ppm-hours during that period. Lowering the mean ozone exposure to 17 ppm-hours, the current NAAQS threshold for protection of ecosystems and people, increases predicted growth rates to 1.65%, a gain of 19% (Figure 16). Notably, the difference between these rates has declined through time, averaging 0.38% in 1991-2000 and 0.14% in 2001-2012. This tapering difference in growth rates under polluted versus compliant air quality, from 23% relative growth loses in the 1990s to 8.4% in the 2000s, closely matches improvements in air quality over the same time frame (Chapter 2, Table A2; National Park Service Air Resources Division 2015, San Joaquin Valley Air Pollution Control District 2010). The predicted growth losses are also remarkably similar to observed measures of growth response, which we characterized via long term re-measurement of trees and visible ozone injury (up to 24%; Chapter 2 Figure 4).

4.4.2 Related findings on ozone impacts

While past estimates of pollution-driven growth losses in Jeffrey and ponderosa pines vary considerably, they are in many ways consistent with our observations. Under field conditions,

Peterson and others recorded growth losses of 11% in mature Jeffrey pines from polluted areas of Sequoia National Park (Peterson et al. 1987). A similar dendroecological study of ponderosa pines throughout the Sierra Nevada, however, found no clear evidence of growth impacts (Peterson et al. 1991, Peterson and Arbaugh 1988). Arbaugh and others observed declines in BAI in the San Bernardino Mountains ranging from 7.8–23.2% during 1950-1974, a period of extreme air pollution in the region. In this system with many stressors, they attributed these changes to the compound effects of ozone, drought, and nitrogen deposition (1999). Growth losses under experimental conditions are typically larger, but have been assessed primarily in juvenile trees with rapid pollutant uptake (thoroughly reviewed in U.S. Environmental Protection Agency 2014 and U.S. Environmental Protection Agency 2013). For field studies, attributing growth losses to ozone has proven difficult, in part due to the complexity of controlling for other influences on growth (Gemmill et al. 1982, Matyssek et al. 2012). Researchers have used both temporal isolation (before and after ozone exposure) and experimental controls (as in Free-Air Carbon dioxide Enrichment sites) to understand ecosystem patterns. We met this challenge by leveraging an existing gradient in ozone pollution in our research design, allowing comparison of tree growth under otherwise comparable climatic conditions.

4.4.3 Additional environmental interactions

Two important additional factors to consider in this study and in ozone response studies more broadly are nitrogen deposition and forest structure, both of which can manifest as additional ecosystem stressors. Although nitrogen deposition is elevated above natural levels in the southern Sierra Nevada, the forest sites in question do not exceed the critical load for nitrate leaching or tree root biomass loss in California mixed conifer forests (17 kg N/ ha/year, Panek et al. 2013b, Fenn et al. 2003, Fenn et al. 2010). Sites nearest pollution sources do likely exceed 5 kg N/ha/year, however, the critical load threshold for sensitive lichen communities. It is therefore possible that our ozone gradient is also a shallow nitrogen gradient. Additional nitrogen inputs could be expected to exacerbate existing ozone impacts by accelerating needle senescence, increasing susceptibility to bark beetle attack, and increasing risk of fire spread; they may also mask growth effects to some degree (Eatough Jones et al. 2004, Grulke 2009, Takemoto et al. 2001).

Southern Sierra Nevada mixed conifer forests are also notably denser and have lower fire frequency compared to their historical analogs (McKelvey et al. 1996, Parsons and Debenedetti 1979, Stephens et al. 2015). The absence of fire or active harvest increases water limitation, with impacts expected on overall tree vigor as well as stomatal behavior, amongst many other changes to forest dynamics (Gray et al. 2005, McIntyre et al. 2015). Our research sites are undoubtedly modified by this management legacy, which could reduce overall growth rates while also amplifying the importance of the interaction between ozone and water limitation. Many mixed conifer stands in the wider region have seen dramatic increases in small tree density over the last half century. Canopy cover increased 25-49% from 1911 to present in parts of Sequoia National Forest, nearby to the south, and the pattern of ingrowth by white fir is common in many sites along the western slope (Levine et al 2016, Knapp et al. 2013, Stephens et al 2015). Density and composition change in the well-drained, open Jeffrey pine stands such as those in our study (17-28 m^2/ha, Figure 4), however, is comparatively small. Low density and high structural variability may combine for increased resilience in these stands, and in some cases, they even have continued presence of low intensity fire (Collins et al. 2007, Stephens and Gill 2005). The mixed

conifer forests of the San Bernardino mountains provide an example of the combined ecosystem effects of ozone, nitrogen deposition, long term fire suppression, and drought. These forests, having first demonstrated marked growth impacts, eventually sustained bark beetle irruptions, high litter loads, nitrate leaching, widespread mortality, and eventual shifts in community composition (Arbaugh et al. 1999, Grulke et al. 1998, McBride and Laven 1999, Miller et al. 1998).

4.5 Impacts of chronic stress on trees and forests

4.5.1 Effects of resource alteration

Ozone pollution has reduced tree growth in polluted southern Sierra Nevada forests, potentially for over forty years. Tropospheric ozone, like other drivers of global change, is characterized not only by its human origin, but also by its continuous and directional press disturbance of ecosystems (Bytnerowicz et al. 2013, Ives and Carpenter 2007). This press disturbance, a long term reduction in air quality, is now a chronic resource alteration of the forest ecosystem. Chronic resource alterations can ultimately lead to modified ecosystem function and reorganization, through both direct and indirect effects (Smith et al. 2009). Higher order impacts and non-linear ecosystem change begin with individual level effects, such as the tree growth responses we have described here. In light of the substantial impacts we observed, it is appropriate to evaluate the potential life history and community implications of long term growth reductions.

Growth indicates tree vitality. Reduced growth rates generally, and oxidative damage specifically, lead to greater susceptibility to disease and damaging attacks by bark beetles and defoliators (Chappelka and Grulke 2016, Krupa et al. 2001, Miller et al. 1998). Slower growing trees are also more vulnerable to common pathogenic fungi (James et al. 1980, Fenn et al. 1990). Tree growth reductions can become self-reinforcing, with initial declines creating positive feedback loops of increasing loss, often mediated by competition or a biological agent. Long term reductions in growth are known to increase likelihood of individual tree mortality (Pedersen 1998a, Das et al. 2007). For example, in Sierra Nevada ponderosa pines, long term (previous 10 years) growth trends are a key control on the probability of mortality (Collins et al. 2014). The influence of growth reductions on mortality is typically as a secondary, contributing factor as opposed to as a primary agent (predisposing versus inciting, sensu Manion 1991; Pedersen 1998b). However, a history of reduced relative growth rates can also mean lower capacity for resilience and recovery when trees face acute stressors (Lloret et al. 2011). Even in the absence of mortality outcomes, differential effects of press disturbance can also alter interspecific interactions (Schmitz 1997). All else being equal, for Sierra Nevada mixed conifer forests with long term growth losses in Jeffrey pine, advantages may accrue to sugar pine and incense-cedar, the least sensitive co-occurring species, and white fir, which is intermediate in ozone sensitivity (Miller et al. 1983). White fir is already favored by long term fire suppression, while sugar pine currently suffers elevated mortality rates due to an introduced pathogen. The disproportionate impacts of ozone on juvenile trees, which take up ambient air at greater rates, could exacerbate community composition effects (McBride and Laven 1999, Pye 1988). In sum, resource alteration in the form of ozone pollution is among the many chronic alterations that pose of risk of pushing ecological systems along novel trajectories of change (National Research Council 2001, Smith et al. 2009).

4.5.2 Chronic stress compounded

Our study has specifically examined the interaction between ozone and annual late-summer water limitation, but the stressors and their outcomes in the ecosystem may also combine with still other factors. There is increasing awareness that novel combinations of anthropogenic stressors, especially in ecosystems with chronic resource alteration, may compromise ecosystem resilience or facilitate shifts to new states (Darling and Cote 2008). The southern Sierra Nevada today is host to both chronic anthropogenic air pollution and the most severe drought in centuries (Griffin and Anchukaitis 2014). We know that as of 2012, before onset of the drought, chronic stress from ozone pollution had produced long term growth impacts in pines. By the summer of 2016, upwards of 66 million trees had succumbed to drought and bark beetle attacks in the Sierra Nevada. Mortality is most severe in Sierra National Forest, Sequoia National Park, and Sequoia National Forest, and water stress is widespread (Asner et al. 2016). We believe that in the areas most impacted by pollution, the effects of this chronic anthropogenic stressor have heightened the already-high risk of drought-induced mortality. Clearly, drought alone would have had substantial mortality effects. Forest densification and fire suppression have certainly also contributed to competition for limited water resources. But even considering these factors, gradual environmental change through degradation of air quality has undeniably set the stage for severe ecosystem impacts during this rare climatic event (Smith et al. 2009).

4.5.3 Long term anthropogenic environmental change

Ozone is just one of the many long term anthropogenic stressors that have the potential to incrementally degrade ecosystems (Ainsworth et al. 2012, Bytnerowicz et al. 2013). Most do not make environmental headlines. The long term, often subtle change of press disturbances and chronic stressors makes their influence notoriously difficult to detect in brief study, but all the more important for explaining underlying patterns and processes in the environment. Drivers of global change like carbon dioxide, nitrogen emissions, and methane often share these signature low and slow attributes. While ecologists may not be surprised to find that a small long term change in an invisible gas has the capacity to alter an ecosystem process, understanding the implications and interactions of these subtle stressors is critical to understanding our changing world. The work of disentangling these interactions also provides a fascinating window into the connections that can make ecosystems simultaneously resilient and vulnerable. As ozone pollution becomes increasingly widespread globally, its long term impacts in California forests might serve as a reminder that the ecosystems rarely adhere to human timescales, nor do they readily reveal their ills. “We are never justified in assuming a force to be insignificant because its measure is unknown, or even because no physical effect can now be traced to it as its origin. The collection of phenomena must precede the analysis of them” (Marsh 1864).

ACKNOWLEDGEMENTS

This research was conducted with the permission of the National Park Service, study SEKI-00380. Air quality data was provided by the National Park Service Air Resources Division, California Air Resources Board, and US Forest Service Region 5 Air Program. For collection and management of ozone exposure data and safekeeping of past research plot information, we thank Annie Esperanza, NPS, and Ricardo Cisneros, USFS/UC Merced. For patient assistance with ozone indexing methods, we thank Don Schweizer, USFS/UC Merced. Thanks to Koren

Nydick and Ginger Bradshaw, NPS, for their guidance with research permitting and logistical support.

Core preparations and measurement, a herculean task, was primarily the work of John Sanders and Debra Swenson, with help from Jeneya Fertel and Natalie Holt. Each contributed many, many, hours at the microscope to the benefit of this project. Field data collection and vegetation measurements took place over the summers of 2011-2013. Debra Swenson was an essential leader of these efforts, and valuable contributions came from research technicians Eric Olliff, David Soderberg, Alex Javier, and Natalie Holt. Short term but critical field assistance was contributed by Hannah Volpi, Maya Hayden, John Sanders, Shelby Semmes, Peter Larson, and Rachel Freund. David Ackerly and Scott Stephens provided helpful feedback on an earlier draft of the manuscript. And finally, a debt of gratitude is owed to Kronk, boss of Cabin A3, and to the pie at the Silver City Store.

REFERENCES

Aber, J., R. Neilson, S. McNulty, J. Lenihan, D. Bachelet, and R. Drapek. 2001. Forest Processes and Global Environmental Change: Predicting the Effects of Individual and Multiple Stressors. BioScience **51**:735-751.

Adams, H. D., M. Guardiola-Claramonte, G. A. Barron-Gafford, J. C. Villegas, D. D. Breshears, C. B. Zou, P. A. Troch, and T. E. Huxman. 2009. Temperature sensitivity of drought-induced tree mortality portends increased regional die-off under global-change-type drought. Proceedings of the National Academy of Sciences **106**:7063-7066.

Ainsworth, E. A., C. R. Yendrek, S. Sitch, W. J. Collins, and L. D. Emberson. 2012. The Effects of Tropospheric Ozone on Net Primary Productivity and Implications for Climate Change. Annual Review of Plant Biology **63**:637-661.

Allen, C. D., and D. D. Breshears. 1998. Drought-induced shift of a forest-woodland ecotone: Rapid landscape response to climate variation. Proceedings of the National Academy of Sciences of the United States of America **95**:14839-14842.

Allen, C. D., A. K. Macalady, H. Chenchouni, D. Bachelet, N. McDowell, M. Vennetier, T. Kitzberger, A. Rigling, D. D. Breshears, E. H. Hogg, P. Gonzalez, R. Fensham, Z. Zhang, J. Castro, N. Demidova, J. H. Lim, G. Allard, S. W. Running, A. Semerci, and N. Cobb. 2010. A global overview of drought and heat-induced tree mortality reveals emerging climate change risks for forests. Forest Ecology and Management **259**:660-684.

Anderegg, W. R. L., C. Schwalm, F. Biondi, J. J. Camarero, G. Koch, M. Litvak, K. Ogle, J. D. Shaw, E. Shevliakova, A. P. Williams, A. Wolf, E. Ziaco, and S. Pacala. 2015. Pervasive drought legacies in forest ecosystems and their implications for carbon cycle models. Science **349**:528-532.

Andreu, L., E. Gutiérrez, M. Macias, M. Ribas, O. Bosch, and J. J. Camarero. 2007. Climate increases regional tree-growth variability in Iberian pine forests. Global Change Biology **13**:804-815.

Arbaugh, M., P. Miller, J. Carroll, and B. Takemoto. 1998. Relationships of ozone exposure to pine injury in the Sierra Nevada and San Bernardino Mountains of California, USA. Environmental Pollution **101**:291-301.

Arbaugh, M. J., and A. Bytnerowicz. 2003. Introduction to a regional passive ozone sampler network in the Sierra Nevada. Pages 157-164 *in* A. Bytnerowicz, M. J. Arbaugh, and R. Alonso, editors. Ozone air pollution in the Sierra Nevada: distribution and effects on forests. Elsevier Science Ltd., Oxford.

Arbaugh, M. J., D. L. Peterson, and P. R. Miller. 1999. Air pollution effects on growth of ponderosa pine, Jeffrey pine, and bigcone Douglas-fir. Pages 179 - 207 *in* P. R. Miller and J. R. McBride, editors. Oxidant Air Pollution Impacts in the Montane Forests of

Southern California: A Case Study of the San Bernardino Mountains. Springer, New York.

Asner, G. P., P. G. Brodrick, C. B. Anderson, N. Vaughn, D. E. Knapp, and R. E. Martin. 2016. Progressive forest canopy water loss during the 2012–2015 California drought. Proceedings of the National Academy of Sciences of the United States of America **113**:E249-E255.

Babst, F., O. Bouriaud, D. Papale, B. Gielen, I. a. Janssens, E. Nikinmaa, A. Ibrom, J. Wu, C. Bernhofer, B. Köstner, T. Grünwald, G. Seufert, P. Ciais, and D. Frank. 2013. Above-ground woody carbon sequestration measured from tree rings is coherent with net ecosystem productivity at five eddy-covariance sites. The New Phytologist.

Baldocchi, D. D., B. B. Hicks, and P. Camara. 1987. A canopy stomatal resistance model for gaseous deposition to vegetated surfaces. Atmospheric Environment (1967) **21**:91-101.

Bates, D., M. Mächler, B. Bolker, and S. Walker. 2015. Fitting Linear Mixed-Effects Models Using lme4. 2015 **67**:48.

Bauer, M., N. Hultman, J. Panek, and A. Goldstein. 2000. Ozone deposition to a ponderosa pine plantation in the Sierra Nevada Mountains(CA)- A comparison of two different climatic years. Journal of Geophysical Research **105**:123–136.

Bender, E. A., T. J. Case, and M. E. Gilpin. 1984. Perturbation Experiments in Community Ecology: Theory and Practice. Ecology **65**:1-13.

Biondi, F., and F. Qeadan. 2008. A Theory-Driven Approach to Tree-Ring Standardization: Defining the Biological Trend from Expected Basal Area Increment. Tree-Ring Research **64**:81-96.

Bowman, D. M. J. S., R. J. W. Brienen, E. Gloor, O. L. Phillips, and L. D. Prior. 2013. Detecting trends in tree growth: not so simple. Trends in Plant Science **18**:11-17.

Boyd, P. W., and D. A. Hutchins. 2012. Understanding the responses of ocean biota to a complex matrix of cumulative anthropogenic change. Marine Ecology Progress Series **470**:125-135.

Braun, S., C. Schindler, and B. Rihm. 2014. Growth losses in Swiss forests caused by ozone: Epidemiological data analysis of stem increment of Fagus sylvatica L. and Picea abies Karst. Environmental Pollution **192**:129-138.

Bunn, A. G., M. Korpela, F. Biondi, F. Campelo, P. Mérian, F. Qeadan, and C. Zang. 2016. dplR: Dendrochronology Program Library in R. R package version 1.6.4., https://CRAN.R-project.org/package=dplR.

Bytnerowicz, A., M. J. Arbaugh, and R. Alonso, editors. 2003. Ozone air pollution in the Sierra Nevada: distribution and effects on forests. . Elsevier Science Ltd.

Bytnerowicz, A., M. Fenn, S. McNulty, F. Yuan, A. Pourmokhtarian, C. Driscoll, and T. Meixner. 2013. Interactive Effects of Air Pollution and Climate Change on Forest Ecosystems in the United States: Current Understanding and Future Scenarios. Pages 333-369 *in* R. Matyssek, N. Clarke, P. Cudlin, T. N. Mikkelsen, J. P. Tuovinen, G. Wieser, and E. Paoletti, editors. Developments in Environmental Science. Elsevier.

Chappelka, A. H., and N. E. Grulke. 2016. Disruption of the 'disease triangle' by chemical and physical environmental change. Plant Biology **18**:5-12.

Cisneros, R., A. Bytnerowicz, D. Schweizer, S. Zhong, S. Traina, and D. H. Bennett. 2010. Ozone, nitric acid, and ammonia air pollution is unhealthy for people and ecosystems in southern Sierra Nevada, California. Environmental Pollution **158**:3261-3271.

Clark, D. A., S. Brown, D. W. Kicklighter, J. Q. Chambers, J. R. Thomlinson, and J. Ni. 2001. Measuring net primary production in forests: Concepts and field methods. Ecological Applications **11**:356-370.

Clark, J. S., D. M. Bell, M. C. Kwit, and K. Zhu. 2014. Competition-interaction landscapes for the joint response of forests to climate change. Global Change Biology **20**:1979-1991.

Clark, J. S., L. Iverson, C. W. Woodall, C. D. Allen, D. M. Bell, D. C. Bragg, A. W. D'Amato, F. W. Davis, M. H. Hersh, I. Ibanez, S. T. Jackson, S. Matthews, N. Pederson, M. Peters, M. W. Schwartz, K. M. Waring, and N. E. Zimmermann. 2016. The impacts of increasing drought on forest dynamics, structure, and biodiversity in the United States. Global Change Biology **22**:2329-2352.

Collins, B. M., A. J. Das, J. J. Battles, D. L. Fry, K. D. Krasnow, and S. L. Stephens. 2014. Beyond reducing fire hazard: fuel treatment impacts on overstory tree survival. Ecological Applications **24**:1879-1886.

Collins, B. M., M. Kelly, J. W. van Wagtendonk, and S. L. Stephens. 2007. Spatial patterns of large natural fires in Sierra Nevada wilderness areas. Landscape Ecology **22**:545-557.

Cook, E. R., and L. A. Kairiukstis. 1990. Methods of dendrochronology: applications in the environmental sciences. Kluwer Academic Publishers, Dordrecht, the Netherlands.

Côté, I. M., E. S. Darling, and C. J. Brown. 2016. Interactions among ecosystem stressors and their importance in conservation. Proceedings of the Royal Society B: Biological Sciences **283**:20152592.

Crawley, M. J. 2002. Statistical Computing: An Introduction to Data Analysis using S-Plus. Wiley, Hoboken, NJ, p. 772.

Darling, E. S., and I. M. Côté. 2008. Quantifying the evidence for ecological synergies. Ecology Letters **11**:1278-1286.

Das, A., J. Battles, N. Stephenson, and P. van Mantgem. 2007. The relationship between tree growth patterns and likelihood of mortality: a study of two tree species in the Sierra Nevada. Canadian Journal of Forest Research **37**:580-597.

Das, A. J., N. L. Stephenson, A. Flint, T. Das, and P. J. van Mantgem. 2013. Climatic correlates of tree mortality in water- and energy-limited forests. PLoS ONE **8**:e69917.

de Bauer, M. d. L., and T. Hernández-Tejeda. 2007. A review of ozone-induced effects on the forests of central Mexico. Environmental Pollution **147**:446-453.

Dobbertin, M. 2005. Tree growth as indicator of tree vitality and of tree reaction to environmental stress: a review. European Journal of Forest Research **124**:319-333.

Dolph, K. L. 1984. Relationships of inside and outside bark diameters for young-growth mixed-conifer species in the Sierra Nevada.*in* F. S. U.S. Department of Agriculture, Pacific Southwest Forest and Range Experiment Station, editor.

Eatough Jones, M., T. D. Paine, M. E. Fenn, and M. A. Poth. 2004. Influence of ozone and nitrogen deposition on bark beetle activity under drought conditions. Forest Ecology and Management **200**.

Fares, S., R. Vargas, M. Detto, A. H. Goldstein, J. Karlik, E. Paoletti, and M. Vitale. 2013. Tropospheric ozone reduces carbon assimilation in trees: estimates from analysis of continuous flux measurements. Global Change Biology **19**:2427-2443.

Feng, Z., J. Sun, W. Wan, E. Hu, and V. Calatayud. 2014. Evidence of widespread ozone-induced visible injury on plants in Beijing, China. Environmental Pollution **193**:296-301.

Fenn, M., M. Poth, A. Bytnerowicz, and J. Sickman. 2003. Effects of ozone, nitrogen deposition, and other stressors on montane ecosystems in the Sierra Nevada. Developments in ….

Fenn, M. E., E. B. Allen, S. B. Weiss, S. Jovan, L. H. Geiser, G. S. Tonnesen, R. F. Johnson, L. E. Rao, B. S. Gimeno, F. Yuan, T. Meixner, and A. Bytnerowicz. 2010. Nitrogen critical loads and management alternatives for N-impacted ecosystems in California. Journal of Environmental Management **91**:2404-2423.

Flint, L. E., A. L. Flint, J. F. Thorne, and R. Boynton. 2013. Fine-scale hydrologic modeling for regional landscape applications: the California Basin Characterization Model development and performance. Ecological Processes **2**.

Fowells, H. A. 1941. The period of seasonal growth of ponderosa pine and associated species. . California Forest and Range Experiment Station, Berkeley, Calif.

Franklin, J. F., H. H. Shugart, and M. E. Harmon. 1987. Tree death as an ecological process. BioScience **37**:550-556.

Fritts, H. C. 1976. Tree rings and climate. Academic Press., London.

Gemmill, B., J. McBride, and R. Laven. 1982. Development of tree-ring chronologies in an ozone air pollution-stressed forest in southern California. Tree-Ring Bull **42**:23-32.

Goldstein, A. H., N. E. Hultman, J. M. Fracheboud, M. R. Bauer, J. A. Panek, M. Xu, Y. Qi, A. B. Guenther, and W. Baugh. 2000. Effects of climate variability on the carbon dioxide, water, and sensible heat fluxes above a ponderosa pine plantation in the Sierra Nevada (CA). Agricultural and Forest Meteorology **101**:113-129.

Goulden, M. L., R. G. Anderson, R. C. Bales, A. E. Kelly, M. Meadows, and G. C. Winston. 2012. Evapotranspiration along an elevation gradient in California's Sierra Nevada. Journal of Geophysical Research: Biogeosciences **117**:n/a-n/a.

Gray, A., H. Zald, R. Kern, and M. North. 2005. Stand conditions associated with tree regeneration in Sierran mixed-conifer forests. Forest Science **51**:198-210.

Griffin, D., and K. J. Anchukaitis. 2014. How unusual is the 2012–2014 California drought? Geophysical Research Letters **41**:9017-9023.

Grulke, N. E., C. P. Andersen, M. E. Fenn, and P. R. Miller. 1998. Ozone exposure and nitrogen deposition lowers root biomass of ponderosa pine in the San Bernardino Mountains, California. Environmental Pollution **103**:63-73.

Grulke, N. E., and L. Balduman. 1999. Deciduous Conifers: High N Deposition and O3 Exposure Effects on Growth and Biomass Allocation in Ponderosa Pine. Water, Air, and Soil Pollution **116**:235-248.

Grulke, N. E., R. Johnson, A. Esperanza, D. Jones, T. Nguyen, S. Posch, and M. Tausz. 2003. Canopy transpiration of Jeffrey pine in mesic and xeric microsites: O3 uptake and injury response. Trees **17**:292-298.

Grulke, N. E., Minnich, R.A., Paine, T.D., Seybold, S.J., Chavez, D.J., Fenn, M.E., Riggan, P.J., Dunn, A., . 2009. Air pollution increases forest susceptibility to wildfires: a case study in the San Bernardino Mountains in southern California. In: Bytnerowicz, A., Arbaugh, M.J., Riebau, A.R., Andersen, C. (Eds.), Wildland Fires and Air Pollution. Developments in Environmental Science, vol. 8. Elsevier, Amsterdam, pp. 365–403.

Gurevitch, J., L. L. Morrow, A. Wallace, and J. S. Walsh. 1992. A Meta-Analysis of Competition in Field Experiments. The American Naturalist **140**:539-572.

Heath, R. L., G. E. Taylor, H. Sandermann, A. R. Wellburn, and R. L. Heath. 1997. Physiological Processes and Plant Responses to Ozone Exposure

Forest Decline and Ozone. Pages 317-368 *in* M. M. Caldwell, G. Heldmaier, R. B. Jackson, O. L. Lange, H. A. Mooney, E. D. Schulze, and U. Sommer, editors. Springer Berlin Heidelberg.

Hicke, J. A., C. D. Allen, A. R. Desai, M. C. Dietze, R. J. Hall, E. H. Hogg, D. M. Kashian, D. Moore, K. F. Raffa, R. N. Sturrock, and J. Vogelmann. 2012. Effects of biotic

disturbances on forest carbon cycling in the United States and Canada. Global Change Biology **18**:7-34.

Holbrook, W. S., C. S. Riebe, M. Elwaseif, J. L. Hayes, K. Basler-Reeder, D. L. Harry, A. Malazian, A. Dosseto, P. C. Hartsough, and J. W. Hopmans. 2014. Geophysical constraints on deep weathering and water storage potential in the Southern Sierra Critical Zone Observatory. Earth Surface Processes and Landforms **39**:366-380.

Hubbert, K. R., J. L. Beyers, and R. C. Graham. 2001. Roles of weathered bedrock and soil in seasonal water relations of Pinus Jeffreyi and Arctostaphylos patula. Canadian Journal of Forest Research **31**:1947-1957.

Hurteau, M., H. Zald, and M. North. 2007. Species-specific response to climate reconstruction in upper-elevation mixed-conifer forests of the western Sierra Nevada, California. Canadian Journal of Forest Research-Revue Canadienne De Recherche Forestiere **37**:1681-1691.

Innes, J., and E. Cook. 1989. Tree-ring analysis as an aid to evaluating the effects of pollution on tree growth. Canadian Journal of Forest Research **19**:1174-1189.

Ives, A. R., and S. R. Carpenter. 2007. Stability and Diversity of Ecosystems. Science **317**:58-62.

Johnson, J. B., and K. S. Omland. 2004. Model selection in ecology and evolution. Trends in Ecology & Evolution **19**:101-108.

Karnosky, D. F., J. M. Skelly, K. E. Percy, and A. H. Chappelka. 2007. Perspectives regarding 50 years of research on effects of tropospheric ozone air pollution on US forests. Environmental Pollution **147**:489-506.

Kellomäki, S., and K. Y. Wang. 1997. Effects of elevated O3 and CO2 concentrations on photosynthesis and stomatal conductance in Scots pine. Plant, Cell & Environment **20**:995-1006.

Knapp, E. E., C. N. Skinner, M. P. North, and B. L. Estes. 2013. Long-term overstory and understory change following logging and fire exclusion in a Sierra Nevada mixed-conifer forest. Forest Ecology and Management **310**:903-914.

Kozlowski, T. T., P. J. Kramer, S. G. Pallardy, and J. Roy. 2012. The Physiological Ecology of Woody Plants. Elsevier Science.

Krupa, S., M. McGrath, C. Andersen, F. Booker, K. Burkey, A. Chappelka, B. Chevone, E. Pell, and B. Zilinskas. 2001. Ambient ozone and plant health. Plant Disease **85**:4-12.

Kurpius, M. R., and A. H. Goldstein. 2003. Gas-phase chemistry dominates O3 loss to a forest, implying a source of aerosols and hydroxyl radicals to the atmosphere. Geophysical Research Letters **30**:n/a-n/a.

Lefohn, A. S., and V. C. Runeckles. 1987. Establishing standards to protect vegetation—ozone exposure/dose considerations. Atmospheric Environment **21**:561-568.

Levine, C.R., F. Krivak-Tetley, N.S. van Doorn, J.-A.S. Ansley, and J.J. Battles. 2016. Long-term demographic trends in a fire-suppressed mixed-conifer forest. Canadian Journal of Forest Research 46:745–752. doi: dx.doi.org/10.1139/cjfr-2015-0406.

Littell, J. S., D. L. Peterson, and M. Tjoelker. 2008. Douglas-fir growth in mountain ecosystems: Water limits tree growth from stand to region. Ecological Monographs 78:349-368.

Lloret, F., E. G. Keeling, and A. Sala. 2011. Components of tree resilience: effects of successive low-growth episodes in old ponderosa pine forests. Oikos **120**:1909-1920.

Lutz, J. A., J. W. v. Wagtendonk, and J. F. Franklin. 2010. Climatic water deficit, tree species ranges, and climate change in Yosemite National Park. Journal of Biogeography **37**:936-950.

Macalady, A. K., and H. Bugmann. 2014. Growth-Mortality Relationships in Pinon Pine (Pinus edulis) during Severe Droughts of the Past Century: Shifting Processes in Space and Time. PLoS ONE **9**:17.

Manion, P. D. 1991. Tree Disease Concepts. Prentice Hall, Englewood Cliffs, NJ.

Marsh, G. P. 1864. Man and Nature. Or, Physical Geography as Modified by Human Action. Reprinted. Belknap Press of Harvard University Press, Cambridge, Massachusetts.

Matyssek, R., H. Sandermann, K. Esser, U. Lüttge, W. Beyschlag, and F. Hellwig. 2003. Impact of Ozone on Trees: an Ecophysiological Perspective. Pages 349-404 *in* U. Lüttge, W. Beyschlag, B. Büdel, and D. Francis, editors. Progress in Botany. Springer.

Matyssek, R., G. Wieser, C. Calfapietra, W. de Vries, P. Dizengremel, D. Ernst, Y. Jolivet, T. N. Mikkelsen, G. M. J. Mohren, D. Le Thiec, J. P. Tuovinen, A. Weatherall, and E. Paoletti. 2012. Forests under climate change and air pollution: Gaps in understanding and future directions for research. Environmental Pollution **160**:57-65.

McBride, J. R., and R. D. Laven. 1999. Impact of Oxidant Air Pollutants on Forest Succession in the Mixed Conifer Forests of the San Bernardino Mountains.*in* P. R. Miller and J. R. McBride, editors. Oxidant Air Pollution Impacts in the Montane Forests of Southern California a Case Study of the San Bernardino Mountains. Springer-Verlag, New York.

McIntyre, P. J., J. H. Thorne, C. R. Dolanc, A. L. Flint, L. E. Flint, M. Kelly, and D. D. Ackerly. 2015. Twentieth-century shifts in forest structure in California: Denser forests, smaller trees, and increased dominance of oaks. Proceedings of the National Academy of Sciences **112**:1458-1463.

McKelvey, K. S., C. N. Skinner, C. Chang, D. C. Erman, S. J. Husari, D. J. Parsons, J. W. van Wagtendonk, and P. C. Weatherspoon. 1996. An Overview of Fire in the Sierra Nevada. In Sierra Nevada Ecosystem Project: Final report to Congress, vol. II, Assessments and scientific basis for management options. Centers for Water and Wildland Resources, University of California, Davis, CA. pp.1033-1040.

McLaughlin, S. B., M. Nosal, S. D. Wullschleger, and G. Sun. 2007. Interactive effects of ozone and climate on tree growth and water use in a southern Appalachian forest in the USA. New Phytologist **174**:109-124.

Meko, D. M., R. Touchan, and K. J. Anchukaitis. 2011. Seascorr: A MATLAB program for identifying the seasonal climate signal in an annual tree-ring time series. Computers & Geosciences **37**:1234-1241.

Meyer, M. D., M. P. North, A. N. Gray, and H. S. J. Zald. 2007. Influence of soil thickness on stand characteristics in a Sierra Nevada mixed-conifer forest. Plant and Soil **294**:113-123.

Millar, C. I., R. D. Westfall, D. L. Delany, M. J. Bokach, A. L. Flint, and L. E. Flint. 2012. Forest mortality in high-elevation whitebark pine (Pinus albicaulis) forests of eastern California, USA; influence of environmental context, bark beetles, climatic water deficit, and warming. Canadian Journal of Forest Research:749-765.

Miller, P., R. Guthrey, S. Schilling, and J. Carroll. 1998. Ozone Injury Responses of Ponderosa and Jeffrey Pine in the Sierra Nevada and San Bernardino Mountains in California. Pacific Southwest Research Station GTR-166:35-42.

Miller, P., K. Stolte, D. M. Duriscoe, and J. Pronos. 1996. Evaluating Ozone Air Pollution Effects on Pines in the Western United States. USDA Forest Service General Technical Report PSW-155:1-87.

Miller, P. R., G. J. Longbotham, and C. R. Longbotham. 1983. Sensitivity of Selected Western Conifers to Ozone. Plant Disease **67**:1113-1115.

Musselman, R. C., A. S. Lefohn, W. J. Massman, and R. L. Heath. 2006. A critical review and analysis of the use of exposure- and flux-based ozone indices for predicting vegetation effects. Atmospheric Environment **40**:1869-1888.

Nakagawa, S., and H. Schielzeth. 2013. A general and simple method for obtaining R2 from generalized linear mixed-effects models. Methods in Ecology and Evolution **4**:133-142.

National Park Service - Air Resources Division. 2015. NPS Gaseous Pollutant and Meteorological Data, Sequoia and Kings Canyon National Park. Gaseous Pollutant Monitoring Program, Denver, CO. Distributed by Air Resource Specialists, Inc. [Available online: http://ard-request.air-resource.com/] Denver, CO.

National Research Council. 2001. Grand challenges in environmental sciences. National Academies Press., Washington, D.C.

Niinemets, Ü. 2010. Responses of forest trees to single and multiple environmental stresses from seedlings to mature plants: Past stress history, stress interactions, tolerance and acclimation. Forest Ecology and Management **260**:1623-1639.

Osborn, T., K. Briffa, and P. Jones. 1997. Adjusting variance for sample size in tree-ring chronologies and other regional mean timeseries. Dendrochronologia **15**:e99.

Paine, R., M. Tegner, and E. Johnson. 1998. Compounded perturbations yield ecological surprises. Ecosystems **1**: 535-545.

Panek, J., and A. Goldstein. 2001. Response of stomatal conductance to drought in ponderosa pine: implications for carbon and ozone uptake. Tree Physiology **21**:337.

Panek, J., D. Saah, A. Esperanza, A. Bytnerowicz, W. Fraczek, and R. Cisneros. 2013a. Ozone distribution in remote ecologically vulnerable terrain of the southern Sierra Nevada, CA. Environmental Pollution **182**:343-356.

Panek, J. A. 2004. Ozone uptake, water loss and carbon exchange dynamics in annually drought-stressed Pinus ponderosa forests: measured trends and parameters for uptake modeling. Tree Physiology **24**:277.

Panek, J. A., D. Saah, and A. Esperanza. 2013b. A natural resource condition assessment for Sequoia and Kings Canyon National Parks: Appendix 2. Air Quality. Air Quality, 2013, National Park Service; Fort Collins, Colorado, National Park Service, Natural Resource Report. NPS/SEKI/NRRd2013/665.2.

Parsons, D. J., and S. H. Debenedetti. 1979. Impact of Fire Suppression on a Mixed-Conifer Forest. Forest Ecology and Management **2**:21-33.

Pavlik, B. M., and M. G. Barbour. 1991. Performance of red and white fir saplings across a Sierra Nevada ecotone. American Midland Naturalist **126**.

Pedersen, B. 1998a. The role of stress in the mortality of midwestern oaks as indicated by growth prior to death. Ecology **79**:79-93.

Pedersen, B. S. 1998b. Modeling tree mortality in response to short- and long-term environmental stresses. Ecological Modelling **105**:347-351.

Peterson, D., M. Arbaugh, and L. Robinson. 1991. Regional growth changes in ozone-stressed ponderosa pine (Pinus ponderosa) in the Sierra Nevada, California, USA. The Holocene **1**:50.

Peterson, D. L., and M. J. Arbaugh. 1988. An Evaluation of the Effects of Ozone Injury on Radial Growth of Ponderosa Pine (Pinus ponderosa) in the Southern Sierra Nevada. Journal of the Air Pollution Control Association **38**:921-927.

Peterson, D. L., M. J. Arbaugh, V. A. Wakefield, and P. R. Miller. 1987. Evidence of Growth Reduction in Ozone-Injured Jeffrey Pine (*Pinus jeffreyi* Grev. and Balf.) in Sequoia and Kings Canyon National Parks. Journal of the Air Pollution Control Association **37**:906-912.

Pinheiro, J., and D. Bates. 2000. Mixed-Effects Models in S and S-PLUS. Springer-Verlag, New York.

Pye, J. M. 1988. Impact of ozone on the growth and yield of trees: a review. Journal of Environmental Quality **17**:347-360.

R Core Team. 2016. R: A language and environment for statistical computing. R Foundation for Statistical Computing, Vienna, Austria. URL https://www.R-project.org/.

Rollinson, C. R., M. W. Kaye, and C. D. Canham. 2016. Interspecific variation in growth responses to climate and competition of five eastern tree species. Ecology **97**:1003-1011.

Royce, E., and M. Barbour. 2001a. Mediterranean Climate Effects. I. Conifer Water Use across a Sierra Nevada Ecotone. American Journal of Botany **88**:911-918.

Royce, E., and M. Barbour. 2001b. Mediterranean Climate Effects. II. Conifer Growth Phenology across a Sierra Nevada Ecotone. American Journal of Botany **88**:919-932.

San Joaquin Valley Air Pollution Control District. 2010. 2010 Ozone Mid-Course Review. Fresno, California June 2010. .

Schmitz, O. J. 1997. Press perturbations and the predictability ofecological interactions in a food web. Ecology **78**:55-69.

Schweingruber, F. H. 1996. Tree rings and environment: dendroecology. Berne, Stuttgart, Vienna, Haupt. , Birmensdorf.

Smith, M. D., A. K. Knapp, and S. L. Collins. 2009. A framework for assessing ecosystem dynamics in response to chronic resource alterations induced by global change. Ecology **90**:3279-3289.

Stephens, S. L., and S. J. Gill. 2005. Forest structure and mortality in an old-growth Jeffrey pine-mixed conifer forest in north-western Mexico. Forest Ecology and Management 205:15-28.

Stephens, S. L., J. M. Lydersen, B. M. Collins, D. L. Fry, and M. D. Meyer. 2015. Historical and current landscape-scale ponderosa pine and mixed conifer forest structure in the Southern Sierra Nevada. Ecosphere 6:1-63.

Stephenson, N. L. 1988. Climatic control of vegetation distribution: the role of the water balance with examples from North America and Sequoia National Park, California. Cornell University, Ithaca, NY.

Stephenson, N. L. 1998. Actual evapotranspiration and deficit: biologically meaningful correlates of vegetation distribution across spatial scales. Journal of Biogeography **25**:855-870.

Sun, G. E., S. B. McLaughlin, J. H. Porter, J. Uddling, P. J. Mulholland, M. B. Adams, and N. Pederson. 2012. Interactive influences of ozone and climate on streamflow of forested watersheds. Global Change Biology **18**:3395-3409.

Takemoto, B., A. Bytnerowicz, and M. Fenn. 2001. Current and future effects of ozone and atmospheric nitrogen deposition on California's mixed conifer forests. Forest Ecology and Management **144**:159-173.

The Royal Society. 2008. Ground-level Ozone in the 21st century: Future Trends, Impacts, and Policy Implications. Royal Society Science Policy Report 15/08, RS1276, 2008; https://royalsociety.org/~/media/Royal_Society_Content/policy/publications/2008/7925.pdf.

U.S. Environmental Protection Agency. 2013. Integrated Science Assessment for Ozone and Related Photochemical Oxidants. Office of Research and Development, National Center for Environmental Assessment. Research Triangle Park, NC.

U.S. Environmental Protection Agency. 2014. Welfare Risk and Exposure Assessment for Ozone.*in* O. o. A. a. Radiation, editor., Office of Air Quality Planning and Standards; Health and Environmental Impacts Division; Risk and Benefits Group Research Triangle Park, NC. Publication No. EPA-452/R-14-005a.

U.S. Environmental Protection Agency. 2015. National Ambient Air Quality Standards for Ozone; Final Rule. Federal Register Vol. 80, No. 206 October 26, 2015. Rules and Regulations 40 CFR Parts 50, 51, 52, 53, and 58. United States Government Printing Office, Washington, D.C. Pages 65292-65468.

Urban, D. L., C. Miller, P. N. Halpin, and N. L. Stephenson. 2000. Forest gradient response in Sierran landscapes: the physical template. Landscape Ecology **15**:603-620.

Ustin, J. A. P. a. S. L. 2004. Ozone Uptake in Relation to Water Availability in Ponderosa Pine Forests: Measurements, Modeling, and Remote Sensing, Final Report.1-51.

Van Ooy, D. J., and J. J. Carroll. 1995. The spatial variation of ozone climatology on the Western slope of the Sierra Nevada. Atmospheric Environment **29**:1319-1330.

Waring, R. H. 1987. Characteristics of Trees Predisposed to Die. BioScience **37**:569-574.

Western Regional Climate Center. 2015. Cooperative climatalogical data summaries. US Cooperative Observer Program, NOAA-NWS. [Available online at: http://www.wrcc.dri.edu/coopmap/].

Williams, A. P., C. D. Allen, A. K. Macalady, D. Griffin, C. A. Woodhouse, D. M. Meko, T. W. Swetnam, S. A. Rauscher, R. Seager, H. D. Grissino-Mayer, J. S. Dean, E. R. Cook, C. Gangodagamage, M. Cai, and N. G. McDowell. 2013. Temperature as a potent driver of regional forest drought stress and tree mortality. Nature Climate Change **3**:292-297.

Yeh, H.-Y., and L. C. Wensel. 2000. The relationship between tree diameter growth and climate for coniferous species in northern California. Canadian Journal of Forest Research **30**:1463-1471.

Zang, C., and F. Biondi. 2015. treeclim: an R package for the numerical calibration of proxy-climate relationships. Ecography **38**:431-436.

Chapter 3 Figures and Tables

Figure 1

Conceptual examples of compound effects in negative (A) and opposing (one negative, one positive) (B) response scenarios. N represents normal conditions with no stressor effects. A, B, and A+B show stressors acting alone and in additive (non-interactive) combination. Shaded zones in A:B illustrate how interactive characteristics of an observed response would be described as additive, antagonistic or synergistic based on the net observed effect of compound stressors. Note that the boundaries of the classifications are dependent on isolated effects. Visualization adapted from Crain et al 2008 and Cote et al 2016.

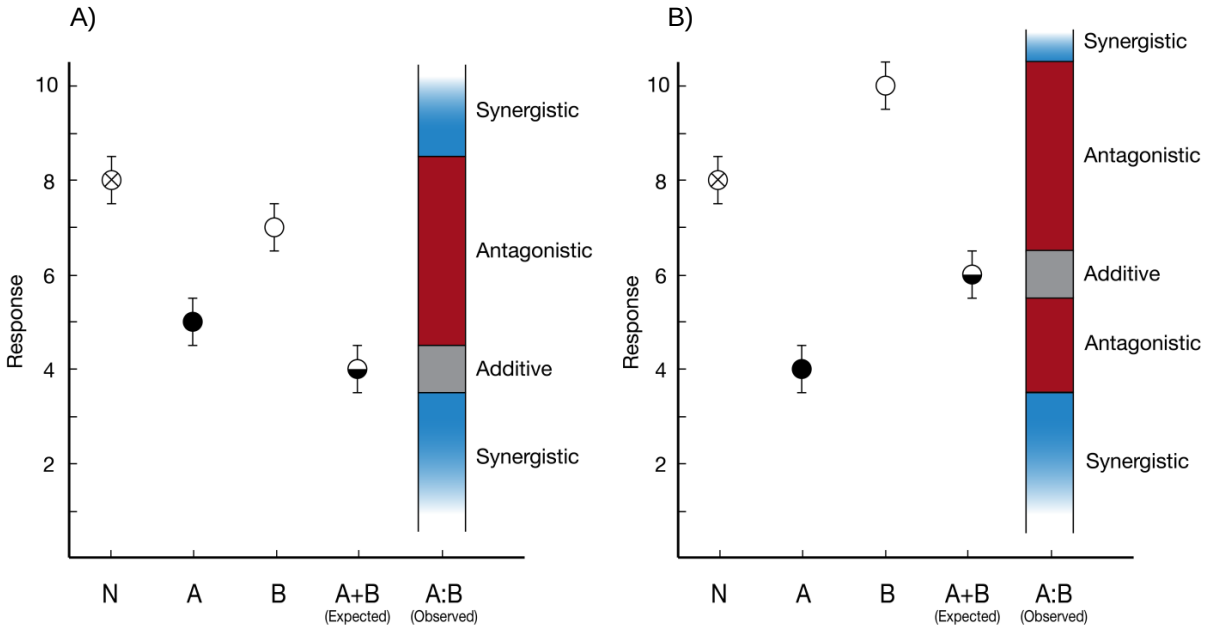

Figure 2

Chlorotic mottle and other damage on Jeffrey pine needles. Chlorotic mottle presents as irregular yellowing in the cells. This injury is a specific bioindicator of ozone damage. It can be distinguished from insect and weather damage by subtle differences in color, pattern, and light transmission. Photo: S. Cousins

Chapter 3 Figures and Tables

Figure 3
Research sites, Sierra National Forest and Sequoia and Kings Canyon National Parks, California. Squares indicate long term study sites, 1991-2012: GG, Grant Grove, and GF, Giant Forest. Circles indicate short term sites, added 2011-2012. FL, Florence Lake; HL, Huntington Lake; SC, Snow Corral; LO, Sugarloaf Basin; AT, Atwell Mill. Photo: AQUA 2014

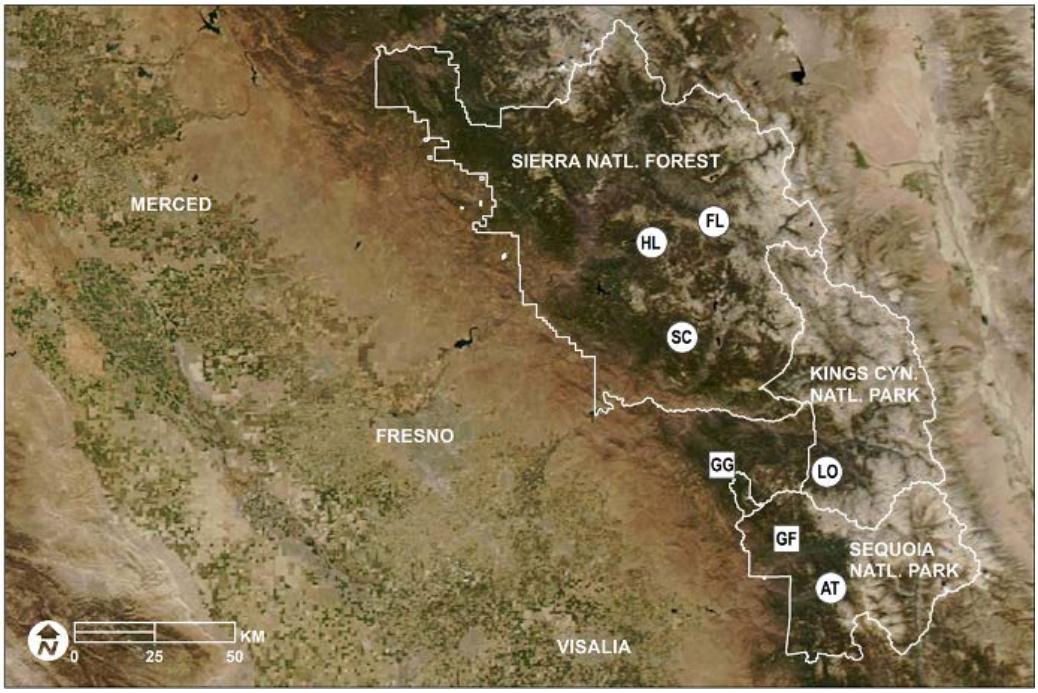

Following pages:

Figure 4
Research sites and personnel: A, Sugarloaf Basin plot 2; B, Florence Lake with Debra Swenson measuring Ozone Injury Index; C, Grant Grove plot 2, Peter Larson and Debra Swenson clipping needles; D, Sugarloaf Basin plot 3; E, Giant Forest plot 1, John Sanders enthusiastically measuring DBH; and F, Huntington Lake, the author recording measurements. Photos: S. Cousins and D. Swenson.

Figure 5
Schematic diagram of analytical steps following ring-width and relative basal area increment chronology development. Analysis proceeds in two main steps: the first describes tree growth in response to climate alone, using the minimum ozone chronology. Once the climate terms are identified by model selection, they become an integral component of the next step.
The second step describes tree growth in response to climate and ozone exposure, while controlling for site and tree characteristics. This stage uses the all sites chronology: all canopy trees at all ozone exposures. Ozone fluxes are potentially related to late summer water availability, so we include both predictors to examine their interaction with respect to growth. The second stage ends with model selection via AIC, followed by three types of model fit and performance testing.
Data shaded with concentric circles signifies indices of tree ring growth. Data shaded dark grey signifies variables that were considered but not selected for incorporation in a growth model (deficit).

Chapter 3 Figures and Tables

Figure 4 *(see caption preceding pages)*

Chapter 3 Figures and Tables

Figure 5 *(see caption preceding pages)*

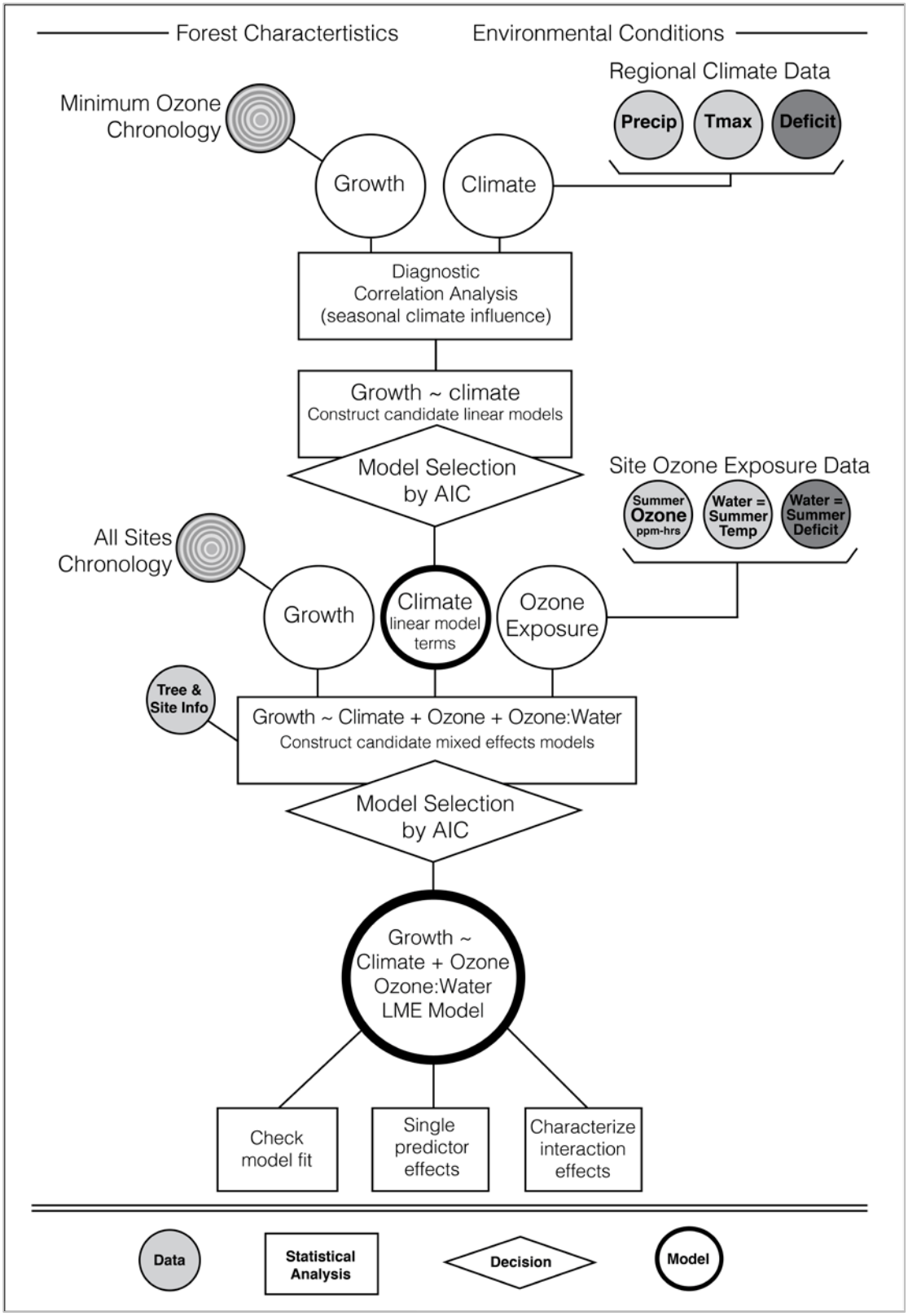

Chapter 3 Figures and Tables

Figure 6

Monthly variation in maximum temperature, precipitation, and climatic water deficit in the southern Sierra Nevada. Unweighted average of all study sites. Data spans 1897-2012 (Flint et al 2013).

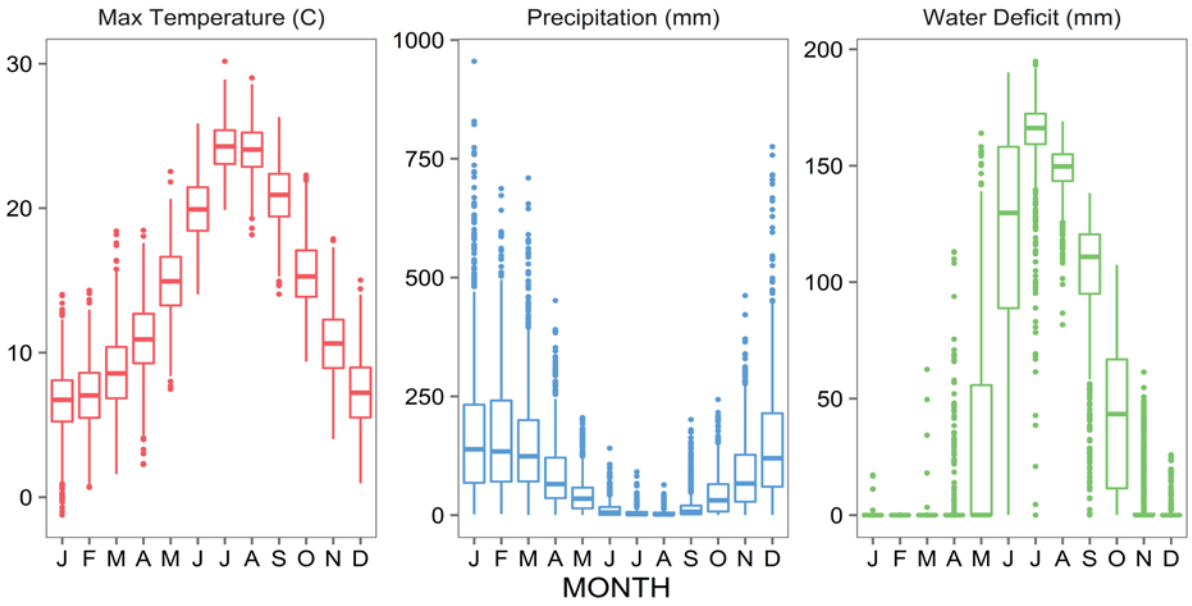

Figure 7

Annual variation and five year mean maximum temperature, precipitation, and climatic water deficit. Temperature is averaged over 12 months, precipitation and deficit are cumulative January through December (Flint et al 2013). Note large interannual variation and shared variation between temperature and deficit.

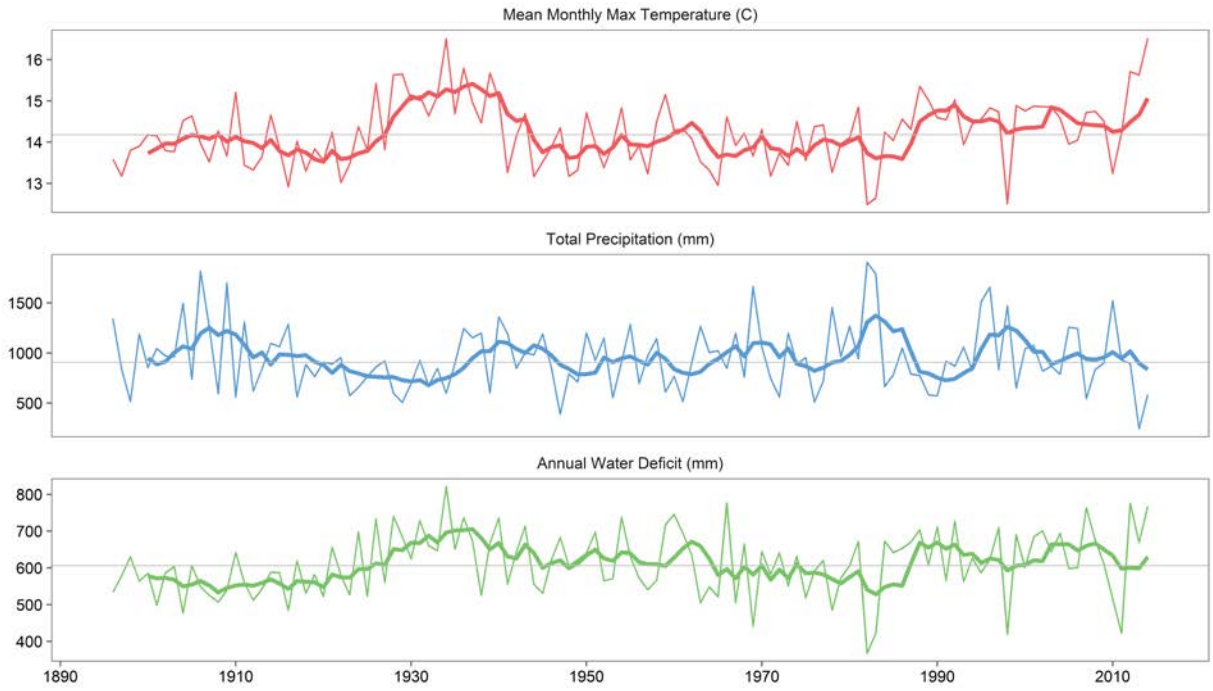

Chapter 3 Figures and Tables

Figure 8
Ring width index chronology for Jeffrey pine at minimum ozone sites (< 45 ppb summer average). Smoothed green line is 5 year mean. Sample depth (grey shading) indicates number of tree ring series, indicated at right hand axis. Note prominence of 1976-77 drought and 1982 El Nino year. Minimum ozone sites include: Florence Lake, Sugarloaf Basin, Huntington Lake, Snow Corral, and Atwell Mill.

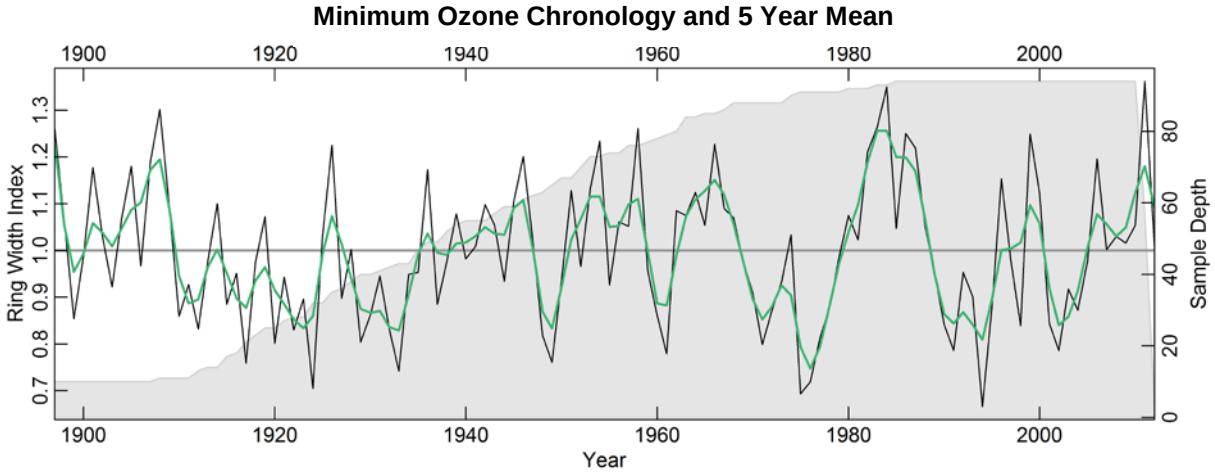

Chapter 3 Figures and Tables

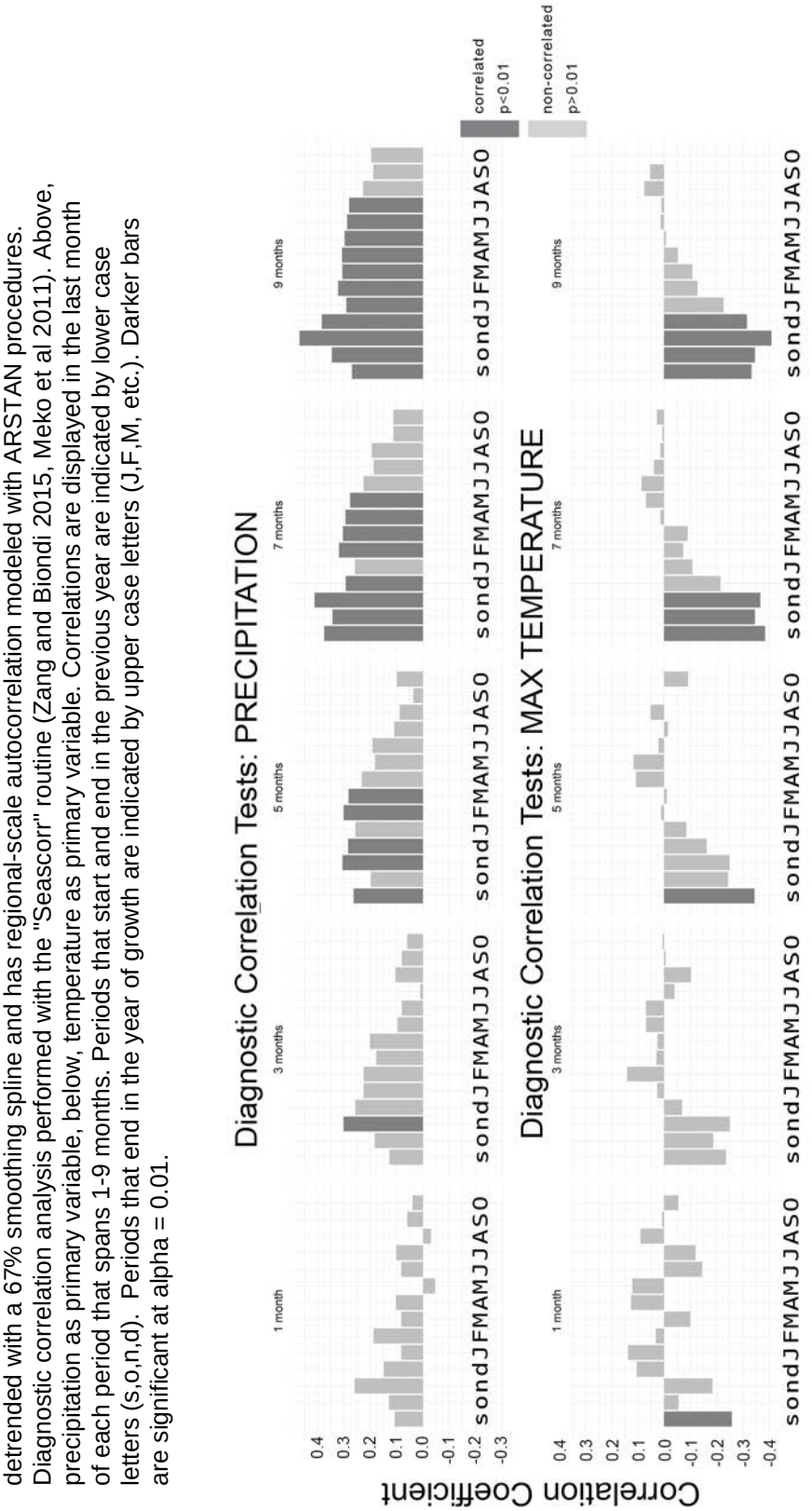

Figure 9
Correlations of the minimum ozone Jeffrey pine chronology with climate averaged across sites. Chronology is detrended with a 67% smoothing spline and has regional-scale autocorrelation modeled with ARSTAN procedures. Diagnostic correlation analysis performed with the "Seascorr" routine (Zang and Biondi 2015, Meko et al 2011). Above, precipitation as primary variable, below, temperature as primary variable. Correlations are displayed in the last month of each period that spans 1-9 months. Periods that start and end in the previous year are indicated by lower case letters (s,o,n,d). Periods that end in the year of growth are indicated by upper case letters (J,F,M, etc.). Darker bars are significant at alpha = 0.01.

Chapter 3 Figures and Tables

Figure 10

Predicted growth response to previous June through February cumulative precipitation and previous March through September mean maximum temperature. Thin lines depict predicted relative growth in the selected climate effects model, Ring Width Index = Precip + Temp + Precip*Temp. Variation in response to high temperatures may be driven by varying soil moisture conditions.

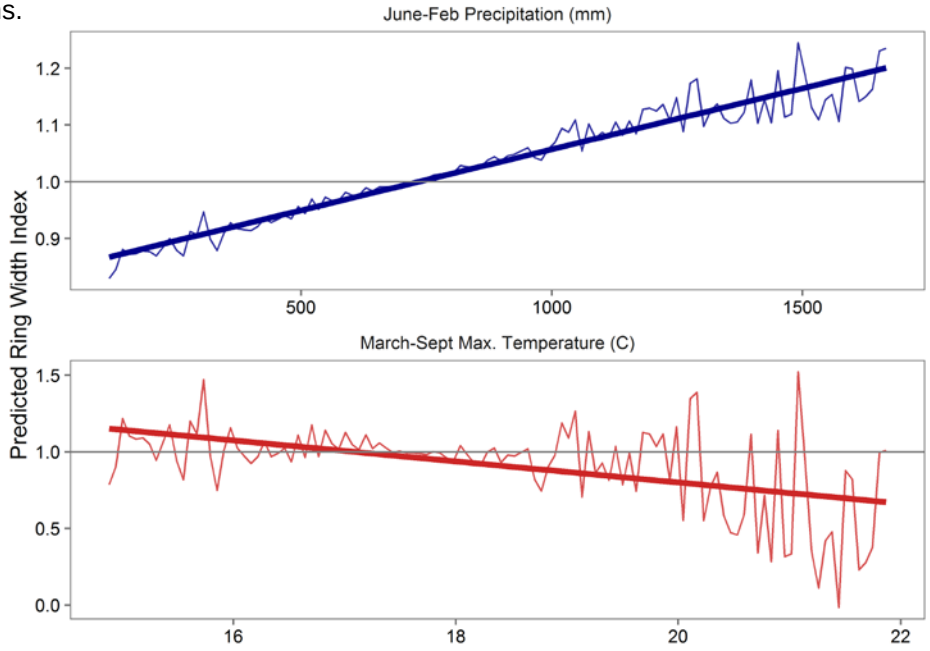

Figure 11

All sites, relative growth (%/ year in rBAI) for each site and overall mean relative growth, 1984-2012. Note that Giant Forest and Grant Grove (GF, GG), the two most severely polluted sites, have relative growth rates consistently below the mean. Values are measured rates. Site abbreviations: AT Atwell Mill; FL Florence Lake; HL Huntington Lake; LO Sugarloaf Basin; SC Snow Corral.

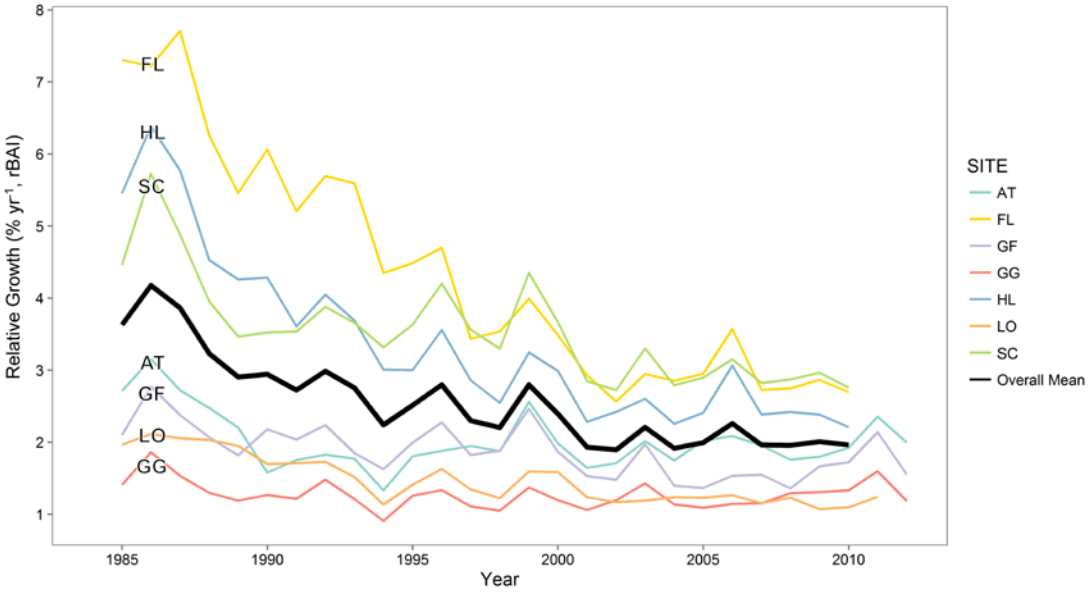

Chapter 3 Figures and Tables

Figure 12
Above: probability density function of relative basal area index for Jeffrey pine relative growth (rBAI) as predicted by the selected linear mixed effects model (black/grey) and as observed (green). Below: distribution of differences between predicted and observed values; note distribution is centered at zero.

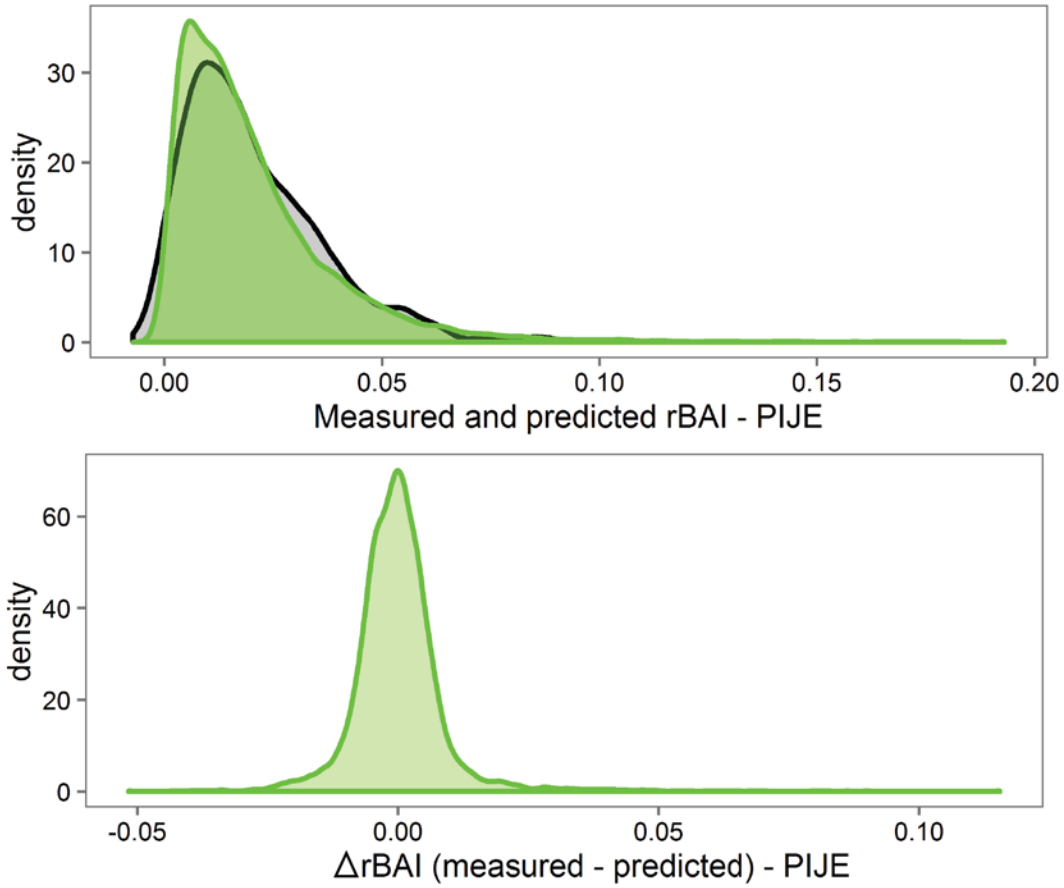

Chapter 3 Figures and Tables

Figure 13
The influence of each fixed effect in isolation on predicted relative growth, based on the linear mixed effects model of relative growth. Values (%/year in relative basal area index) are predicted using the full model, varying each isolated fixed effect across its full range while holding all other effects at their observed median values. Random effects are also set at median values (zero).

Clockwise from upper left: growth steeply declines with increasing ozone exposure (W126 ppm-hours), and increases slightly with summer maximum temperature (June-September); increases with precipitation in the previous June through February; and decreases with temperature of the previous year (March-September). Fixed effects estimates and confidence intervals, Table 3.

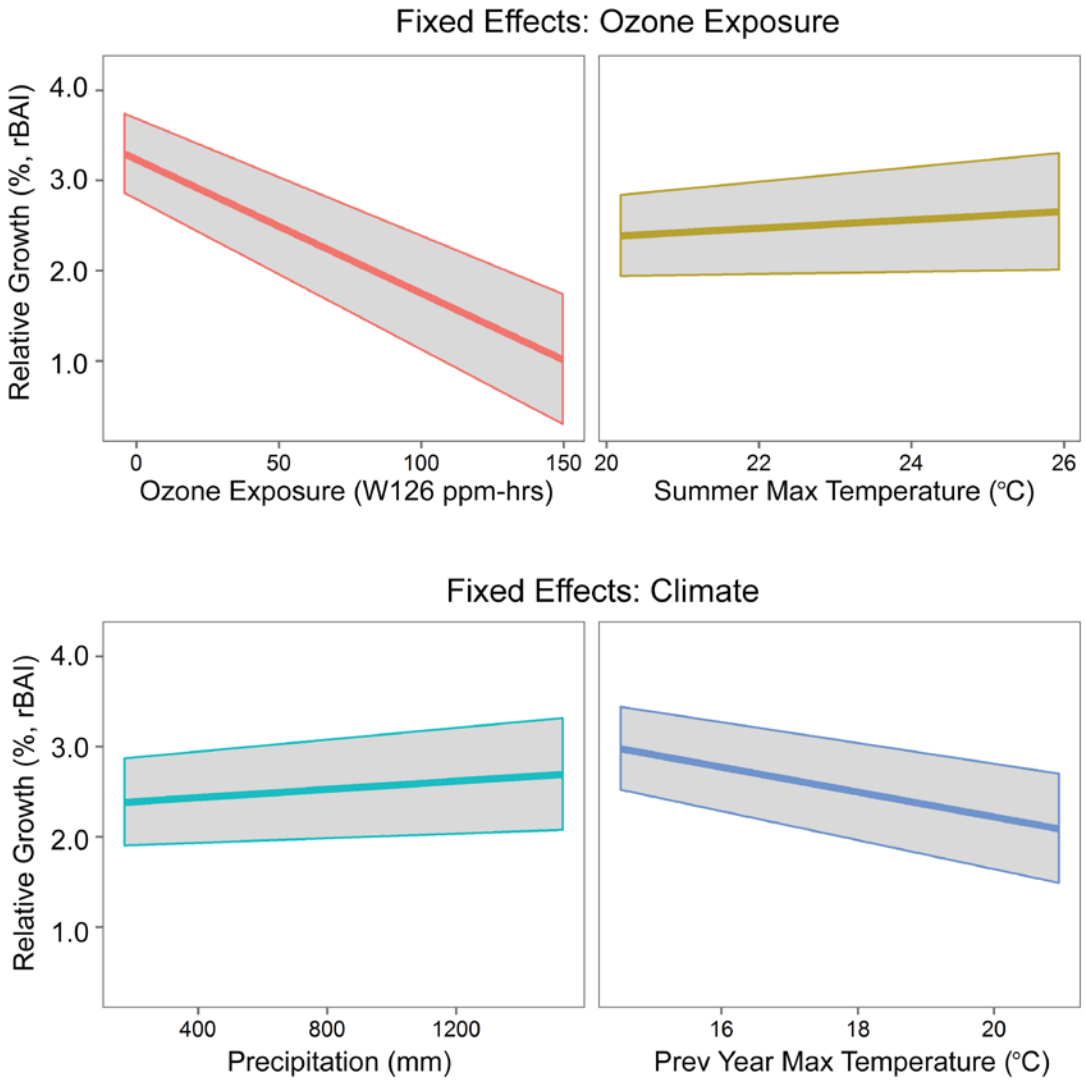

Chapter 3 Figures and Tables

Figure 14
Response of predicted growth (percent relative basal area index) to ozone exposure at two levels of summer water limitation: maximum temperatures below the 1984-2012 mean (< 22.3 degrees C) and maximum temperatures above the mean (> 22.3 degrees C). Effects shown are observed values in the selected linear mixed effects model, with all other fixed effects at median values. At lower temperatures, increasing ozone exposure leads to lower predicted tree growth rates, with many observations at very low exposure and growth above 2.5% annually. At temperatures above the mean, growth increases with rising temperatures, the opposite effect. This shift may be attributable to the difference between ambient ozone concentration and total ozone flux made possible through stomatal closure at high temperatures.

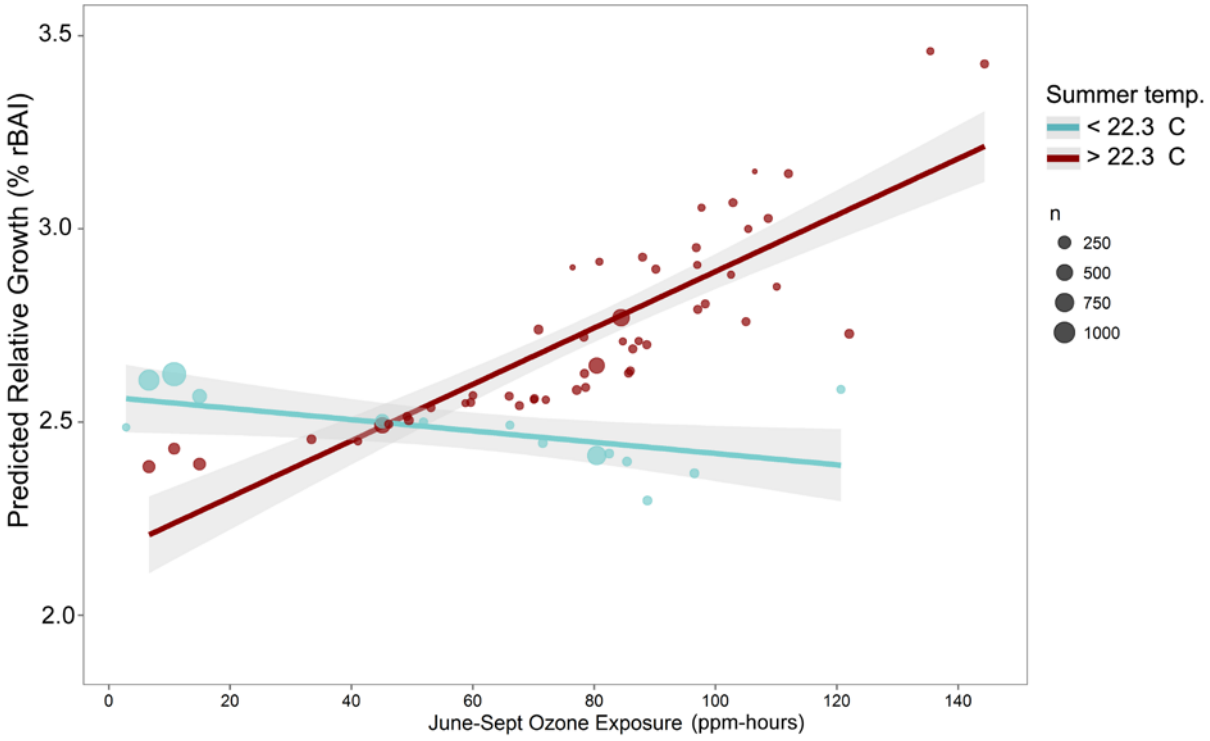

Chapter 3 Figures and Tables

Figure 15

Predicted effects of ozone exposure and summer maximum temperature, a proxy for water availability, individually and interactively. Each isolated effect size is estimated using a fixed effect value one standard deviation beyond the mean and all other variables are held at median values. The Ozone + Temp (Expected) term represents the null hypothesis, a linearly additive sum of the isolated effects, as in Figure 1. The full linear mixed effects model of growth, based on our tree ring and ozone exposure observations, predicts relative growth outside the expected additive range (see Ozone + Temp (Observed)). Note that temperature elicits a small positive response in this case, as in Figure 1 part B. The shaded bar at right depicts a classification of interaction types based on the relative differences and confidence intervals of the isolated and additive effects, per Crain et al., 2008 and Côté et al., 2016. The difference between the additive (expected) range the observed growth rate indicates that the interaction of ozone exposure and summer maximum temperature is an antagonistic one.

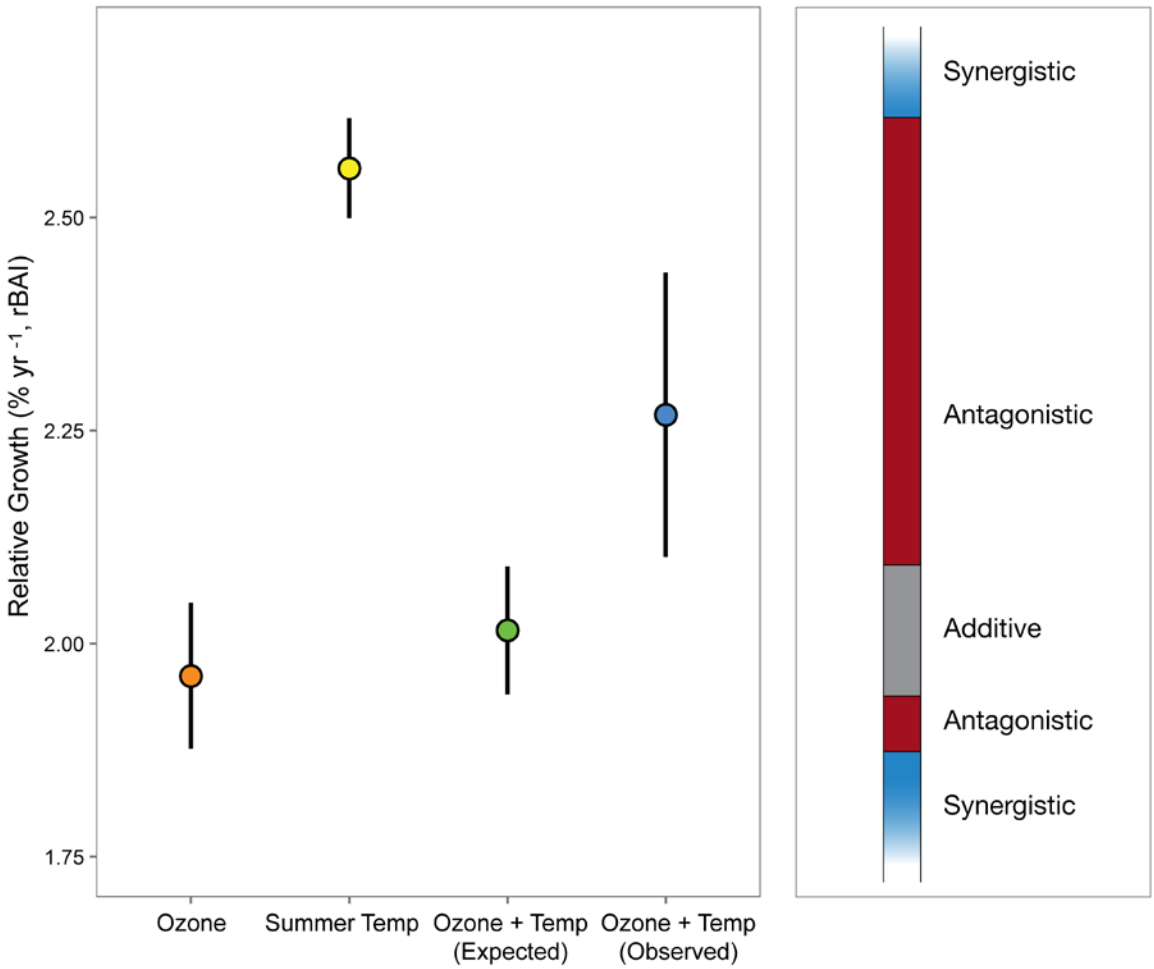

Chapter 3 Figures and Tables

Figure 16
Growth response to ozone exposure at Giant Forest and Grant Grove, 1984-2012. Two responses to ozone exposure are shown: in black, the predicted relative growth rate at observed ozone exposure (averaging 75.5 ppm-hours). In green, the predicted growth response with ozone exposure simulated at an average of 17 ppm-hours, the 3 year mean National Ambient Air Quality Standard (NAAQS) for protection of ecosystems and people from ozone damage. This simulated exposure level would mean a significant improvement in air quality. Points below indicate the difference between growth predicted at extant pollution exposure and at the NAAQS standard. The trend line for this difference shows that the size of this difference has decreased since the 1980s ($p < 0.001$), possibly as a result of declining ozone exposure.

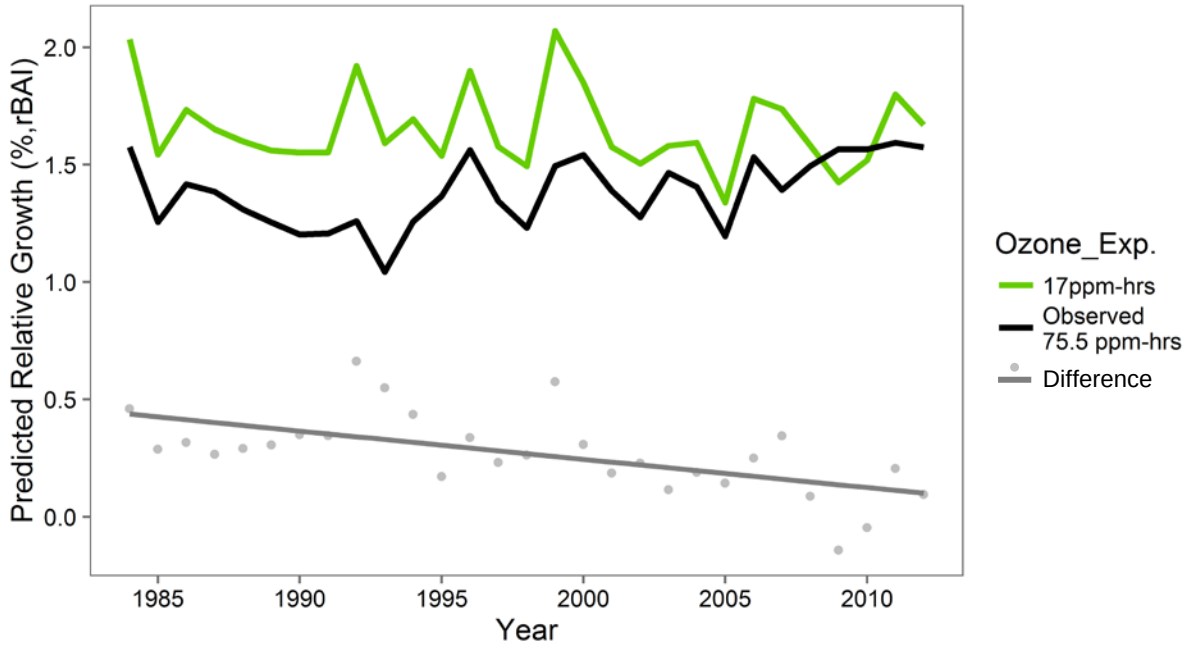

Table 1
Overview of diagnostic chronology statistics for region-wide chronologies used in models of tree growth response to climate and ozone exposure.

Chronology Statistics

Chronology	Growth Index	Series	Trees	Series length (max. years)	Mean length (years)	Series intercorrelation	Standard Deviation	Rbar	Sensitivity	Expressed Pop. Signal
Minimum ozone chronology *P. Jeffreyi*	Ring width index (RWI)	94	77	287	83	0.517	0.057	0.386	0.207	0.932
All sites chronology, *P. Jeffreyi*	Relative basal area index (rBAI)	494	323	343	104	0.42	0.11	0.257	0.209	0.971

Series intercorrelation by Spearman correlation test (dplR)

Table 2
Model selection AIC table. Fixed and random effects of all candidate linear mixed effects models for the response of tree growth to climate, ozone exposure, and the interaction of summer ozone exposure with coincident water availability. Alternative proxies for June through September water availability were maximum temperature or deficit. Random effects terms were the same for all candidate models. The selected model is listed in bold; ΔAIC to nearest model is 132.8.

Parameters						**Criteria**		
Random effects	**Prev. Year Climate**	**DBH, Year**	**Summer ozone exposure**	**Summer water availability**	**Ozone:Water**	**K**	**AICc**	**ΔAIC**
1| SITE/ID	**Precip, Temp, Precip:Temp**	**DBH, Year**	**W126**	**Temp**	**W126: Temp**	**12**	**12544.22**	**0**
1| SITE/ID	Precip, Temp, Precip:Temp	Year only	W126	Temp	W126: Temp	11	12677.02	132.8
1| SITE/ID	Precip, Temp, Precip:Temp	DBH, Year	W126	Temp	--	11	12684.46	140.23
1| SITE/ID	Precip, Temp, Precip:Temp	DBH, Year	W126	--	W126: Temp	9	12689.82	145.6
1| SITE/ID	Precip, Temp, Precip:Temp	DBH, Year	W126	Deficit	--	11	12703.11	158.88
1| SITE/ID	Precip, Temp, Precip:Temp	DBH, Year	W126	--	W126: Deficit	12	12703.96	159.73
1| SITE/ID	Precip, Temp, Precip:Temp	DBH, Year	--	--	W126: Temp	10	12792.01	247.78
1| SITE/ID	Precip, Temp, Precip:Temp	DBH, Year	--	--	--	9	12810.99	266.76
1| SITE/ID	--	DBH, Year	W126	Deficit	W126: Deficit	9	12814.33	270.1
1| SITE/ID	Precip, Temp, Precip:Temp	DBH only	W126	--	W126: Temp	11	13607.85	1063.63

Chapter 3 Figures and Tables

Table 3

Maximum likelihood estimates and confidence limits for fixed parameters in the selected linear mixed effects model of tree growth. P values were obtained via likelihood ratio tests. Parameter groups are likelihood ratio tests on groups of variables representing climate (precipitation and temperature of the previous year through winter) and ozone exposure (ozone exposure value in ppm-hours and growing season summer maximum temperatures).

Species	Parameter	MLE	Lower Limit	Upper Limit	t-value	p-value
P. Jeffreyi	Intercept	0.080	-0.190	0.356	0.66	0.894
	Jun-Feb Precip	0.031	0.017	0.045	4.43	<0.001
	Mar-Sep Temp	-0.086	-0.100	-0.071	-11.89	<0.0001
	Precip * Temp	0.004	-0.010	0.017	0.55	0.326
	DBH	-0.483	-0.557	-0.410	-13.02	<0.0001
	Year	-0.243	-0.257	-0.229	-33.75	<0.0001
	Ozone ppm-hrs	-0.257	-0.288	-0.225	-15.87	<0.0001
	Jun-Sep Temp	0.028	0.007	0.049	2.64	<0.001
	Ozone * Jun-Sep Temp	0.087	0.073	0.101	11.98	<0.0001
	Parameter groups				degrees freedom	
	"Climate" (Precip, Mar-Sep Temp)		-	-	3	<0.0001
	"Ozone Exposure" (Ozone, Jun-Sep Temp)		-	-	3	<0.0001

All maximum likelihood estimates (MLE) from standardized data. Upper and lower limits are 95% confidence intervals computed from likelihood profiles (Pinheiro and Bates 2000). Ozone Exposure: W126, 24 hour cumulative exposure index, in ppm-hours, June - September. June-September Temperature is included as a modifier of ozone exposure. DBH: Diameter at breast height, cm, 2011. Model is based on tree growth and environmental conditions 1984-2012. P-values from likelihood ratio tests.

Chapter 3 Appendix A

Figure A1
Correlations of the minimum ozone Jeffrey pine chronology with climate averaged across sites. Chronology is detrended with a 67% smoothing spline and has regional-scale autocorrelation modeled with ARSTAN procedures. Diagnostic correlation analysis performed with the "Seascorr" routine (Zang and Biondi 2015, Meko et al 2011). Above, climatic water deficit as primary variable; Below, maximum temperature as primary variable. Correlations are displayed in the last month of each period that spans 1-9 months. Periods that start and end in the previous year are indicated by lower case letters (s,o,n,d). Periods that end in the year of growth are indicated by upper case letters (J,F,M, etc.). Darker bars are significant at alpha = 0.01.

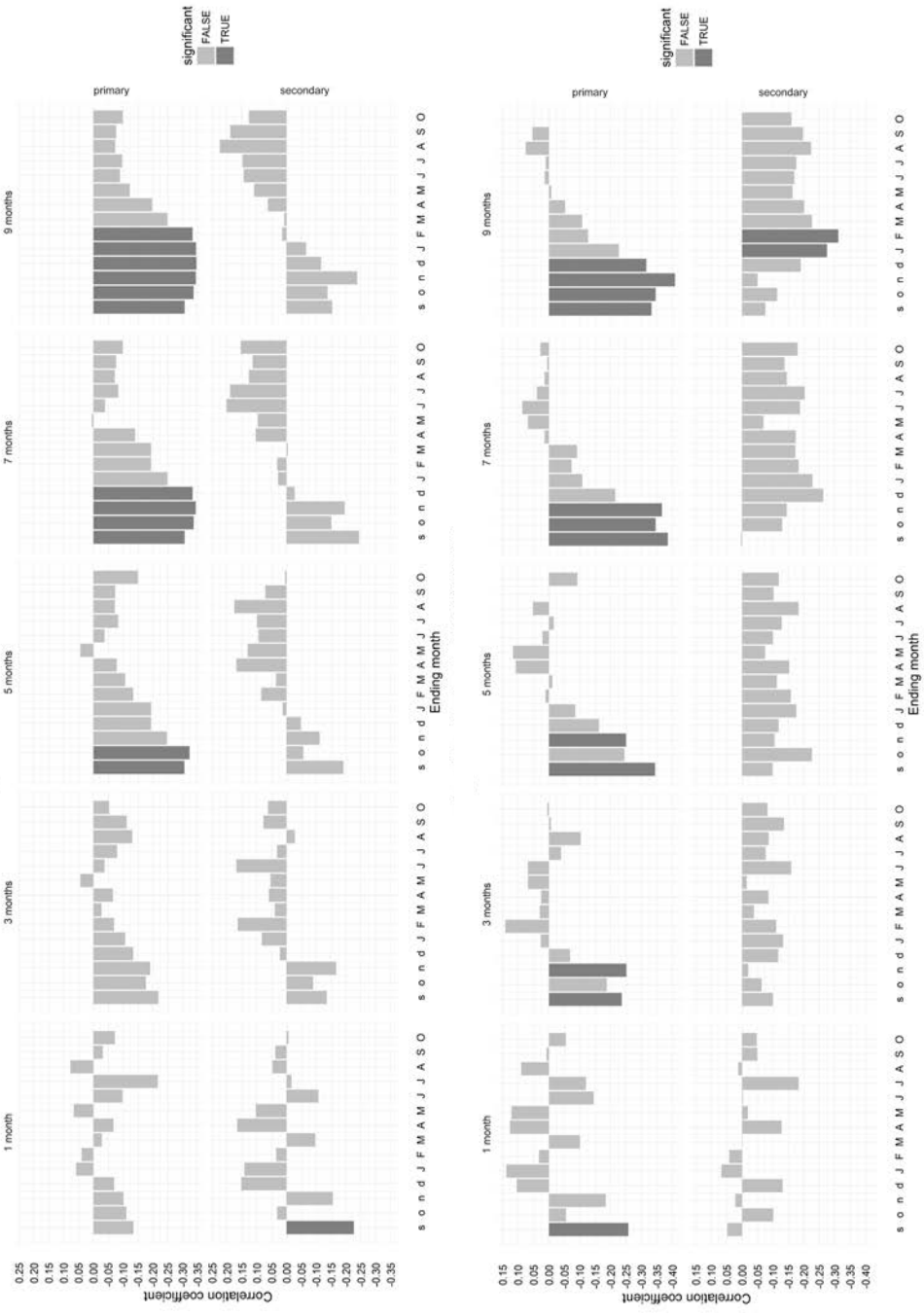

Chapter 3 Appendix A

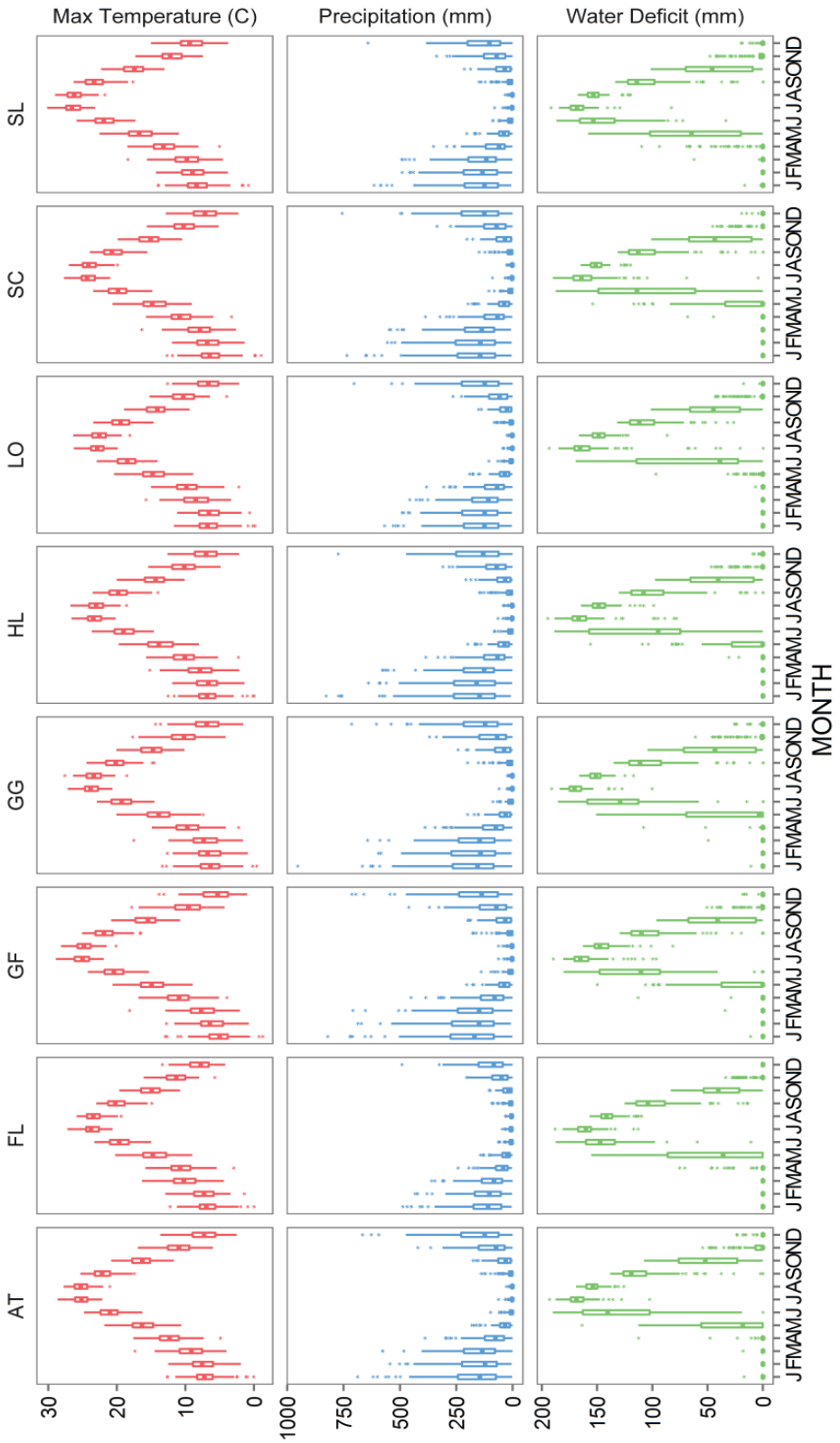

Figure A2
Site-by-climate variable display of monthly maximum temperature, precipitation, and climatic water deficit. Note site-to-site consistency throughout the region. Data are site averages from the California Basin Characterization Model (Flint et al 2013).

Chapter 3 Appendix A

Figure A3

Five year mean temperature and precipitation superimposed over minimum ozone chronology of relative growth (Ring Width Index, RWI). Climate data is scaled to mean = 1.0 and SD = SD_{RWI} for visualization. The chronology does not reflect all variation in climate, and responses may be lagged by one or more years. See Figure 8 for the corresponding annual resolution chronology.

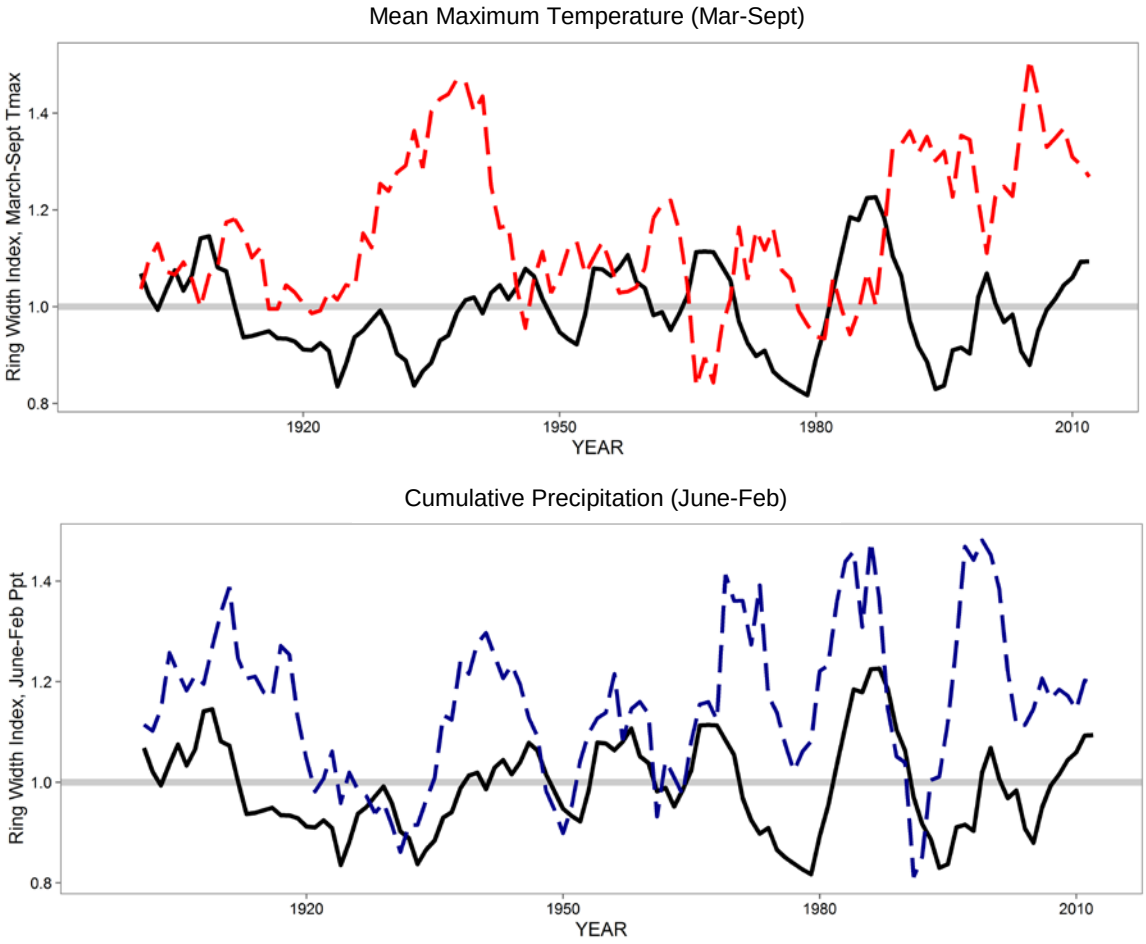

Chapter 3 Appendix A

Figure A4

Diagnostic plots of linear mixed effects residual distributions: fitted versus residual, quantile-quantile, and scale-location plots. While variance does directionally increase, this is a characteristic attribute of tree growth (i.e. increasing with size) and not a serious violation of model assumptions.

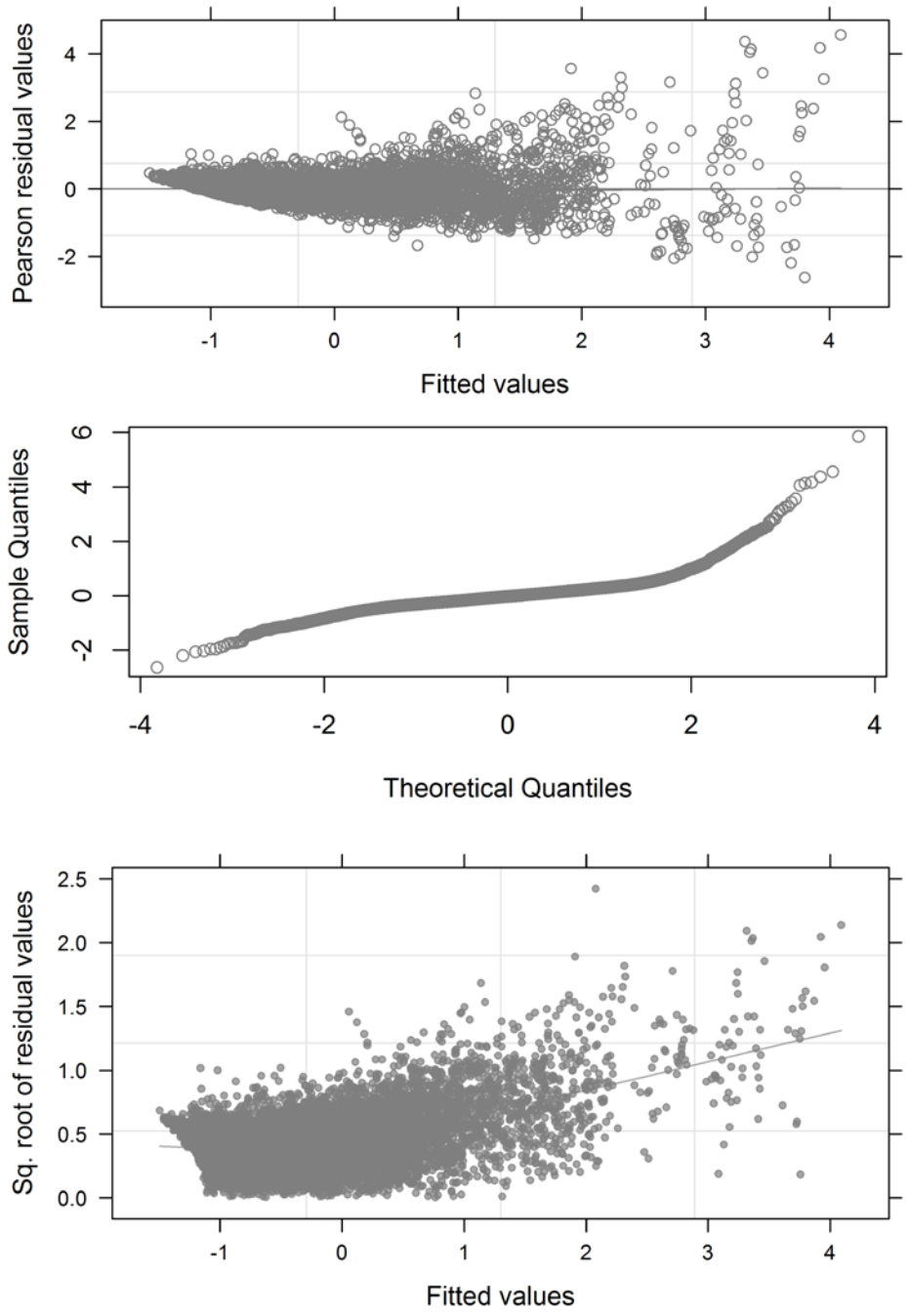

Chapter 3 Appendix A

Table A1

Growth response to ozone exposure, climate, and interaction of ozone and water limitation: details of the selected linear mixed effects model. Precipitation is cumulative from June through February of the year previous to growth; temperature is averaged daily maximums March through September the year previous; or, June-September temperatures refer to the growth year. Fixed and random effect information in Table 3.

Variance Explained:

Conditional R2	Marginal R2
0.783	0.363

Random effects:

	Variance	SD
ID:Site	0.315	0.561
Site	0.092	0.303
Residual	0.225	0.474

Observations:

Total	ID:Site	Site
8426	316	7

Correlation of Fixed Effects:

	Intercept	Jun-Feb Precip	Mar-Sep Temp	Ozone	Jun-Sep Temp	DBH	Year	Precip * Temp
Jun-Feb Precip	-0.017	-0.087						
Mar-Sep Temp	-0.017	-0.087						
Ozone exposure	0.014	0.085	0.186					
Jun-Sep Temp	-0.024	0.4	-0.104	-0.037				
DBH	0.031	0	0	-0.004	0.001			
Year	0.021	-0.35	-0.005	0.134	-0.584	-0.002		
Precip * Temp	-0.013	-0.349	-0.182	-0.056	0.178	0	-0.071	
Ozone * Jun-Sep Temp	-0.029	-0.119	-0.12	-0.534	-0.147	0.001	-0.034	0.132